

Molecular studies of coronavirus replication and pathogenesis

Li, Qisheng

2007

Li, Q. S. (2007). Molecular studies of coronavirus replication and pathogenesis. Doctoral thesis, Nanyang Technological University, Singapore.

<https://hdl.handle.net/10356/6584>

<https://doi.org/10.32657/10356/6584>

Nanyang Technological University

Downloaded on 20 Mar 2024 19:41:05 SGT

MOLECULAR STUDIES OF CORONAVIRUS REPLICATION AND PATHOGENESIS



LI QISHENG

**SCHOOL OF BIOLOGICAL SCIENCES
NANYANG TECHNOLOGICAL UNIVERSITY**

2007

Molecular Studies of Coronavirus Replication and Pathogenesis

Li Qisheng

School of Biological Sciences

A thesis submitted to the Nanyang Technological University
in fulfillment of the requirement for the degree of
Doctor of Philosophy

2007

Abstract

Host factors participate in most steps of virus life cycle. Concomitantly, host gene expression and defenses are modulated by viruses to optimize viral replication. Identifying virus-host interactions can help define mechanisms of viral pathogenesis within the host cell as well as the roles of individual viral protein during infection.

Coronaviruses are a diverse group of large, enveloped, positive-stranded RNA viruses. Severe acute respiratory syndrome coronavirus (SARS-CoV) encodes a highly basic and extensively phosphorylated nucleocapsid (N) protein, the primary function of which is to package viral genomic RNA to form ribonucleoprotein complex (RNP) and assemble into the nucleocapsid core, due to its RNA-binding activities and self-association properties. In this study, we identified Ubc9, an E2 small ubiquitin-like modifier (SUMO)-conjugating enzyme, as a binding partner of the N protein in a yeast two-hybrid screen. This interaction was verified by GST pull-down assay, coimmunoprecipitation and colocalization of the two proteins in cells. Subsequent biochemical characterization studies demonstrated that SARS-CoV N protein was posttranslationally modified by covalent attachment to SUMO. The major sumoylation site was mapped to the ⁶²lysine residue of the N protein. Further expression and characterization of wild-type N protein and K62A mutant revealed that sumoylation of the N protein drastically promotes its homo-oligomerization, and played certain roles in its subcellular localization and the N protein-mediated interference of host cell division. This is the first report showing that a coronavirus structural protein undergoes posttranslational modification by sumoylation, and the functional implication of this modification in the formation of coronavirus ribonucleoprotein complex, virion assembly and virus-host interactions.

There was evidence that coronaviruses and their encoded proteins would induce host cell cycle perturbation and apoptosis. Nevertheless, little is known about how these effects are brought out, and how the manipulation of host-cell functions influences coronavirus replication. This study examined the two major biological events in cells infected with the avian coronavirus infectious bronchitis virus (IBV). We demonstrated that IBV infection imposed a growth-inhibitory effect on cultured cells by inducing cell cycle arrest at both S and G₂/M phases. The arrest was associated with the modulation of various cell cycle regulatory genes and the accumulation of hypophosphorylated RB, but was independent of p53 status in host cells. Proteasome inhibitors such as lactacystin and NLVS could bypass the S-phase arrest by restoring the expression of corresponding cyclin/Cdk complexes. Our data also showed that both S-phase and G₂/M-phase arrest were manipulated by IBV for the enhancement of viral replication. In addition, the late-stage apoptosis induced by IBV infection in cultured cells was shown to be p53-independent, since it was detected in both p53-null cell line (H1299) and cell line expressing wild-type p53 (Vero), and IBV infection did not affect the expression of p53 in host cells.

This thesis is dedicated to
my parents,
my wife, Jinwen,
my son, Xuheng (Nathan),
and my family.

Acknowledgements

First and foremost, I would like to express my deepest appreciation to my supervisor, Dr. Liu Ding Xiang, for his meticulous guidance and continuous financial support. As a role model, his excellent scientific skills, and more importantly, his great passion for science, has taught me so much during my PhD studies, and will be valuable to me for the rest of my career path.

My deepest gratitude also goes to Dr. James P. Tam, my supervisor and Dean of SBS. He has been an excellent mentor, role model, and facilitator for the work in this dissertation. I greatly appreciate his unyielding encouragement and financial support throughout the years of my research.

I am also grateful to my wonderful pals and colleagues in Dr. Liu's labs both at NTU and at IMCB, and Dr. Tam's lab at NTU. The success of my PhD work would be impossible without the help of all these people. As much as I enjoyed working with them, I enjoyed the passionate discussions on both science and life, in a truly friendly atmosphere.

I am especially indebted to Dr. Lim Siew Pheng, who was my first PhD advisor between years 2002 to 2003, before she moved her lab to the Novartis Institute for Tropical Diseases. I have benefited a tremendous amount from her scientific insights and brilliant approaches.

I am also grateful to Dr. Julian Lescar and members of Julian's lab for their scientific instructions, helpful discussions, as well as generously lending chemicals, sharing equipments, and giving some plasmids.

I also highly appreciate all members in my dissertation committee for their evaluation of my thesis work, and valuable comments and suggestions.

Several people in SBS deserve special thanks for their professional assistance: May Chong, Tan Kim Yin, Tan Lay Tin, Eileen Tan, Yee Lee Choo, Oh Seok Fen,, Christabell Chua, and Eugene Lee, our administration staff; Alexander Lim, Joseph Chua, etc, our technical executives, for their great help in all confusing and time-consuming matters. Joyce Leo and Dr. Zheng Zeyi in Dr. Valerie Lin's lab are appreciated for their help in using the FACS Calibur, and sharing some chemicals.

My heartfelt gratitude also goes to Dr. Alex Law, Vice-Dean (Research) of SBS, for his kind and meticulous taking care of all the graduate students from the very beginning when the school was established.

I would also like to take this opportunity to give special thanks to my wife Jinwen, who has been there for me with tremendous support, love, patience, and sacrifice through those good as well as bad times.

I am always so proud of my wonderful family! My father, Li Ke; mother, Geng Meiyun; sister, Yongmei; brother-in-law, Minggang and my cousins have supported me so much with LOVE throughout my life and I know that the most precious award for them from me is they can be proud of me as well.

Lastly, but not the least, I would like to thank the beloved Brothers and Sisters of Bukit Panjang Chapel and Shalom Baptist Chapel in Singapore, especially Sisters Zeng Zuan, and Dai Yin, Borthers Xiaodong, Yong Liang, Wong, and Lin, for all the love, caring, and prayers.

This work was supported by the Agency for Science, Technology and Research, Singapore, and grants from the Biomedical Research Council, Agency for Science, Technology and Research, Singapore.

Table of Contents

Abstract	iii
Dedication	v
Acknowledgements	vi
Table of Contents	viii
List of Figures and Tables	xvi
List of Abbreviations	xviii
Chapter 1 – Literature Review	1
1.1. Overview of Coronaviruses	2
1.1.1. Coronaviruses – important pathogens of human and animals -	2
1.1.1.1. Infectious bronchitis	3
1.1.1.2. SARS	4
1.1.2. Taxonomy and classification	7
1.1.3. Viron morphology and structure	8
1.1.4. Genome organization	10
1.1.5. Structural proteins	12
1.1.5.1. Nucleocapsid (N) protein	12
(1) N protein, an essential structural protein	
wrapping the viral genome	12
(2) Biochemical features and multi-functions	
of the coronavirus N protein	13
(3) SARS-CoV N protein	15
1.1.5.2. Spike (S) protein	16
1.1.5.3. Envelope (E) protein	17
1.1.5.4. Membrane (M) protein	19

1.1.5.5. Hemagglutinin-Esterase (HE) protein -----	20
1.1.6. Nonstructural proteins -----	20
1.1.6.1. Replicase proteins -----	20
1.1.6.2. Accessory proteins -----	21
1.1.7. The coronavirus life cycle -----	22
1.1.7.1. Attachment and penetration -----	22
1.1.7.2. Replication and transcription -----	22
1.1.7.3. Viral assembly -----	23
1.1.8. Treatment and vaccine strategies -----	24
1.1.9. Coronavirus-host interactions -----	25
1.1.9.1. Cytopathic effect (CPE) of coronavirus infection ----	26
1.1.9.2. Effect of coronavirus infection on host cell transcription and translation -----	27
1.1.9.3. Effect of coronavirus infection on cell cycle and apoptosis -----	27
1.1.9.4. Immunopathogenesis of coronavirus infection -----	27
1.2. Viruses and Sumoylation -----	28
1.2.1. Post-translational modification of proteins by small ubiquitin-like modifiers -----	28
1.2.1.1. The family of small ubiquitin-like modifiers -----	29
1.2.1.2. SUMO conjugation pathways -----	29
1.2.1.3. Functional features of SUMO modification -----	31
1.2.2. Viral interactions with the host cell sumoylation system -----	32
1.3. Viruses and the Cell Cycle -----	34
1.3.1. Cell cycle control -----	34

1.3.2. RB phosphorylation is controlled in the cell cycle -----	35
1.3.3. Cdk inhibitors (CKIs) -----	36
1.3.4. The ubiquitin-proteasome pathway in cell cycle regulation --	37
1.3.5. Manipulation of cell cycle progression by viruses and viral-encoded proteins -----	37
1.4. Viruses and Apoptosis -----	39
1.4.1. Cell cycle arrest versus apoptosis: crosstalk -----	39
1.4.2. Role of viral proteins in the induction and suppression of apoptosis -----	40
1.4.3. Coronavirus-induced apoptosis -----	42
1.5. Objectives of Dissertation Study -----	42
Figures and Tables -----	44
Chapter 2 – Materials and Methods -----	55
2.1. Materials -----	56
2.1.1. Viruses -----	56
2.1.2. Cells -----	56
2.1.3. Bacteria strains -----	57
2.1.4. Yeast -----	57
2.1.5. Chemicals, radiochemicals and reagents -----	57
2.1.6. Enzymes -----	58
2.1.7. Antibodies -----	59
2.1.8. Vectors -----	62
2.2. Methods -----	64
2.2.1. DNA manipulations -----	64
2.2.1.1. Construction of plasmids -----	64

2.2.1.2. Cloning techniques	65
(1) Polymerase chain reaction (PCR)	65
(2) Site-directed mutagenesis by two rounds of PCR	66
(3) Agarose gel electrophoresis and gel purification of nucleic acid fragments	66
(4) Restriction endonuclease digestion of PCR products and DNA fragments	67
(5) Dephosphorylation of plasmid DNA	67
(6) Ligation reactions	67
(7) Preparation of competent <i>E. coli</i> cells	67
(8) Transformation of competent <i>E. coli</i> cells by plasmid DNA by heat shock	68
2.2.1.3. Plasmid DNA purification	68
(1) Small scale preparation of plasmid DNA (Miniprep) – <i>Alkaline lysis</i>	68
(2) Phenol/chloroform extraction and ethanol precipitation	69
2.2.1.4. Automated DNA sequencing	69
2.2.2. Preparation of RNA, cDNA and RT-PCR	70
2.2.2.1. Extraction of RNA from HeLa cells	70
2.2.2.2. Reverse transcription – polymerase chain reaction (RT-PCR)	70
2.2.3. Protein characterizations	71
2.2.3.1. SDS-polyacrylamide gel electrophoresis	

(SDS-PAGE) -----	71
2.2.3.2. Expression of GST fusion protein -----	71
2.2.3.3. GST pull-down assay -----	71
2.2.3.4. In vitro translation -----	72
2.2.3.5. Autoradiography -----	72
2.2.3.6. Immunoprecipitation -----	73
2.2.3.7. Western blot analysis -----	73
2.2.4. Yeast two-hybrid screen -----	73
2.2.5. Virus manipulations -----	74
2.2.5.1. Preparation of recombinant vaccinia	
virus-T7 (vTF7-3) working stock -----	74
2.2.5.2. Preparation of working stock of IBV -----	74
2.2.5.3. Infection of mammalian cells by IBV -----	75
2.2.5.4. Virus titration assays -----	75
2.2.6. Tissue culture -----	76
2.2.6.1. Passage of continuous cell line -----	76
2.2.6.2. Preparation and resuscitation of	
frozen cell line stock -----	76
2.2.6.3. Cell transfection -----	76
2.2.6.4. Transient expression of viral proteins	
in mammalian cells -----	76
2.2.7. Cell cycle and apoptosis assays -----	76
2.2.7.1. Measurement of cell proliferation and viability -----	76
2.2.7.2. Determination of cell division -----	78
2.2.7.3. Cell cycle manipulation -----	78

2.2.7.4. Cell cycle analysis by flow cytometry -----	79
2.2.7.5. TUNEL assay -----	79
2.2.8. IF and confocal microscopy -----	80
2.2.8.1. Indirect immunofluorescence (IF) -----	80
2.2.8.2. Confocal microscopy -----	80
2.2.9. Statistical analysis -----	81
Chapter 3 – Sumoylation of the Nucleocapsid Protein of Severe Acute	
Respiratory Syndrome Associated Coronavirus by Ubc9 -----	82
3.1. Introduction -----	83
3.2. Results -----	84
3.2.1. Expression of SARS-CoV N protein in bacterial	
and mammalian cells -----	84
3.2.2. Identification of Ubc9 as a SARS-CoV	
N-interacting protein -----	84
3.2.3. Posttranslational modification of SARS-CoV	
N protein by sumoylation -----	86
3.2.4. Mapping of the sumoylation site on SARS-CoV N protein ---	87
3.2.5. Promotion of homo-oligomerization of SARS-CoV	
N protein by sumoylation -----	88
3.2.6. Further characterization of sumoylation-mediated	
homo-oligomerization of SARS-CoV N protein -----	89
3.3.7. Nucleolar localization of SARS-CoV N protein -----	90
3.2.8. Effects of sumoylation on the subcellular	
localization of SARS-CoV N protein -----	91
3.2.9. Effects of sumoylation on SARS-CoV N protein-mediated	

disruption of host cell division -----	92
3.3. Discussion -----	94
Figures -----	98
Chapter 4 – Cell Cycle Arrest and Apoptosis Induced by the Coronavirus IBV	
in the Absence of p53 -----	110
4.1. Introduction -----	111
4.2. Results -----	113
4.2.1. IBV efficiently infects p53-null H1299 cells -----	113
4.2.2. IBV replication inhibits cell proliferation -----	113
4.2.3. IBV infection induces cell cycle arrest	
in the S and G ₂ /M phases -----	114
4.2.4. IBV infection stimulates cell cycle reentry	
in quiescent cells -----	115
4.2.5. IBV infection does not inhibit cytokinesis or mitotic exit ---	115
4.2.6. Quantitative analysis of cyclins and Cdks	
in IBV infected cells -----	116
4.2.7. IBV infection causes the accumulation of	
hypophosphorylated RB -----	117
4.2.8. Effect of IBV infection on the expression of	
cellular p53 and p21 -----	118
4.2.9. Bypass of IBV-induced S-phase arrest by	
proteasome inhibitors -----	119
4.2.10. IBV-induced cell cycle arrest is not catalyzed by	
the spike protein-mediated cell fusion -----	120
4.2.11. Cell cycle arrest in the S phase promotes IBV replication -	121

4.2.12. G ₂ /M-phase-dependent replication of IBV -----	122
4.2.13. p53-independent apoptosis induced by IBV -----	122
4.3. Discussion -----	124
Figures -----	130
Chapter 5 – General Discussion and Future Directions -----	143
5.1. Virus-host interactions -----	144
5.2. Interaction of SARS-CoV N protein with Ubc9 -----	145
5.3. Sumoylation of the SARS-CoV N protein	
promotes its homo-oligomerization -----	147
5.4. Aberrant cell cycle progression induced by IBV	
infection enhances viral replication -----	147
5.5. Cell cycle arrest and apoptosis in IBV-infected cells	
are p53-independent -----	149
5.6. Novelty and significance of our work -----	150
5.7. Future directions -----	151
5.7.1. Systematic characterization of	
coronavirus-host interactions -----	151
5.7.2. Post-translational modifications of coronavirus N proteins -	152
5.7.2.1. Phosphorylation -----	152
5.7.2.2. Sumoylation -----	153
5.7.3. Crosstalk between IBV-induced	
cell cycle arrest and apoptosis -----	153
5.7.4. Further characterization of IBV-induced apoptosis -----	153
5.7.5. Other questions remain to be elucidated -----	154
References -----	155

List of Figures and Tables

Chapter 1

Figure 1.1	Structure of the coronavirus virion -----	44
Figure 1.2	Comparison of coronavirus genome organization -----	45
Figure 1.3	Schematic representation of the SARS-CoV N protein -----	46
Figure 1.4	Replication of coronavirus and steps in coronavirus life cycle that are potential targets for antiviral drugs and vaccines -----	47
Figure 1.5	Specificity in SUMO signaling and conjugation -----	49
Figure 1.6	The cell cycle control -----	50
Figure 1.7	Roles of viral proteins in the induction and suppression of apoptosis --	51
Table 1.1	Coronavirus groups, species, hosts, and principal associated diseases –	52
Table 1.2	Summary of SARS-CoV proteins-----	53

Chapter 3

Figure 3.1	Analysis of the expression of N protein in bacterial and mammalian cells -----	98
Figure 3.2	Interaction of SARS-CoV N protein with Ubc9 -----	99
Figure 3.3	Modification of SARS-CoV N protein by SUMO-1 -----	101
Figure 3.4	Mapping of the major sumoylation site on SARS-CoV N protein ----	103
Figure 3.5	Analysis of the homo-oligomerization of SARS-CoV N protein -----	104
Figure 3.6	Further analysis of the homo-oligomerization of SARS-CoV N protein -----	105
Figure 3.7	Nucleolar localization of SARS-CoV N protein -----	107
Figure 3.8	Subcellular localization of SARS-CoV N protein constructs -----	108
Figure 3.9	Effects of sumoylation of SARS-CoV N protein on its interference of host cell division -----	109

Chapter 4

Figure 4.1	IBV efficiently infects p53-null H1299 cells -----	128
Figure 4.2	IBV replication in both H1299 and Vero cells inhibits cell proliferation -----	129
Figure 4.3	IBV infection induces S and G ₂ /M arrest in both asynchronously growing and synchronized H1299 and Vero cells -----	130
Figure 4.4	IBV infection stimulates cell cycle reentry in quiescent cells -----	131
Figure 4.5	IBV infection does not inhibit cytokinesis and mitotic exit -----	132
Figure 4.6	Immunoblot analysis of cyclins and Cdks -----	133
Figure 4.7	Immunoblot analysis of RB -----	135
Figure 4.8	Immunoblot analysis of p53 and p21 -----	136
Figure 4.9	Bypass of IBV-induced S-phase arrest by proteasome inhibitors -----	137
Figure 4.10	IBV-induced cell cycle arrest is not catalyzed by the spike protein-mediated cell fusion -----	138
Figure 4.11	S-phase arrest promotes IBV replication -----	139
Figure 4.12	G ₂ /M-phase-dependent replication of IBV -----	140
Figure 4.13	IBV infection induces apoptotic cell death in both H1299 and Vero cells -----	141

List of Abbreviations

2'-O-MT	2'-O-methyltransferase
3CLpro	3C-like proteinase
aa	amino acid
ACE2	angiotensin-converting enzyme 2
APN	aminopeptidase N
ATCC	American Type Culture Collection
BCoV	Bovine coronavirus
CCoV	Canine coronavirus
Cdk	cyclin-dependent kinase
CEA	carcinoembryonic antigen
CIP	calf intestinal alkaline phosphatase
CKI	Cdk inhibitor
CMV	Cytomegalovirus
CNS	central nervous system
CPE	cytopathic effect
DMEM	Dulbecco's modified Eagle's medium
DNA	deoxyribonucleic acid
dNTP	deoxynucleoside triphosphate
E	envelope protein
EBV	Epstein-Barr virus
<i>E. coli</i>	<i>Escherichia coli</i>
ECoV	Equine coronavirus
EGFP	enhanced green fluorescent protein
EM	electron microscopy

ER	endoplasmic reticulum
ETM	transmembrane domain of E protein
FACS	fluorescence-activated cell sorting
FeCoV	Feline enteric coronavirus
FIPV	Feline infectious peritonitis virus
GCoV	Goose coronavirus
GFL	growth factor-like domain
GFP	green fluorescence protein
h	hours
HCMV	Human cytomegalovirus
HCoV-229E	Human coronavirus 229E
HCoV-OC43	Human coronavirus OC43
HDAC	histone deacetylase
HE	hemagglutinin-esterase protein
HEV	Porcine hemagglutinating encephalomyelitis virus
HHV6	Human herpes virus-6
HPV	Human papillomaviruses
HSV	Herpes simplex virus
IAA	iodoacetamide
IBV	Avian coronavirus infectious bronchitis virus
IF	indirect immunofluorescence
IFN	interferon
IP	immunoprecipitation
IPTG	isopropanol- β -D-thiogalactoside
IRES	internal ribosome entry site

ISG15	interferon stimulated gene 15
KSHV	Kaposi's sarcoma-associated herpesvirus
M	membrane protein
MAPK	mitogen-activated kinase
MCS	multiple cloning site
MHV	Murine hepatitis virus
MOI	multiplicity of infection
MuLV	Moloney murine leukemia virus
N	nucleocapsid protein
NES	nuclear export signal
NEM	<i>N</i> -ethylmaleimide
NLS	nuclear localization signal
NLVS	NIP-leu-leu-leu-vinylsulfone
NoRS	nucleolar retention signal
NSP	nonstructural protein
ORF	open reading frame
PAGE	polyacrylamide gel electrophoresis
PBS	phosphate buffered-saline
PCD	programmed cell death
PCR	polymerase chain reaction
PEDV	Porcine epidemic diarrhea virus
P.F.U.	plaque forming units
PhCoV	Pheasant coronavirus
p.i.	postinfection
PI	propidium iodide

PLP	papain-like protease
<i>Pol</i>	polymerase
PRCoV	Porcine respiratory virus
RB	retinoblastoma tumor suppressor protein
RBD	RNA binding domain
RdRp	RNA-dependent RNA polymerase
RNA	ribonucleic acid
RNP	ribonucleocapsid structure
RT-PCR	reverse transcription- polymerase chain reaction
S	spike protein
SARS	severe acute respiratory syndrome
SDS	Sodium dodecyl sulfate
sgRNA	subgenomic RNA
SGT	small glutamine-rich tetratricopeptide repeat-containing protein
S/R	serine/arginine
ssRNA	single strand RNA
STDEV	standard deviation
SUMO	small ubiquitin-like modifier
TCID ₅₀	50% tissue culture infective dose
TCoV	Turkey coronavirus
TGEV	Porcine coronavirus transmissible gastroenteritis virus
TUNEL	the terminal deoxynucleotidyltransferase-mediated dUTP-biotin nick end labeling
Ubc9	ubiquitin-conjugating enzyme 9

Ubl	ubiquitin-like proteins
UTR	untranslated region
w/v	weight/volume
VLP	virus-like particle
v/v	volume/volume
VV	Poxvirus vaccinia virus

Chapter 1

Literature Review

1.1. Overview of Coronaviruses

1.1.1. Coronaviruses – important pathogens of human and animals

Coronaviruses, a genus in the family of *Coronaviridae*, are a diverse group of large, enveloped, non-segmented, positive-stranded RNA viruses that replicate by a unique mechanism, which results in a high frequency of recombination (Lai and Holmes, 2001).

Coronaviruses are important pathogens of human and animals that cause highly prevalent diseases. Most coronaviruses naturally infect only one host species, or a limited number of closely related species (Lai and Holmes, 2001). Virus replication *in vivo* can either cause systemic infections, or be restricted to a few cell types, often the epithelial cells of the respiratory or enteric tracts, leading to localized infections (Lai and Holmes, 2001). The strict species and tissue specificity of coronaviruses is determined by both viral and host factors, such as virus receptors, cell permissivity for virus replication and host immune response (Wege et al., 1982).

This group of viruses is associated with a wide variety of respiratory, gastrointestinal and central nervous system (CNS) diseases in animals and humans (Lai and Cavanagh, 1997; Masters, 2006; McIntosh, 1974) (Table 1.1). Avian coronavirus infectious bronchitis virus (IBV) causes an acute and highly contagious disease in chickens, with a significant impact on the poultry industry worldwide (King and Cavanagh, 1991; Picault et al., 1986). Porcine coronavirus transmissible gastroenteritis virus (TGEV) is a major cause of viral enteritis and fetal diarrhea in swine; it is most severe in neonates, with mortality resulting in significant economic loss (Enjuanes and van der Zeijst, 1995). Porcine respiratory virus (PRCoV) is an attenuated variant of TGEV, which infects lung epithelial cells, resulting in interstitial

pneumonia (Enjuanes and van der Zeijst, 1995). Bovine coronavirus (BCoV) causes both respiratory and enteric disease, including calf diarrhea, winter dysentery in adults, and respiratory infections in cattle of all ages. Feline enteric coronavirus (FeCoV) generally causes mild or asymptomatic infections, mainly of domestic cats. Feline infectious peritonitis virus (FIPV), a virulent variant of FeCoV, has the ability to replicate in macrophages, causing a severe and lethal disease (de Groot-Mijnes et al., 2005). Murine hepatitis virus (MHV) is a well-known cause of hepatic and neurologic diseases of mice and thus provides animal models for encephalitis and hepatitis as well as the immune-mediated demyelinating disease (Matthews et al., 2002; Perlman, 1998; Stohlman et al., 1999). In humans, coronaviruses cause respiratory disease and, to a lesser extent, gastroenteritis. The viruses human coronavirus OC43 (HCoV-OC43) and human coronavirus 229E (HCoV-229E) have long been known to be causative agents of neonatal enteritis and approximately 30% of common colds (McIntosh, 1974).

At the end of 2002, the first cases of severe acute respiratory syndrome (SARS) were reported, and in the following year, SARS had spread to affect more than 8,000 people in 26 countries across 5 continents (Ksiazek et al., 2003; Marra et al., 2003; Rota et al., 2003). SARS is caused by a novel species of coronavirus (SARS-CoV) and is the first example of the association of human coronaviruses with serious human illness. Since the identification of SARS-CoV, two new human coronaviruses, HCoV-NL63 and HCoV-HKU1, have been reported to cause severe, although rarely fatal, infections of the upper and lower respiratory tract (Fouchier et al., 2004; van der Hoek et al., 2004; Woo et al., 2005).

1.1.1.1. Infectious bronchitis

Infectious bronchitis is an acute, highly contagious viral respiratory disease of chicken characterized by tracheal rales, coughing, and sneezing (Cavanagh and Naqi, 2003). The causative agent of the disease is IBV, the prototype species of the family *Coronaviridae*. Since first described and isolated in 1930s, IBV has remained a primary concern in all countries with an intensive poultry industry (Beaudette and Hudson, 1937; Schalk and Hawn, 1931). The most economically detrimental consequences of IBV infection are poor egg quality and markedly poor growth in chicks that survive.

The control of IBV depends mainly on vaccination. Live, attenuated vaccines containing strains of IBV of multiple serotypes have been routinely used in commercial chicken flocks (Bijlenga et al., 2004; Farsang et al., 2002; Ladman et al., 2002). However, vaccination is only partially successful due to the continuous emergence of genetic and antigenic variants (Bacon et al., 2004; Collisson et al., 1992; Gelb et al., 2005). A better understanding of the molecular biology aspects and pathogenesis of the virus may lead to the development of more effective control measures.

1.1.1.2. SARS

In the winter of 2002-2003, a novel viral disease, SARS, emerged in Guangdong Province, China and rapidly spread throughout the world (Parry, 2003; World Health Organization, 2003). Within several months, 8,437 cases of SARS, resulting in 813 deaths, were reported to the World Health Organization by 29 countries across 5 continents (Holmes and Enjuanes, 2003; Ksiazek et al., 2003; Peiris et al., 2004; Skowronski et al., 2005; World Health Organization, 2003). The SARS epidemic almost paralyzed the Asian economy, till it was officially controlled by July

2003, through a tremendous global effort (Ashraf, 2003). However, perhaps the longer and deeper influence by the outbreak of SARS is people's fear and a huge change of their life styles. As we can imagine, at that time, even young ballet students in Hong Kong would have to wear face masks while performing to protect themselves from SARS.

The aetiological agent of SARS, a new coronavirus, was identified using virus-isolation techniques, cell culture, electron-microscopical and histologic studies, and sequencing of the viral genome (Drosten et al., 2003a; Drosten et al., 2003b; Fouchier et al., 2003; Ksiazek et al., 2003; Marra et al., 2003; Peiris et al., 2003a; Rota et al., 2003; Snijder et al., 2003).

Infection of humans with SARS-CoV typically exhibits an influenza-like syndrome of malaise, rigors, fatigue, headache, chills, and high fevers. In two-thirds of infected patients, the disease progresses to an atypical pneumonia, with shortness of breath and poor oxygen exchange in the alveoli (Booth et al., 2003; Lee et al., 2003; Tsui et al., 2003). Up to 70% of these patients also develop watery diarrhoea with active virus shedding, which might increase the transmissibility of the virus (Leung et al., 2003). Respiratory insufficiency leading to respiratory failure is the most common cause of death among those infected with SARS-CoV (Peiris et al., 2003a; Peiris et al., 2003b).

However, the pathology induced by SARS-CoV infection remains unknown. A SARS disease model was proposed, consisting of three stages: viral replication, immune hyperactivity, and pulmonary destruction (Tsui et al., 2003). SARS pathology of the lung has been correlated with diffuse alveolar damage, epithelial cell proliferation, and an increase of macrophages (Weiss and Navas-Martin, 2005). Similar to many coronavirus infections, multinucleate giant-cell infiltrates of

macrophage or epithelial origin have been associated with putative syncytium-like formation (Nicholls et al., 2003). Severe cases of SARS are associated with neutrophilia, mild thrombocytopaenia and coagulation defects (Wong et al., 2003). As those reported in the fatal influenza subtype H5N1 disease in 1997, lymphopenia, hemophagocytosis in the lung and white-pulp atrophy of the spleen are also observed during severe SARS-CoV infection (To et al., 2001). This hemophagocytosis is an indicator of cytokine dysregulation (Fisman, 2000), which may play a role in the pathogenesis of SARS due to the proinflammatory cytokines being released by stimulatory macrophages in the alveoli (Nicholls, 2003; Wang et al., 2004).

The new virus probably circulated among wild animals (Chinese SARS Molecular Epidemiology Consortium, 2004; Guan et al., 2003; Song et al., 2005), which was subsequently transmitted to humans and caused human to human transmission mainly by contacting with infectious respiratory droplets (Holmes, 2003b; Poon et al., 2004; Zhong et al., 2003). Healthcare workers had been a most susceptible group because of their close contact with patients at their most infectious stage (Peiris, 2003b; World Health Organization, 2004).

The SARS outbreak provided an excellent model that the power of modern science leads to rapid solutions to a public health emergency. The syndrome appears as a life-threatening form of pneumonia, and the rapid transmission by aerosols (probably also the fecal-oral route) and the high mortality rate make it a global threat. Although currently there is no efficacious therapy available, and vaccines are still under development, many achievements have been made for understanding this new virus, including sequencing its genome, developing animal models of infection and determining where the pathogen originated in nature and how it was globally spread

in human communities. Nevertheless, a broad range of research needs are still here to challenge the researchers.

1.1.2. Taxonomy and classification

The *Coronaviridae* family includes two subfamilies, the coronaviruses and the toroviruses, which share many features in the genome organization and replication strategies but have different nucleocapsid structure and genome lengths. The *Coronaviridae*, together with the *Arteviridae* and *Roniviridae* families, are classified in the order *Nidovirales*, in which enveloped, positive-stranded RNA viruses that synthesize a 3' nested set of multiple subgenomic mRNAs during infection of host cells are grouped in (Cavanagh, 1997; Mayo, 2002). Toroviruses cause enteric diseases in cattle and possibly in humans (Cavanagh and Horzinek, 1993). The *Arteviridae* family includes swine and equine pathogens, and the *Roniviridae* family is composed of invertebrate viruses (Weiss and Navas-Martin, 2005).

Coronaviruses are divided into three antigenic groups, among which groups I and II contain mammalian viruses, whereas group III contains only avian viruses. (Lai and Holmes, 2001) (Table 1.1). Within each serogroup, the viruses are classified into distinct species according to their host ranges, serological relationships, and genome organizations (Lai and Cavanagh, 1997). Group I coronaviruses include animal pathogens, such as TGEV, porcine epidemic diarrhea virus (PEDV), canine coronavirus (CCoV) and FIPV, as well as HCoV-229E and the newly identified HCoV-HKU1, which cause respiratory infections. Group II also includes pathogens of veterinary relevance, such as BCoV, porcine hemagglutinating encephalomyelitis virus (HEV), and equine coronavirus (ECoV), as well as HCoV-OC43 and another recently identified human respiratory coronavirus, HCoV-NL63. Group II also

includes MHV, which infects both mice and rats, causing a number of diseases, such as hepatitis, enteritis, and respiratory disorders, as well as encephalitis and chronic demyelination. Group III so far includes only avian coronaviruses, such as IBV, turkey coronavirus (TCoV), pheasant coronavirus (PhCoV), and goose coronavirus (GCoV) (Cavanagh, 2005; Cavanagh et al., 2002). Over the past few years, genome sequences of SARS-CoV isolates obtained from a number of patients have been published (Marra et al., 2003; Rota et al., 2003; Ruan et al., 2003). By comparison, the genome organization is similar to that of other coronaviruses, but phylogenetic and sequencing analyses showed that SARS-CoV is not closely related to any of the previously characterized coronaviruses (Rota et al., 2003). There has been controversy about whether SARS-CoV defines a new group of coronaviruses or whether it is a distant member of group II. Currently available evidence shows that it is more closely allied with the group II coronaviruses and has not sufficiently diverged to constitute a fourth group (Goebel et al., 2004; Gorbalenya et al., 2004).

Following the SARS epidemic, three distinct bat coronaviruses have been isolated, two of which are members of group 1. The third, in group 2, is a likely precursor of the human SARS-CoV (Lau et al., 2005; Li et al., 2005b; Poon et al., 2005). In addition, using reverse transcription-PCR (RT-PCR) technique, new IBV-like viruses have been detected that infect geese, pigeons, and ducks (Jonassen et al., 2005). Phylogenetic analyses of the replicase and nucleocapsid protein sequences suggest that these viruses belong to group III, but as yet they have not been isolated or characterized (Weiss and Navas-Martin, 2005).

1.1.3. Viron morphology and structure

The basic structure of coronavirus virions is depicted in Fig. 1.1. The virions are spherical, enveloped particles about 80 to 120 nm in diameter. Interior to the virion is a single-stranded, positive-sense RNA genome ranging from 27 to 32 kb in length, the largest of all RNA virus genomes reported to date (Bournsnell et al., 1985; Eleouet et al., 1995; Lai and Cavanagh, 1997; Lai and Holmes, 2001; Lee et al., 1991). The RNA genome is associated with the nucleocapsid (N) phosphoprotein to form a long, flexible, helical nucleocapsid (Macnaughton et al., 1978; Sturman et al., 1980). A corona of large, distinctive spikes in the envelope makes possible the identification of coronaviruses by electron microscopy (EM). The spike (S) glycoprotein binds to receptors on host cells and fuses the viral envelope with host cell membranes. The envelope also contains the membrane (M) glycoprotein, which spans the lipid bilayer three times and is thought to be a component of both the “internal core structure” and the envelope (Machamer et al., 1990; Machamer and Rose, 1987); and the highly hydrophobic envelope (E) protein, which is present in much smaller amounts than the other viral envelope proteins (Godet et al., 1992; Vennema et al., 1996; Yu et al., 1994).

SARS-CoV contains a single-stranded, positive-sense RNA genome of 29.7 kb in length (Thiel, et al., 2003). The morphology of SARS-CoV virion is typical of a coronavirus (Ksiazek et al., 2003). The N protein binds to the viral RNA forming the helical nucleocapsid in the interior cavity of the virion, whereas M and E proteins are important for the assembly of the viral envelope. S protein is a membranous glycoprotein with prominent petal-shaped spikes on the surface of the virion. This glycoprotein is important for viral entry and defines host range, tissue tropism and virulence. Extraordinary three-dimensional images have been obtained for SARS-CoV virions by using advanced imaging techniques (Ng et al., 2004). These scanning

electron micrographs and atomic force micrographs reveal knobby, rosette-like viral particles resembling tiny cauliflowers. The applications of advanced imaging techniques would substantially aid our understanding of coronavirus structure (Masters, 2006).

1.1.4. Genome organization

Coronaviral genome RNAs are capped, polyadenylated, positive-stranded RNAs of 27 to 32 kb in length (Lai and Stohlman, 1978; Lai and Stohlman, 1981) (Fig. 1.2). Since the genomes are positive stranded, they are able to function as mRNAs and it has been shown that the purified genomic RNA is infectious (Lomniczi, 1977). At the 5' end of the genome is a sequence of 65 to 98 nucleotides, termed the leader RNA, which is also present at the 5' end of all subgenomic mRNAs (Lai et al., 1984). This leader sequence is followed by an untranslated region (UTR) of approximately 210 to 530 nucleotides. At the 3' end of the RNA genome is another UTR of approximately 270 to 500 nucleotides, followed by a poly(A) tail that varies in length. Both UTRs are believed to interact with host and perhaps viral proteins to control RNA replication, which includes the synthesis of positive- and negative-strand genomic-length RNA. Unlike most eukaryotic mRNAs, coronavirus genomes contain multiple open reading frames (ORFs). Specifically for SARS-CoV, the genome contains 10 ORFs encoding the replicase gene, 6 structural proteins, and a variety of potential nonstructural genes (Rota et al., 2003; Thiel et al., 2003). The replicase gene products are encoded within two very large ORFs, 1a and 1b, which are translated into two large polypeptides, pp1a and pp1ab, via a frameshifting mechanism involving a pseudoknot structure formed by the genomic RNA (Bredenbeek et al., 1990; Lee et al., 1991). The order of the genes encoding the polymerase (*pol*) and the

four structural proteins that are present in all coronaviruses is 5'-*Pol*-S-E-M-N-3'. These genes are interspersed with several ORFs encoding various nonstructural proteins and the HE glycoprotein, which differ markedly among coronaviruses in number, nucleotide sequence, gene order, and method of expression (Lai and Cavanagh, 1997). The functions of most of the nonstructural proteins are unknown.

The genome organization of IBV is similar to that of other coronaviruses, such as HCoV-229E, MHV, and TGEV, in having the “5'-*Pol*-S-E-M-N-3'” gene order together with interspersed small nonstructural proteins, such as 3a, 3b, 5a, and 5b (Fig. 1.2.). Due to its smaller genome size (27 kb) as compared to other coronaviruses, the IBV genome is more efficient and compact. Some of the ORFs overlap with neighbour ORFs (Casais et al., 2003).

By analogy with other coronaviruses, SARS-CoV gene expression involves complex transcriptional, translational and post-translational regulatory mechanisms (Snijder et al., 2003; Thiel et al., 2003). In SARS-CoV-infected cells, a 3'-coterminal nested set of nine mRNAs species, including the genome-length mRNA (mRNA1) and eight subgenomic mRNA species (mRNA2–9), is expressed (Fig. 1.2). The genome-length mRNA1 encodes two overlapping replicase proteins in the form of polyproteins 1a and 1a/b, which are processed by virus-encoded proteinases into at least 16 putative nonstructural proteins (NSP1–NSP16) (Table 1.2). The four major structural proteins, S, E, M, and N, are encoded by subgenomic mRNA 2, 4, 5, and 9, respectively (Table 1.2). Two accessory genes, 3a and 7a, encoded by subgenomic mRNA 3, and 7, respectively, have recently been shown to be viral structural proteins (Huang et al., 2006; Ito et al., 2005; Shen et al., 2005) (Table 1.2). In addition, six putative nonstructural proteins, 3b, 6, 7b, 8a, 8b, 9b, are encoded by subgenomic

mRNA 3, 6, 7, 8, and 9, respectively (Snijder et al., 2003; Thiel et al., 2003) (Table 1.2).

1.1.5. Structural proteins

Coronaviruses have four essential structural proteins. These include nucleocapsid (N) protein, spike (S) glycoprotein, small envelope (E) protein, and integral membrane (M) protein. Besides these elements, some strains of groups I and II coronaviruses have an additional glycoprotein, the hemagglutinin-esterase (HE) protein. The I protein of MHV (Fischer et al., 1997), and the SARS-CoV 3a and 7a proteins (Huang et al., 2006; Ito et al., 2005; Shen et al., 2005), have also been shown to be components of virions.

1.1.5.1. Nucleocapsid (N) protein

(1) N protein, an essential structural protein wrapping the viral genome

The N protein is a major structural component of virions. Its RNA binding properties are consistent with the fact that it packages viral genomic RNA during formation of the nucleocapsid in viral assembly. This packaging process is necessary for the assembly and morphogenesis of virus particles.

Assembly of enveloped virus particles is an essential step for a productive viral replication cycle, and requires complex interactions between the lipid envelope, envelope proteins, and internal viral components. During this process, the nucleocapsid becomes progressively wrapped in a cellular membrane that is modified by virus-specific envelope proteins. Budding, a process referred to the acquisition of

virion membrane, results in pinching off the virion from the host membrane, thereby releasing the virus into the extracellular space.

(2) Biochemical features and multi-functions of the coronavirus N protein

All coronaviruses encode an extensively phosphorylated, highly basic N protein. It varies from 377 to 455 amino acids in length and has high serine content (7-11%), which are potential targets for phosphorylation. Sequence conservation of the N proteins within the genus is low. Based on sequence comparisons, three relatively conserved structural domains have been identified in the protein (Lai and Cavanagh, 1997), of which the middle domain is a potential RNA-binding domain, capable of binding both coronavirus- and non-coronavirus-derived RNA sequences in vitro (Masters 1992; Stohlman et al., 1988). Coronavirus-specific RNA substrates that have been identified for N protein include the positive-sense transcription regulating sequence (Chen et al., 2005; Nelson et al., 2000; Stohlman et al., 1988), regions of the 3' UTR (Zhou et al., 1996) and the N gene (Cologna et al., 2000), and the genomic RNA packaging signal (Cologna and Hogue, 2000).

In IBV, two separate RNA-binding sites have been found to map, respectively, to amino- and carboxy-terminal fragments of the N protein (Zhou and Collisson, 2000; Hiscox et al., 2001). The crystal structure of the N-terminal domain reveals a protein core composed of a five-stranded antiparallel beta sheet with a positively charged beta hairpin extension and a hydrophobic platform that are probably involved in RNA binding (Fan et al., 2005a). The C-terminal domain forms a tightly intertwined dimer with an intermolecular four-stranded central beta-sheet platform flanked by alpha helices, indicating that the basic building block for coronavirus nucleocapsid formation is a dimeric assembly of N protein (Jayaram et al., 2006). Data from our

group showed that ⁷⁶Arg and ⁹⁴Tyr in the N-terminal domain of IBV N protein are critical for RNA binding and essential to the infectivity of the viral RNA to cultured cells, thus linking the RNA binding capacity of the coronavirus N protein to viral infectivity directly (Tan et al., 2006). The RNA-binding sites reported for SARS-CoV N protein contain the N-terminal one third region (Huang et al., 2004a). It was recently revealed that the C-terminus is also able to associate with nucleic acids and residues 363-382 are the responsible interaction partner, demonstrating that this fragment might involve in genomic RNA binding (Luo et al., 2006). In addition, the RNA-binding ability of the SARS-CoV N protein would promote its homo-oligomerization (Luo et al., 2006).

The N protein localizes either to the cytoplasm alone or to the cytoplasm and a structure in the nucleus (Hiscox et al., 2001; Li et al., 2005a). This nucleolar localization of the N protein has been shown to be a common feature of the coronavirus family (Wurm et al., 2001). Putative nucleolar retention signals (NoRSs) and nuclear export signal (NES) of the N protein have been identified, and the N protein may use these signals to traffic to and from the nucleolus and the cytoplasm (Reed et al., 2006). It must be noted, however, that nucleolar localization of the N protein was not observed in TGEV-infected or SARS-CoV-infected cells by some groups (Calvo et al., 2005; Rowland et al., 2005; You et al., 2005).

Multiple functions have been postulated for the coronavirus N protein throughout the virus life cycle. Primarily, it complexes with the genomic RNA to form a ribonucleocapsid structure (RNP) and together with the M protein, constitute a component of the viral core (Davies et al., 1981; Escors et al., 2001; Hurst et al., 2005; Narayanan et al., 2000; Risco, 1996). It also plays an important role in the replication of the genomic RNA (Chang and Brian, 1996), and in the transcription and translation

of a subgenomic RNA (sgRNA) (Baric et al., 1988; Stohlman et al., 1988; Tahara et al., 1994). Through binding to cellular membranes and phospholipids, it may facilitate both virus assembly and formation of RNA replication complexes (Lai and Holmes, 2001). It was reported that assembly of SARS-CoV RNA packaging signal into virus-like particles is nucleocapsid dependent (Hsieh et al., 2005). Specifically, two negatively charged residues, ⁴⁴⁰Asp and ⁴⁴¹Asp, in the C-terminus of MHV A59 N protein, are key residues that are involved in virus assembly (Verma et al., 2006). In addition, expression of N protein is necessary for efficient recovery of virus from infectious cDNA clones (Yount et al., 2003; Yount et al., 2002), and enhances the efficiency of replication of coronavirus genome RNA in reverse genetic systems (Almazan et al., 2004; Schelle et al., 2005). N protein might also inhibit host cell proliferation or delay cell growth, possibly by disrupting cytokinesis (Chen et al., 2002; Li et al., 2005a; Wurm et al., 2001). Last but not least, coronavirus N protein may modulate host gene expression and anti-viral defense mechanism by targetting certain host factors. Studies of such modulations have been recognized as an increasingly important area in current virology research.

(3) SARS-CoV N protein

Similar to other coronaviruses, SARS-CoV N protein is highly basic and extensively phosphorylated (Surjit et al., 2005), but it only shares a 20-30% identity to N proteins of other coronaviruses (Marra et al., 2003; Rota et al., 2003). Our recent data showed that besides phosphorylation, SARS-CoV N protein can also be post-translationally modified by sumoylation through interaction with human ubiquitin-conjugating enzyme 9 (Ubc9) (Li et al., 2005a). The most prominent function of the protein is to wrap up the RNA genome to form RNP complex and assemble into

nucleocapsid core, due to its RNA-binding activities and self-association properties. Among its 422 aa, there are several regions rich in basic residues, that may function as NuLs and RNA-binding motifs, and a serine/arginine (S/R) rich motif, which plays a pivotal role in recombinant SARS-CoV N protein multimerization (Luo et al., 2005) (Fig. 1.3). Sequence comparison and structural studies indicated that both the N-terminal one third region (amino acids 49 to 178) and the C-terminus (amino acids 363 to 382) may contain the RNA binding domain (RBD) (Huang et al., 2004a; Luo et al., 2006) (Fig. 1.3). The C-terminal region is responsible for its self-association and homo-oligomerization (He et al., 2004; Luo et al., 2006; Surjit et al., 2004b; Yu et al., 2005) (Fig. 1.3). Crystal structure of the dimerization domain shows a dimer with extensive interactions between the two subunits, suggesting that the dimeric form of the N protein is the functional unit *in vivo* (Yu et al., 2006). Furthermore, the N protein may disrupt host cell cytokinesis, retard S-phase progression and induce apoptosis (Li et al., 2005a; Surjit et al., 2006; Surjit et al., 2004a). The N protein can also stimulate strong humoral cellular immune response, making it a potential vaccine candidate (Kim et al., 2004; Zhao et al., 2005).

1.1.5.2. Spike (S) protein

The coronavirus S proteins are large, heavily glycosylated membrane bound type I glycoproteins (Holmes et al., 1981). They form the large, petal-shaped spikes on the surface of the virion, which can be easily seen under EM (Fig. 1.1). In most group II and all group III coronaviruses, the S protein is cleaved into two subunits, S1 and S2, of roughly equal sizes, by a furin-like enzymatic activity during processing in the Golgi. The amino-terminal S1 subunit contains a receptor binding domain, and it is the most divergent region of the molecule, both across and within the three

coronavirus groups (Masters, 2006). Even among strains and isolates of a single coronavirus species, the sequence of S1 can vary extensively (Lai and Holmes, 2001). In contrast, S2 sequences are more conserved. The carboxy-terminal S2 subunit contains two or three heptad repeat (HR) domains as well as the putative fusion peptide (Weiss and Navas-Martin, 2005). The coronavirus S protein plays vital roles in viral entry, cell-to-cell spread, and tissue tropism (Casais et al., 2003; Matsuyama and Taguchi, 2002; Popova and Zhang, 2002). In addition, the S proteins of most coronaviruses are immunogenic and are immune targets for viral inhibition. Monoclonal antibodies against S can neutralize virus infectivity (He et al., 2006; Zhou et al., 2006).

1.1.5.3. Envelope (E) protein

The coronavirus E protein is a small (8.4 to 12 kDa) integral membrane protein. It was first recognized as a small but essential virion component in 1991 in IBV (Liu and Inglis, 1991), and then in TGEV (Godet et al., 1992) and MHV (Yu et al., 1994). E protein sequences are extremely divergent across the three coronavirus groups and in some cases, among members of a single group. Nevertheless, the same general architecture can be discerned in all E proteins: a short hydrophilic region on the amino terminus, followed by a large hydrophobic region, preceding a large hydrophilic carboxy-terminal region (Liu and Inglis, 1991). In contrast to other viral structural proteins, the coronavirus E protein is expressed by a cap-independent translation mechanism that uses the internal ribosome entry site (IRES) located between ORFs 3a and 3b in the IBV genome and in the 5a region in the MHV genome (Liu and Inglis, 1992; Thiel and Siddell, 1994).

The topology of the E protein in the membrane has been extensively investigated, and results show that different coronavirus E proteins assume distinct topologies. TGEV E protein was reported to have a $C_{\text{exo}}N_{\text{cyto}}$ membrane orientation (Godet et al., 1992). However, studies on the IBV E protein demonstrated an $N_{\text{exo}}C_{\text{cyto}}$ topology (Corse and Machamer, 2000), while MHV E protein spans the lipid bilayer twice, with both its N- and C-terminal regions exposed to the cytoplasm ($N_{\text{cyto}}C_{\text{cyto}}$) (Maeda et al., 2001; Raamsman et al., 2000). The putative transmembrane domain of SARS-CoV E protein has been shown to adopt a highly unusual topology, consisting of a unique, very short transmembrane helical hairpin (Arbely et al., 2004; Khattari et al., 2005). However, latter studies suggested controversial models, in which the topology of transmembrane domain of E protein (ETM) is consistent with a regular TM alpha-helix (Torres et al., 2005; Torres et al., 2006). Data from our group revealed two distinct membrane topologies of a coronavirus E protein. We showed that both the N- and C-terminal regions of SARS-CoV E protein are located in the cytoplasm ($N_{\text{cyto}}C_{\text{cyto}}$), meanwhile a certain proportion of the protein may also adopt either an $N_{\text{cyto}}C_{\text{exo}}$ or $N_{\text{exo}}C_{\text{exo}}$ topology (Yuan et al., 2006a).

The main function of the E protein is its role in the formation of the coronavirus envelope. Along with the M protein, E plays an important role in viral assembly (Vennema et al., 1996). The putative peripheral domain of the E protein interacts with the M protein, thereby retaining the M protein in the pre-Golgi compartment where the virus buds (Lim and Liu, 2001). E protein was also shown to localize to the Golgi and then interacts with the M protein via the carboxyl terminal tail (Corse and Machamer, 2000, 2002, 2003). E protein, when expressed alone or when expressed together with M, forms virus-like particles (VLPs) (Baudoux et al., 1998; Corse and Machamer, 2000; Vennema et al., 1996). The E:M stoichiometry in

the VLPs have not been determined. For the SARS-CoV, however, expression of M and E alone is not sufficient for VLP formation, although expression of M and N is sufficient for capsid formation (Huang et al., 2004b). Another function of the E protein is its ability to induce apoptosis in the infected cell (An et al., 1999).

Several studies of the SARS-CoV E protein have shown additional properties that may be specific to the SARS-CoV. The E protein has the ability to alter membrane permeability and form cation-selective ion channels (Liao et al., 2004; Liao et al., 2006; Wilson et al., 2004). In addition, it appears to have a unique structural feature by forming a highly unusual palindromic transmembrane helical hairpin around a previously unidentified pseudo-center of symmetry (Arbely et al., 2004).

1.1.5.4. Membrane (M) protein

The M protein, a type III integral membrane protein, is the most abundant glycoprotein in the viral envelope. It differs from other coronavirus glycoproteins in that only a short amino terminal domain of M is exposed on the exterior of the viral envelope (Lai and Holmes, 2001). Glycosylation is O-linked for group II coronaviruses and N-linked for groups I and III coronaviruses. One of the main functions of the M protein is to direct the incorporation of the S protein (Nguyen and Hogue, 1997) and the N protein (Narayanan et al., 2000) into the budding virion particle. For several coronaviruses, cells expressing the M and E proteins alone produce VLPs which are exported from the cell (Baudoux et al., 1998; Corse and Machamer, 2000; Vennema et al., 1996). Additionally, the glycosylation status of M can influence organ tropism *in vivo* and induce alpha interferon *in vitro* (Charley and Laude, 1988; de Haan et al., 2003).

1.1.5.5. Hemagglutinin-Esterase (HE) protein

The HE glycoprotein exists as a homodimer of a 65 to 70 kDa protein that forms short spikes on the virions of some group II coronaviruses as well as TCoV (group III) (Lai and Holmes, 2001). HE appears to be a “luxury” protein and is not absolutely necessary for virus infection in culture. However, the presence of HE in a virus may alter its pathogenicity in animals (Smits et al., 2005). The HE protein of various coronaviruses binds 9-*O*-acetylated neuraminic acid residues which is comparable to the binding activity of S in BCoV and HCoV-OC43. This activity contributes to the hemagglutination and hemadsorption activities of coronaviruses, implying that HE may be involved in either virus entry or virus release from infected cells (Brian et al., 1995).

1.1.6. Nonstructural proteins

1.1.6.1. Replicase proteins

Two coronavirus replicase polyproteins, termed pp1a and pp1ab, are produced from ORFs 1a and 1b. Pp1a has been predicted to include a papain-like protease (PLP), a picornavirus 3C-like protease (3CLpro), and several other products of unknown function. Pp1ab is generated through a ribosomal frameshifting mechanism (Brierley et al., 1989; Liu et al., 1994). A set of nonstructural proteins, produced from the autoproteolytic cleavage of pp1a and pp1ab, are predicted to assemble into a membrane-associated viral replication complex (Lim et al., 2000; Liu et al., 1997; Liu et al., 1998; Snijder et al., 2003; Stadler et al., 2003; Thiel et al., 2003; Xu et al., 2001). Essential functions of the replication complex are carried out as follows: 1) transcription of genome-length negative- and positive-stranded RNAs, 2) transcription

of a 3'-coterminal nested set of subgenomic mRNAs that have a common 5' leader sequence derived from the 5' end of the genome, and 3) transcription of the subgenomic derived negative-stranded RNAs with common 5' ends and complementary leader sequences at their 3' ends (Lai and Holmes, 2001; Thiel et al., 2003). The replicase proteins could affect viral tropism and pathogenesis by determining the efficiency of viral replication, perhaps via interactions with noncoding 5' or 3' UTRs, with specific host factors, or with elements of the immune response (Weiss and Navas-Martin, 2005).

The basic properties and major roles of individual SARS-CoV nonstructural protein are summarized in Table 1.2.

1.1.6.2. Accessory proteins

Interspersed among the canonical genes, replicase, S, E, M, and N, all coronavirus genomes contain additional small ORFs, which encode a set of accessory genes. Although some of them have been shown to be components of virions, such as SARS-CoV 3a and 7a proteins (Huang et al., 2006; Ito et al., 2005; Shen et al., 2005) (Table 1.2), most of these coronavirus accessory genes are nonstructural. In all cases examined so far, accessory proteins have been found to be nonessential in viral replication. This dispensability has been determined for genes ns2, ns4 and ns5a of MHV (Schwarz et al., 1990; Yokomori and Lai, 1991), gene 7 of TGEV (Ortego et al., 2003), and genes 3b, 5a, and 5b of IBV (Casais et al., 2005; Shen et al., 2003; Youn et al., 2005). It should be noted that SARS-CoV 3a protein was recently found to function as an ion channel that may modulate virus release (Lu et al., 2006) (Table 1.2).

1.1.7. The coronavirus life cycle

A general schematic view of the major events in the coronavirus life cycle is depicted in Fig. 1.4. Coronaviruses replicate in the cytoplasm of infected cells. However, there is evidence showing that host nuclear factors may be involved in replication of some coronaviruses.

1.1.7.1. Attachment and penetration

Attachment and penetration are complex processes that have not been fully characterized for most coronaviruses. The virion binds to the cell membrane receptors by either the S glycoprotein, or by sequential binding of HE followed by binding of S. Conformational changes either in the S protein or the receptor or both, may be induced by virus binding and lead to fusion of the viral envelope with host cell membranes. Given its role in viral attachment, the S protein is the main determinant of viral tropism. The receptors for some coronaviruses have been identified. The MHV receptor is a glycoprotein which belongs to the carcinoembryonic antigen (CEA) family in the Ig superfamily (Williams et al., 1991). Both TGEV and HCoV-229E utilize aminopeptidase N (APN) glycoproteins as receptors (Delmas et al., 1992). Angiotensin-converting enzyme 2 (ACE2) was identified as a functional receptor for SARS-CoV (Li et al., 2003). Recently, however, CD209L (LSIGN) has been reported to be another receptor for SARS-CoV (Jeffers et al., 2004). After virion attachment to its cellular receptor, virus will be internalized and targeted to the cellular organelles where the virus will replicate.

1.1.7.2. Replication and transcription

Similar to most other positive-stranded RNA viruses, after the release of viral RNA into host cells, replication of genome and transcription of mRNAs must occur. Depending on the strain of the virus, coronaviruses produce five to eight subgenomic mRNAs, each of which translates one or, occasionally, more than one protein (Fig. 1.4). All of the subgenomic mRNAs have a 3' coterminal nested set of structure. The mechanism by which the subgenomic mRNAs are synthesized involves a unique discontinuous transcription mechanism that is not completely understood. The current model is that discontinuous transcription occurs during subgenomic negative-strand RNA synthesis (Sawicki and Sawicki, 2005). This process can be viewed as a number of consecutive events. (i) Negative-strand synthesis is initiated at the 3' end of a genomic RNA. (ii) Elongation and translocation of nascent negative-strand RNA. (iii) The completed negative-strand RNA would then serve as a template for mRNA synthesis. The original model involved leader-primed transcription in which discontinuous transcription occurred during positive-stranded RNA synthesis (Zhang et al., 1994). It was postulated by another model that, after virus entry, subgenomic mRNAs were used directly as templates for the synthesis of negative-stranded subgenomic RNAs, which, in turn, served as templates for additional copies of subgenomic mRNAs. However, this model is not compatible with the discontinuous nature of coronavirus RNA synthesis.

1.1.7.3. Viral assembly

Once the viral gene expression is in progress, through transcription, translation, and genome replication, progeny viruses may begin to assemble. Coronavirus virion assembly is a complex process, involving a series of cooperative interactions among the canonical set of structural proteins. The assembly occurs at the pre-Golgi

membranes of the intermediate compartment (IC) early in infection and in the rough endoplasmic reticulum (ER) at late times of the infection. The E protein can physically interact, via a putative peripheral domain, with the M protein, thereby retaining the M protein in the pre-Golgi compartment where the virus buds (Lim and Liu, 2001). E protein, when expressed alone or when expressed together with M, forms VLPs (Baudoux et al., 1998; Corse and Machamer, 2000; Vennema et al., 1996). The VLPs produced in this manner form a homogeneous population that is morphologically indistinguishable from normal virions, and are released from cells by a pathway similar to that used by virions. Thus, coronavirus virion assembly does not require the participation of the nucleocapsid, defining a new mode of virion budding (Mortola and Roy, 2004; Narayanan et al., 2003; Vennema et al., 1996). In addition, the reverse genetic approach was used to show that S protein is also dispensable in the viral assembly (Narayanan and Makino, 2001). However, in a separate study of SARS-CoV, M and N proteins were reported to be necessary and sufficient for VLP formation, whereas E protein was dispensable (Huang et al., 2004b). This contradiction remains to be resolved.

1.1.8. Treatment and vaccine strategies

Currently, there are no specific antiviral drugs that are highly effective against coronaviruses. However, many steps unique to coronavirus replication could be targeted for development of antiviral drugs and vaccines (Fig. 1.4). The S glycoprotein is a good candidate because neutralizing antibodies are directed against S. Blockade of the specific virus receptor on the surface of the host cell by monoclonal antibodies or other ligands can prevent virus entry. Receptor-induced conformational changes in the S protein can be blocked by peptides that inhibit membrane fusion and

virus entry. Inhibitors of HIV-1 entry and membrane fusion are good models for new drugs that target this first step in coronavirus infection. The large polyprotein of the replicase protein must be cleaved into functional units by virus-encoded proteinases. Protease inhibitors may block virus replication, and those developed to treat other viral diseases as well as new ones are being tested for SARS-CoV (Holmes et al., 2003b). The assembly of polymerase complex, coronavirus transcription, translation, budding and release are also potential targets for drug development. Noticeably, if specific host factors are found to be associated with the most severe cases, it may be possible to modulate their expression or activity in order to prevent progression of the disease.

Control of SARS is most likely to be achieved by vaccination. Live attenuated vaccines prevent serious diseases caused by porcine and avian coronaviruses (Lai and Holmes, 2001). It is likely that a similar inactivated vaccine could be developed for SARS-CoV. Other approaches include adenovirus or vaccinia virus vector recombinants expressing the S glycoprotein. DNA-based vaccine expressing S is also in development (Yang et al., 2004b). In addition, human monoclonal antibodies against the S protein can inhibit virus replication in both cell cultures and ferret models (ter Meulen et al., 2004)

Although progress has been made, the development of effective drugs and vaccines for SARS-CoV that could be rapidly and safely administered to humans in the event of an outbreak needs to be based in a better understanding of SARS pathogenesis, and it is likely to take a long time.

1.1.9. Coronavirus-host interactions

In coronavirus-infected cells, extensive morphological and biochemical changes may occur, such as alterations in the translational and transcriptional patterns, cell cycle, cytoskeleton, and apoptosis pathways. In addition, coronavirus infection may cause inflammation, alter immune and stress responses, and modify the coagulation pathways. The alterations of novel signaling pathways such as mitogen-activated kinases (MAPKs), AP-1, and Akt have also been identified more recently (Enjuanes et al., 2006). Concomitantly, coronavirus replication employs complex mechanisms that involve both viral and cellular proteins, and although yet poorly defined, it is believed that host factors participate dynamically in most steps of coronavirus life cycle. These cellular proteins are hijacked from their normal functions in the cell to assist the virus in its replication (Bushell and Sarnow, 2002). Some of them have been identified and are now increasingly scrutinized as targets to intervene with coronavirus infection (de Haan and Rottier, 2006).

1.1.9.1. Cytopathic effect (CPE) of coronavirus infection

Typical CPE induced by coronavirus infection appears as: rounding up and fusion of infected cells to form multinucleated giant syncytia, detachment of infected cells from the culture dish, and eventually cell lysis and death (Liu et al., 2001). However, it may vary with the virus strain and host cell. Some coronaviruses, such as MHV, IBV, or SARS-CoV, induce cell fusion in infected cells. Intercellular fusion is mediated by the S glycoprotein expressed on the infected cell surface and may aid in the dissemination of virus to neighboring cells. In contrast, some other coronaviruses do not cause host cell fusion, but rather a cell-rounding type of CPE. Host factors could affect coronavirus-induced CPE. For example, MHV-induced cell fusion could

be determined by host cell proteases, which mediate S protein cleavage (Frana et al., 1985).

1.1.9.2. Effect of coronavirus infection on host cell transcription and translation

It is well documented that coronavirus infection leads to inhibition, but not a complete shut off, of host protein translation (Hilton et al., 1986; Tahara et al., 1994); accompanied by a continuous increase of viral protein synthesis. mRNAs of coronaviruses and their host are structurally similar, and thus they share, but compete for the same host-translation machinery. The reduced levels of some host proteins may be due to a loss of their mRNAs in coronavirus-infected cells. In addition to the downregulation of genes involved in host cell translation and maintenance of cytoskeletal network, the upregulation of host genes related to stress response, proapoptosis, proinflammation, and procoagulation was observed (Leong et al., 2005; Tang et al., 2005).

1.1.9.3. Effect of coronavirus infection on cell cycle and apoptosis

In general, viruses regulate host cell cycle and modulate apoptosis for their own replication advantage. The effect of coronavirus infection on cell cycle and apoptosis will be described later.

1.1.9.4. Immunopathogenesis of coronavirus infection

Coronavirus infection results in certain typical host immune responses, which are initiated by the innate immune system, followed by the engagement of the adaptive immune system, which consists of T cells that can kill virus-infected cells and B cells that produce pathogen-specific antibodies. Initiation of the immune

response results in the production of chemokines and other cytokines that induce a pro-inflammatory response and attract certain cells to sites of infection to “clear” the infection. However, the immune response also contributes to progress of the disease or tissue destruction, which is termed “immunopathogenesis” (Perlman and Dandekar, 2005).

In many cases, immunopathogenesis is the outcome of immune dysregulation via the following three ways. First, coronavirus infection might result in an intense inflammatory response mediated by certain proinflammatory cytokines, which help produce toxic agents or induce apoptosis (Banerjee et al., 2002). Second, direct infection of immune cells by a coronavirus might cause increased or dysregulated production of immune mediators (Bergmann et al., 2006). Third, adaptive immune responses might result in autoimmune reactions. Several such mechanisms of autoimmune immunopathogenesis have been described for models of both coronavirus infection and non-coronavirus infection (Perlman and Dandekar, 2005).

1.2. Viruses and Sumoylation

1.2.1. Post-translational modification of proteins by small ubiquitin-like modifiers

Posttranslational modification of proteins is an efficient way to modulate protein-protein interaction, stability, function and localization. A wide range of posttranslational modifications have been determined, including phosphorylation, acetylation, glycosylation, isgylation, ubiquitination as well as sumoylation. Increasing attention has been paid to modifications by ubiquitin-like proteins (UbIs), among which, the SUMO modification, or sumoylation, is the best studied one.

1.2.1.1. The family of small ubiquitin-like modifiers

Ubiquitin, a highly conserved 76 residue polypeptide, is covalently linked to lysine residues of target proteins via an enzymatic cascade involving E1 activating, E2 conjugating, and E3 ligase enzymes (Hershko and Ciechanover, 1998). Since its initial discovery, ubiquitination has been recognized in a wide variety of biological processes, ranging from signal transduction to endocytosis.

About a dozen UbIs have been identified in humans, including the highly related Nedd8 (Kawakami et al., 2001), the interferon-inducible ISG15 (Malakhova et al., 2003; Ritchie et al., 2004), and the SUMO.

In vertebrates four paralogs, designated SUMO-1, SUMO-2/3 and SUMO-4 are expressed. Human SUMO-1, a 101 amino acid polypeptide, is 18% identical and 48% homologous to human ubiquitin (Müller et al., 2001). SUMO-2 and SUMO-3 only differ from one another by three N-terminal residues and have yet to be functionally differentiated. They form a distinct subfamily known as SUMO-2/3 and are 50% identical in sequence to SUMO-1 (Saitoh and Hinchey, 2000). Recently discovered SUMO-4, 86% homologous to SUMO-2, is expressed only in kidney cells (Bohren et al., 2004). Although all SUMO family members utilize the same set of enzymes for conjugation pathway, it appears that functions of SUMO-1 are different from those of SUMO-2/3, which conjugate certain proteins under stress conditions and protect the cells from apoptosis. Whether SUMO-1 and SUMO-2/3 compete for the same substrates is not clear. However, a number of substrates have been shown to be readily modified by both SUMO-1 and SUMO-2/3 at the same site (Seeler and Dejean, 2003).

1.2.1.2. SUMO conjugation pathways

Covalent interactions between SUMO and its targets are achieved by formation of an isopeptide bond between the carboxyl group of a C-terminal glycine of mature SUMO and the ϵ -amino group of lysine in the substrate protein, provided that the lysine is part of a SUMO conjugation consensus motif (Hay, 2005). This reaction is an ATP-dependent, tetra-step process. The four steps are: maturation, activation, conjugation, and ligation, mediated by SUMO protease Ulp, E1, E2 and E3 enzymes respectively (Seeler and Dejean, 2003) (Fig. 1.5).

In the second step of the reaction, SUMO is transferred from SAE1/SAE2 complex to the E2 conjugating enzyme Ubc9 (Desterro et al., 1997; Schwarz et al., 1998). As a result, a new thioester bond between the C-terminal Gly97 of SUMO and the Cys93 of Ubc9 is formed. To date only one E2 enzyme has been identified for SUMO modification compared with the many for ubiquitin. Ubc9 shares the same three-dimensional structure and considerable sequence homology with E2s of the ubiquitination pathway. However, its enzymatic activity is specific to the SUMO conjugation pathway (Desterro et al., 1997). One of the functions of Ubc9 is the transfer of SUMO to the ϵ -amino group of a lysine side chain in a target protein. A unique ability of Ubc9 to interact with a large number of SUMO substrates suggests that it directly recognize SUMO substrates and participates in their modification. Routinely, SUMO substrates are identified by yeast two-hybrid interaction with Ubc9.

The SUMO modification consensus motif is a tetrapeptide, ψ KxE (where ψ is a large hydrophobic residue and x is any residue) (Rodriguez et al., 2001). Although it is clear that modification of most substrates takes place within the SUMO modification consensus motif, certain substrates are modified on lysine residues where the surrounding sequence does not conform to this consensus. It should also be

note that not all proteins containing the ψ KxE sequence are modified by SUMO. This indicates that other factors such as subcellular localization or appropriate presentation of the sequence on the substrate protein may be required for modification. Recently, a new SUMO-binding motif, V/I-X-V/I-V/I, was identified by NMR spectroscopic characterization of interactions among SUMO-1 and peptides derived from proteins that are known to bind SUMO or sumoylated proteins. This motif binds all SUMO paralogues (SUMO-1 to -3), and exists in nearly all proteins known to be involved in SUMO-dependent processes, suggesting its general role in sumoylation-dependent cellular functions (Song et al., 2004).

Sumoylation of proteins is a highly dynamic and reversible process. The control over of this process is carried out by a family of proteases called SUMO hydrolases. Modified substrates are subject to de-sumoylation by the isopeptidase activity of these hydrolases (Melchior et al., 2003). Thus isopeptidase inhibitors such as *N*-ethylmaleimide (NEM) and iodoacetamide (IAA) were used in this study to stabilize SUMO conjugation.

1.2.1.3. Functional features of SUMO modification

Diverse consequences have been ascribed to SUMO modification, such as nuclear transport (Pichler and Melchior, 2002), DNA repair (Müller et al., 2004), cell cycle progression (Dieckhoff et al., 2004), transcriptional regulation (Gill, 2003), and modulation of protein-protein and protein-nucleic acid interactions (Verger et al., 2003).

The list of proteins found to be modified by SUMO is growing all the time. Although some of them are cytoplasmic (for example, RanGAP1, I κ B α , GLUT1, GLUT4 and yeast proteins), it seems that sumoylation is a largely nuclear process

(Seeler and Dejean, 2003). In fact, a short peptide that contains the SUMO consensus motif and a nuclear localization signal (NLS) is sufficient to produce a SUMO conjugate *in vivo* (Rodriguez et al., 2001).

As with other post-translational modifications, the functional consequence of SUMO modification is dependent on the particular substrate that is being modified. Although it is clear that sumoylation pervades many cellular processes, the stoichiometry of modified substrates is generally very low, comparing with the coexistent unmodified substrates. This raises the question as to how these low levels of modification could lead to such obvious regulatory consequences. Perhaps the dynamic and reversible property of the modification makes it unstable and hard to capture experimentally. Alternatively, the dynamics of the modification, rather than the stoichiometry, may be relevant for function.

There are crosstalks among sumoylation, ubiquitination, phosphorylation, methylation and acetylation. Noticeably, all sumoylation, ubiquitination, methylation and acetylation take place on lysine residues (Freiman and Tjian, 2003). The potential cascades of modifications on a protein serve as molecular rheostats that fine-tune the control of its functions.

1.2.2. Viral interactions with the host cell sumoylation system

A well established and widespread virus-host interaction is the modulation of viral protein properties and functions by post-translational modifications such as phosphorylation, glycosylation, ubiquitinylation, and the more recently defined sumoylation. While the interplay between viruses and host cell sumoylation system remains to be dissected, it is clear that a reciprocal relationship exists. Viral proteins can be sumoylated, and this modification can regulate protein functions and/or

intracellular location, and has functional consequences that are important for the viral life cycle. Viruses can also influence the sumoylation state of cellular proteins. There is both direct and indirect evidence that reducing sumoylation of critical cell proteins may help overcome cellular antiviral defense mechanisms or promote a more favourable intracellular environment for viral reproduction (Wilson and Rangasamy, 2001). SUMO appears to facilitate viral infection of cells, making it a possible target for antiviral therapies (Boggio and Chiocca, 2006). As sumoylation is a tetra-step reaction, viral proteins may inhibit the conjugation at multiple sites, including interference with E1–SUMO thioester formation, transfer of SUMO from E1 to E2 or transfer of SUMO from E2 to substrate (Boggio and Chiocca, 2006). For example, Gam1 binds to the E1 heterodimer and inhibits its function, resulting in a complete block of the sumoylation pathway both in vivo and in vitro (Boggio et al., 2004).

In recent years a plethora of reports has been published concerning various viruses and their interference with the host cell sumoylation machinery. Among the DNA viruses, all of the known sumoylated viral proteins are immediate-early or early nuclear proteins, as observed for the herpes simplex virus (HSV) immediate-early protein ICP0 (Parkinson and Everett, 2000), human cytomegalovirus (HCMV) immediate-early 1 and 2 proteins (IE1 and IE2) (Müller and Dejean, 1999), Kaposi's sarcoma-associated herpesvirus (KSHV) K-bZIP (Izumiya et al., 2005), Epstein-Barr virus (EBV) Zta, Rta and BMRF1 (Adamson and Kenny, 2001; Chang et al., 2004), and human herpes virus-6 (HHV6)-IE1 (Gravel et al., 2004). In both adenovirus type 5 and papillomavirus (PV), sumoylation is important for nuclear targeting of their early proteins (Rangasamy and Wilson, 2000). In the past two years, it was found that viral Gag capsid proteins of Moloney murine leukemia virus (MuLV) and HIV type 1 (HIV-1), as well as HIV-1 regulatory proteins Tet and Rev, are modified by SUMO

(Col et al., 2005; Gurer et al., 2005; Roisin et al., 2004; Yueh et al., 2006). The poxvirus vaccinia (VV) provides the first case of a DNA virus for which sumoylation is a prerequisite for its localization to cytoplasmic entities (Palacios et al., 2005). In our study, SARS-CoV N protein provides the first evidence that a coronavirus structural protein undergoes sumoylation, and this modification might play an important regulatory role in the SARS-CoV replication cycles (Li et al., 2005a).

1.3. Viruses and the Cell Cycle

1.3.1. Cell cycle control

The cell cycle is comprised of four phases: G_1 (Gap 1), S, G_2 (Gap 2) and M (Fig. 1.6). In the presence of inhibitory signals, many cells may enter a prolonged, quiescent state called G_0 . Under favorable conditions, cells may re-enter the cell cycle and initiate a new round of DNA synthesis. S phase is a stage of DNA replication and chromosome duplication. The M phase is made up of mitosis and cytokinesis. Chromosome segregation and cell division occur during this phase (Murray and Hunt, 1993; Nurse, 2004).

Progression of the cell cycle is triggered by the activation of a series of cyclin-dependent kinase (Cdks), which form complexes with cyclins, and are regulated by the availability of the cyclin subunit, changes in phosphorylation state, and association with cellular Cdk inhibitors (CKIs), whose expression is also tightly controlled (Morgan, 1995; Nurse, 2004; Sherr and Roberts, 1999) (Fig. 1.6). cyclin D/Cdk4 and cyclin D/Cdk6 initiate progression through G_1 by phosphorylating substrates, which eventually leads to the transcription activation of genes necessary for DNA synthesis and subsequent cell cycle progression; cyclin E/Cdk2 promotes the G_1 /S transition,

where levels peak at the restriction point; cyclin A/Cdk2 is important during S-phase progression; cyclin A/Cdk1 activity peaks during the G₂ phase; and cyclin B/Cdk1 promotes the G₂/S transition, as well as modulates mitotic exit (cytokinesis) (Murry, 2004; van den Heuvel and Harlow, 1993) (Fig. 1.6).

The control of cyclin expression is regulated at the transcriptional level, and is balanced by their degradation. The transcriptional regulation of these genes has been correlated with the E2F family of transcription factors, leading to a model in which E2F-containing complexes are critical to the cell proliferation.

In response to cellular stress signals, cells activate checkpoint pathways and subsequently delay the progression of cell cycle by inhibiting Cdk activity. Four major checkpoints are involved in DNA damage-induced cell cycle arrest: G₁/S checkpoint, replication checkpoint, G₂/M checkpoint, and mitosis checkpoint. These checkpoints may serve to maintain genomic stability, allow DNA damage repair, and ensure proper DNA replication and progression through mitosis.

1.3.2. RB phosphorylation is controlled in the cell cycle

A crucial substrate of the Cdks is the retinoblastoma tumor suppressor protein (RB), which functions as a signal transducer connecting the cell cycle clock with the transcriptional machinery. In its active hypophosphorylated state, RB is a transcriptional repressor when bound to the E2F family of transcription factors, and hyperphosphorylation of RB results in its inactivation and the release of E2F, allowing the transcription of genes important for DNA synthesis (Chellappan et al., 1991; DeCaprio et al., 1989; Dyson, 1998; Harbour and Dean, 2000; Weinberg, 1995). RB is unphosphorylated in the quiescent G₀ phase, while during G₁ phase, it is first hypophosphorylated by cyclin D/Cdk4/6 and sequentially inactivated by

hyperphosphorylation by cyclin E/Cdk2 (Lundberg and Weinberg, 1998). The hyperphosphorylated state is maintained till late M phase (Mittnacht, 1998; Xiao et al., 1996). However, cell checkpoint pathways may activate the RB protein to its hypophosphorylated form, leading to G₀/G₁, S, or G₂/M cell cycle arrest (Chew et al., 1998; Knudsen et al., 1998; Saudan et al., 2000; Zhang et al., 2000). In addition, the hypophosphorylated RB also regulates both p53-dependent and p53-independent apoptosis through an unknown mechanism (Sherr and McCormick, 2002; Wang, 1997). The importance of RB was further emphasized by the findings that RB phosphorylation would promote cell cycle progression as well (Malanchi et al., 2004).

The molecular basis for the RB-imposed cell cycle control, however, is still unclear. HDAC-Rb-hSWI/SNF and Rb-hSWI/SNF appear to maintain the order of cyclins E and A expression during the cell cycle, which in turn regulates exit from G₁ and from S phase, respectively (Zhang et al., 2000).

1.3.3. Cdk inhibitors (CKIs)

Activities of certain cyclin/Cdk complexes are regulated by Cdk inhibitors (CKIs), which can be grouped into two families (Morgan, 1995; Sherr and Roberts, 1999). The INK4 (Inhibitors of Cdk4) family includes p16^{INK4a}, p15^{INK4b}, p18^{INK4c}, and p19^{INK4d}. INK4 proteins exclusively associate with and inhibit D-type Cdk, and appear to play a role in cellular differentiation and tumor suppression (Roussel, 1999).

CKIs of the Cip/Kip family contain p21^{Cip1}, p27^{Kip1}, and p57^{Kip2}, which share a Cdk inhibition domain at the N-terminal regions and bind to and inhibit Cdk2/cyclin E, Cdk2/cyclinA, and, to a less extent, Cdk4/cyclin D and Cdk1/cyclin B (Nakayama, 1998; Sherr and Roberts, 1999). p53 exerts its anti-proliferative effect by activating p21 (el-Deiry et al., 1993), the first transcriptional target of p53 identified and which

plays important roles in regulating cell cycle progression or arrest (Niculescu, 1998; Harper et al., 1993; Harper et al. 1995). p21 overexpression has been seen to inhibit two critical checkpoints in the cell cycle, namely G₁ and G₂, through both p53-dependent and p53-independent pathways (Macleod et al., 1995). p21 also retards S phase progression primarily by inhibition of Cdk's (Ogryzko et al., 1997). Counterintuitive to the roles it plays in cell cycle arrest, p21 has also been implicated as a positive regulator of cell survival and a suppressor of apoptosis (Asada et al., 1999). p21 might inhibit the Cdk1 activity, whose aberrant activation induced apoptosis in a variety of cell types (Shi et al., 1994; Shimizu et al., 1995; Tan et al., 2002). Down-regulation of p21 was shown to contribute to apoptosis induced by HPV E6 in human mammary epithelial cells (Fan et al., 2005b).

1.3.4. The ubiquitin-proteasome pathway in cell cycle regulation

The ubiquitination-mediated proteasomal degradation system plays a vital role in controlling the levels of various cellular proteins and thus regulates a wide range of basic cellular processes such as cell cycle progression, signal transduction and apoptosis (Murray, 2004). Cyclin/Cdk complexes work hand-in-hand with proteolysis to provide the logical framework for cell cycle regulation (Koepp et al., 1999). Modulating the ubiquitination-dependent degradation is a major mechanism for cells to control p21 and p53 levels as well (Liu and Lozano, 2005; Yang et al., 2004a).

1.3.5. Manipulation of cell cycle progression by viruses and viral-encoded proteins

Many viruses have been shown to manipulate host cell cycle regulations in order to facilitate viral replication (Op De Beeck and Caillet-Fauquet, 1997; Schang,

2003; Swanton and Jones, 2001). Small DNA tumor viruses, such as simian virus 40 (DeCaprio et al., 1988; Lehman et al., 2000), adenovirus (Howe et al., 1990), human T-cell leukemia virus (Neuveut et al., 1998)), and human papillomavirus (Malanchi et al., 2004), encode proteins that stimulate host cell entry into the S phase of the cell cycle to support viral DNA replication. These viruses do not code for their own DNA polymerase or other accessory factors that support DNA replication. All of these oncoproteins exhibit binding activities to RB, and this binding may prematurely induce cells into the S phase by disrupting RB-E2F complexes.

Viruses also regulate the cell cycle by blocking the progression at a certain stage. Virus-induced cell cycle arrest may create a more favorable environment for its successful propagation. Many viruses, such as human immunodeficiency virus type 1 (Goh et al., 1998; Poon et al., 1998), herpesviruses (Flemington, 2001), the paramyxovirus simian virus 5 (Lin and Lamb, 2000), measles virus (McChesney et al., 1988; Naniche et al., 1999), coxsackievirus (Luo et al., 2003), and human cytomegalovirus (Lu and Shenk, 1996), maximize virus production by preventing cell proliferation and progression of the cell cycle. Various proteins of hepatitis C virus have the potential to modulate the normal regulation of the cell cycle as well (Arima et al., 2001; Honda et al., 2000). Specifically, G₁/S arrest was reported to be induced by Simian Immunodeficiency Virus Nef Protein (Ndolo et al., 2002) and Kaposi's Sarcoma-Associated Herpesvirus K-bZIP (Izumiya et al., 2003), accompanied by an upregulation of CKIs p21 and p27. G₂ arrest has been shown to be a feature of several viral proteins. These include the human papillomaviruses (HPV) E2 protein (Fournier et al., 1999), the human immunodeficiency virus Vpr protein (He et al., 1995; Re et al., 1995; Rogel et al., 1995), and the reovirus δ 1s protein (Poggioli et al., 2001). Adeno-associated virus Rep78 protein (Saudan et al., 2000; Berthet et al., 2005), aleutian

mink disease parvovirus (Oleksiewicz and Alexandersen, 1997), polyoma viruses (Dahl et al., 2005), and Epstein-Barr Virus (Kudoh et al., 2005) have been shown to cause cell cycle arrest at the S phase.

A number of reports have highlighted the cell cycle perturbation properties of coronaviruses and their encoded proteins. MHV and its nonstructural protein p28 were shown to induce G₀/G₁ arrest (Chen and Makino, 2004; Chen et al., 2004a). The nucleocapsid protein of SARS-CoV blocks S-phase progression in mammalian cells by inhibiting the activity of cyclin-Cdk complex (Surjit et al., 2006). SARS-CoV infection increased the number of hepatocytes undergoing mitosis (Chau et al., 2004). Furthermore, SARS-CoV 3b and 7a proteins arrest cell cycle at the G₀/G₁ phase (Yuan et al., 2005; Yuan et al., 2006b). Recently, there was a report that infection of Vero cells with IBV induced G₂/M cell cycle arrest (Dove et al., 2006).

1.4. Viruses and Apoptosis

1.4.1. Cell cycle arrest versus apoptosis: crosstalk

Crosstalk exists between cell cycle and apoptosis (Gil-Gomez et al., 1998; King and Cidlowski, 1998). Apoptosis is sometimes an end point of stalled cell cycle progression, but in other cases, it appears to require smooth progression through the cell cycle (Santiago-Walker et al., 2005; Zhu and Anasetti, 1995).

It has been reported that apoptosis is frequently associated with the G₁ phase of the cell cycle (King and Cidlowski, 1998). Nevertheless, arrest at either late G₁, or S, or G₂/M phase may accelerate or potentiate apoptosis, especially in the absence of wild-type p53 (Meikrantz et al., 1994).

Such a crosstalk is also a prevalent phenomenon in virus-infected cells. Apoptosis is a consequence of the S-phase arrest imposed by IFN- β in human papilloma virus-infected cervical carcinoma cell line ME-180. The cell cycle arrest and apoptosis were shown to be independent of p53, but the apoptosis was mediated by the tumor necrosis factor-related apoptosis-inducing ligand (TRAIL) in a manner dependent on the S-phase deregulation (Vannucchi et al., 2005). HIV Vpr inhibits cell proliferation by arresting the cell cycle at the G₂ phase, followed by apoptosis (Stewart et al., 1997). However, C81, a carboxy-terminally truncated form of Vpr induces apoptosis via G₁ arrest of the cell cycle (Nishizawa et al., 2000).

1.4.2. Role of viral proteins in the induction and suppression of apoptosis

Apoptosis constitutes part of the host cell defense against viral infection (Hay and Kannourakis, 2002; Benedict et al., 2002). Viral infection may activate a variety of signal transduction pathways that lead to either induction or suppression of apoptosis of infected cells (Fig. 1.7).

A good few of viral gene products have been found to regulate apoptosis (Roulston et al., 1999; Teodoro and Branton, 1997). Apoptosis induction can be seen as a mechanism for releasing progeny viruses while limiting the inflammatory and immune responses or as an innate immune response of the cell to viral infection. Viruses trigger the pro-apoptotic stimuli in different ways. In most cases, certain viral proteins can activate some cellular mediators of apoptosis, such as the dsRNA-dependent protein kinase (PKR) (Der et al., 1997). Virus infection may also trigger apoptotic pathways through the activation of cell surface death receptors. Recently, several viruses, including Japanese encephalitis virus (Su et al., 2002), bovine diarrhea virus (Jordan et al., 2002), and Tula virus (Li et al., 2005c) have been shown

to induce apoptosis mediated by ER stress (He, 2006). Undoubtly, ER stress-mediated apoptosis induced by virus would be related to the pathogenesis of viral infection.

Since the induction of early apoptosis after infection would potentially limit virus production and reduce the spread of progeny virus in the host, most viruses have evolved strategies to disrupt early apoptosis. These include the suppression of IFN action, as in the case of human adenovirus and HPV (Barber, 2001). IFNs play a critical role in mounting innate response to viral infections, and, in some circumstances, may promote apoptosis of virus-infected cells. Viruses can also disrupt apoptosis by inactivating p53. For example, the SV40 large T antigen binds to p53 and sequesters it in an inactive complex. HPV E6, adenovirus E1B-55K, and E4orf6 promote ubiquitination and degradation of p53. Additionally, HBV pX protein complexes with p53 and inhibits p53-mediated transcriptional activation as well as p53-dependent apoptosis (Benedict et al., 2002).

Viruses are also known to encode antiapoptotic Bcl-2 homologs to prevent the premature death of the infected host cell to sustain virus replication (Cuconati and White, 2002). A pertinent example is adenovirus E1B-19K, which is similar both in sequence and function to Bcl-2. Human herpesviruses, EBV, KSHV, and mouse γ -herpesvirus MHV-68, however, encode Bcl-2 orthologs to block apoptosis. Some other viral proteins such as HTLV-1 Tax protein and HIV-1 Nef inhibit apoptosis by modulating Bcl-2 family members at the transcriptional level or via post-translational modification (Benedict et al., 2002). In addition, poxviruses, myxoma virus, human CMV, and adenovirus can specifically target members of TNF receptor (TNFR), which are potent inducers of apoptosis, to block apoptosis for their own advantage (Benedict et al., 2002).

1.4.3. Coronavirus-induced apoptosis

Various coronaviruses and their encoded proteins have been reported to be inducers of apoptosis. Eleouet et al. demonstrated that infection of TGEV induces caspase-dependent apoptosis via cellular oxidative stress (Eleouet et al., 1998; Eleouet et al., 2000). IBV also induces caspase-dependent apoptosis in cultured cells, probably mediated by a 58-kDa protein encoded by IBV ORF 1b (Liu et al., 2001). Apoptosis induced by MHV (Liu et al., 2003; Liu et al., 2006) and its E protein (An et al., 1999) has also been characterized, while it is not clear whether the apoptosis is caspase-dependent or not. Chen and Makino reported that MHV-induced apoptosis involves a mitochondria-mediated pathway and its downstream caspase-8 activation and bid cleavage (Chen and Makino, 2002). Interestingly, diverse proteins of SARS-CoV (Chau et al., 2004), including N (Surjit et al., 2004a), E (Yang et al., 2005), S (Chow et al., 2005), 3C-like protease (Lin et al., 2006), 3a (Law et al., 2005), 3b (Yuan et al., 2005), and 7a (Tan et al., 2004) have been shown to have pro-apoptotic properties, which may be responsible for pathogenesis of SARS.

1.5. Objectives of Dissertation Study

The major goal of the work in this dissertation is to elucidate coronavirus-host interactions, which may constitute the basis of viral pathogenesis, and provide potential antiviral targets. The approaches involved two distinct avenues of research. The first was discovery of SARS-CoV N protein-interacting partners through biochemical characterizations and the yeast two-hybrid screen: the results from this part of work are presented in chapter 3. By analogy with other coronavirus N proteins, SARS-CoV N protein expression involves complex transcriptional, translational and posttranslational regulatory mechanisms. However, these complicated characteristics

of the N protein remain to be dissected. We attempted to screen host factors that may interact with SARS-CoV N protein, and identified human Ubc9, an E2 SUMO-conjugating enzyme. We next found that SARS-CoV N protein is a sumoylated protein, mediated by Ubc9. The roles of N protein sumoylation in promoting its homo-oligomerization, changing its subcellular localization, and modulating its interference of host cell division were subsequently characterized.

Two major biological events, cell cycle arrest and apoptosis, have been previously described in coronavirus-infected cells. However, crucial details remain to be clarified, for examples, how exactly these two events are brought out, and how the manipulation of host-cell functions may influence coronavirus replication. In the second part of this dissertation study, using IBV as a model, we demonstrated that IBV infection imposes a growth-inhibitory effect on cultured cells by inducing cell cycle arrest at both S and G₂/M phases. To source the molecular basis of IBV-induced cell cycle arrest, we systematically analyzed the regulation of host cell gene expression imposed by IBV infection, particularly roles of cellular growth regulatory proteins p53 and RB. We also investigated the effect of cell cycle arrest on IBV replication. As our lab has characterized the caspase-dependent apoptosis induced following IBV infection in cultured cells, another objective of the work described in this dissertation was to investigate whether p53 is involved in IBV-mediated apoptosis, as well as cell cycle arrest described previously. To facilitate the work, both wild-type p53 containing Vero cells and p53-null H1299 cells were used. Results of this study are described in chapter 4.

Figures and Tables

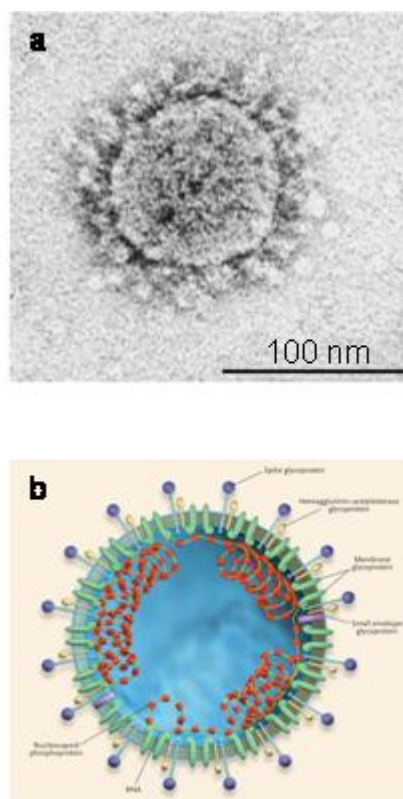


Fig. 1.1. Structure of the coronavirus virion. a| Negative-stain electron micrograph of SARS-CoV that was cultivated in Vero cells (Ksiazek et al., 2003). b| A schematic diagram of the coronavirus virion (Holmes, 2003a).

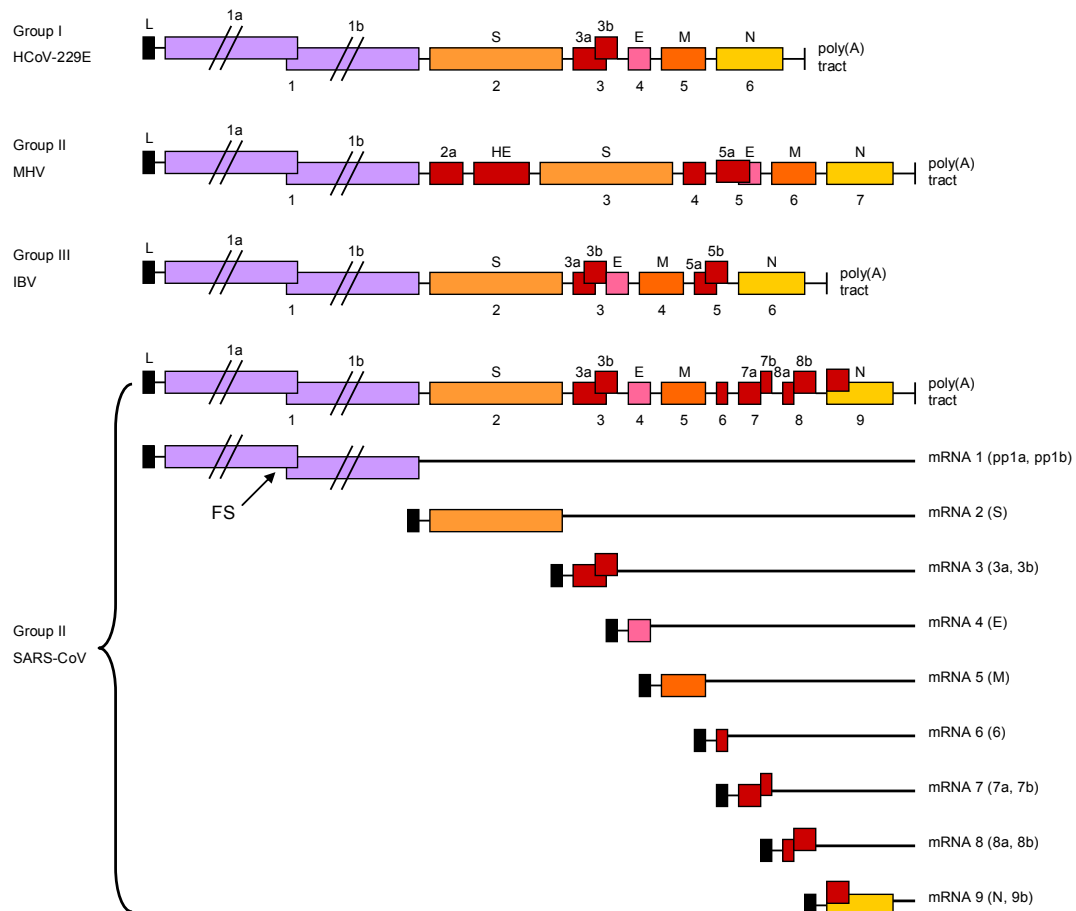


Fig. 1.2. Comparison of coronavirus genome organization. Genome organization of coronavirus representatives of group 1 (HCoV-229E), group 2 (MHV; SARS-CoV) and group 3 (IBV) are shown. All genes, except for gene 1 (pp1ab) are drawn approximately to scale. Red boxes represent the accessory genes. The positions of the leader sequence (L) and poly(A) tract are indicated. The SARS-CoV ORFs, frameshift (FS), and genomic and subgenomic mRNAs, are also shown. Also indicated are the viral proteins predicted to be expressed from a given mRNA's 'unique' region. Modified from Stadler et al., 2003; Thiel et al., 2003.

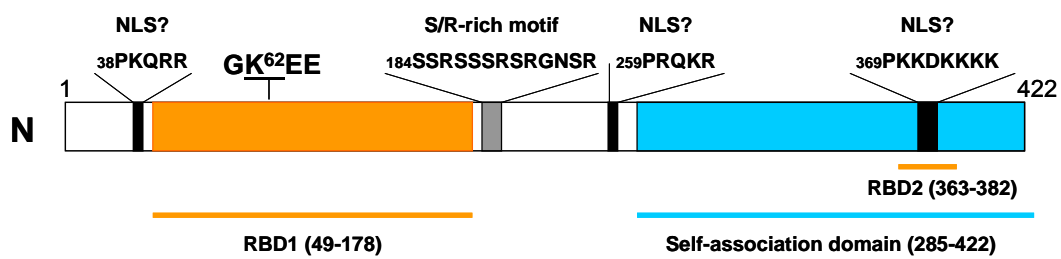


Fig. 1.3. Schematic representation of the SARS-CoV N protein, showing the SUMO-1 conjugation site (K⁶²), three putative nucleolar localization signals, the S/R-rich motif, the RNA-binding domains (RBD) and self-association domain.

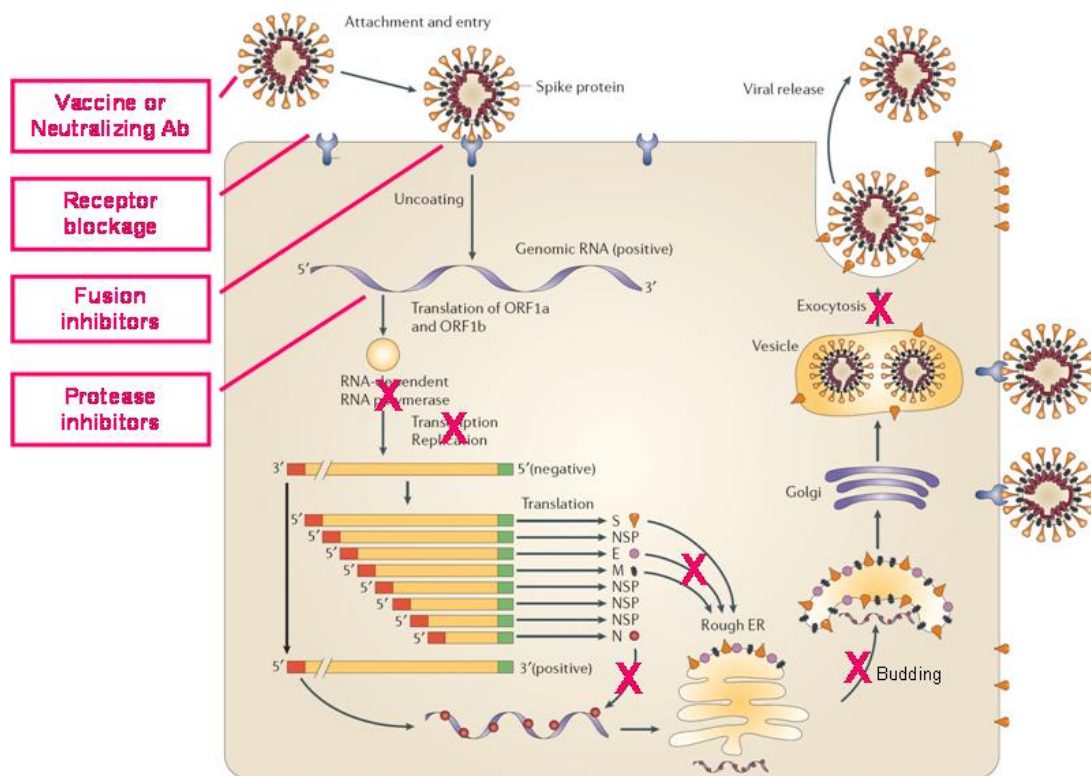


Fig. 1.4. Replication of coronavirus and steps in coronavirus life cycle that are potential targets for antiviral drugs and vaccines. Coronavirus binds to the host-cell receptor through interaction of the S (spike) glycoprotein. Virus entry into the host cell can occur through fusion with the surface of the host cell, with the subsequent release of the genomic RNA into the cytoplasm. Translation of the positive-strand genomic RNA gives rise to a large polyprotein that undergoes proteolytic processing to generate an RNA-dependent RNA polymerase. Through the action of the RNA polymerase, a full-length, antisense negative-strand template is generated. Subgenomic mRNAs are synthesized, presumably from subgenomic negative-strand templates. Translation of subgenomic mRNAs gives rise to structural viral proteins. Virus assembly occurs within vesicles, followed by virus release by fusion of virion-containing vesicles with the plasma membrane. The S glycoprotein is a good candidate because neutralizing antibodies are directed against S. Blockade of the specific virus receptor on the surface of the host cell by monoclonal antibodies or other ligands can prevent virus entry. The large polyprotein of the replicase protein must be cleaved into functional units by virus-encoded proteinases. Protease inhibitors may block virus replication. The assembly of polymerase complex, coronavirus transcription, translation, budding and release are also potential targets for drug development. E, envelope protein; ER, endoplasmic reticulum; M, membrane protein; N, nucleocapsid protein; ORF, open reading frame. Modified from Bergmann et al., 2006.

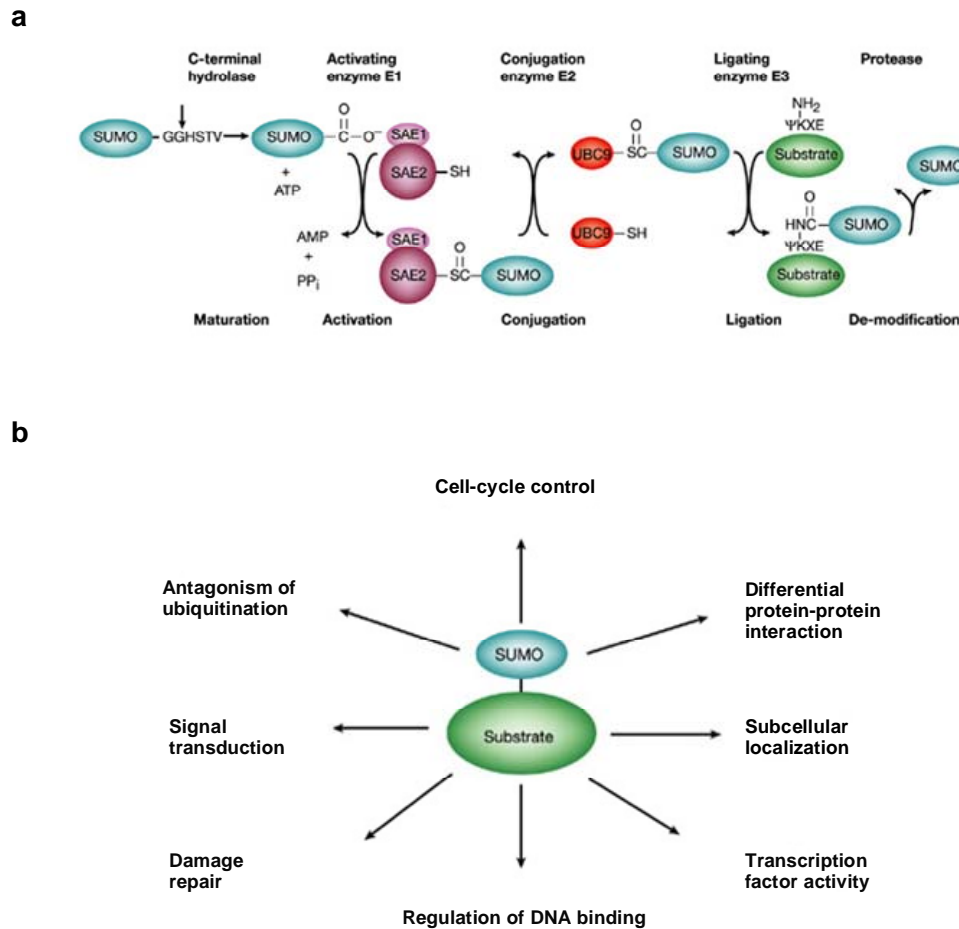


Fig. 1.5. Specificity in SUMO signaling and conjugation. a| The SUMO pathway. SUMO is synthesized as a precursor and processed by hydrolases to make the carboxy-terminal double-glycine motif available for conjugation. It is subsequently conjugated to proteins by means of E1 activating (SAE1/SAE2), E2 conjugating (Ubc9) and E3 ligating enzymes. The E3-like proteins might serve to increase the affinity between Ubc9 and the substrates by bringing them into close proximity in catalytically favourable orientations, allowing sumoylation to occur at a maximal rate. The disruption of the resulting isopeptide bond requires a desumoylating enzyme. b| Diverse consequences of SUMO modification. Modified from Verger et al., 2003.

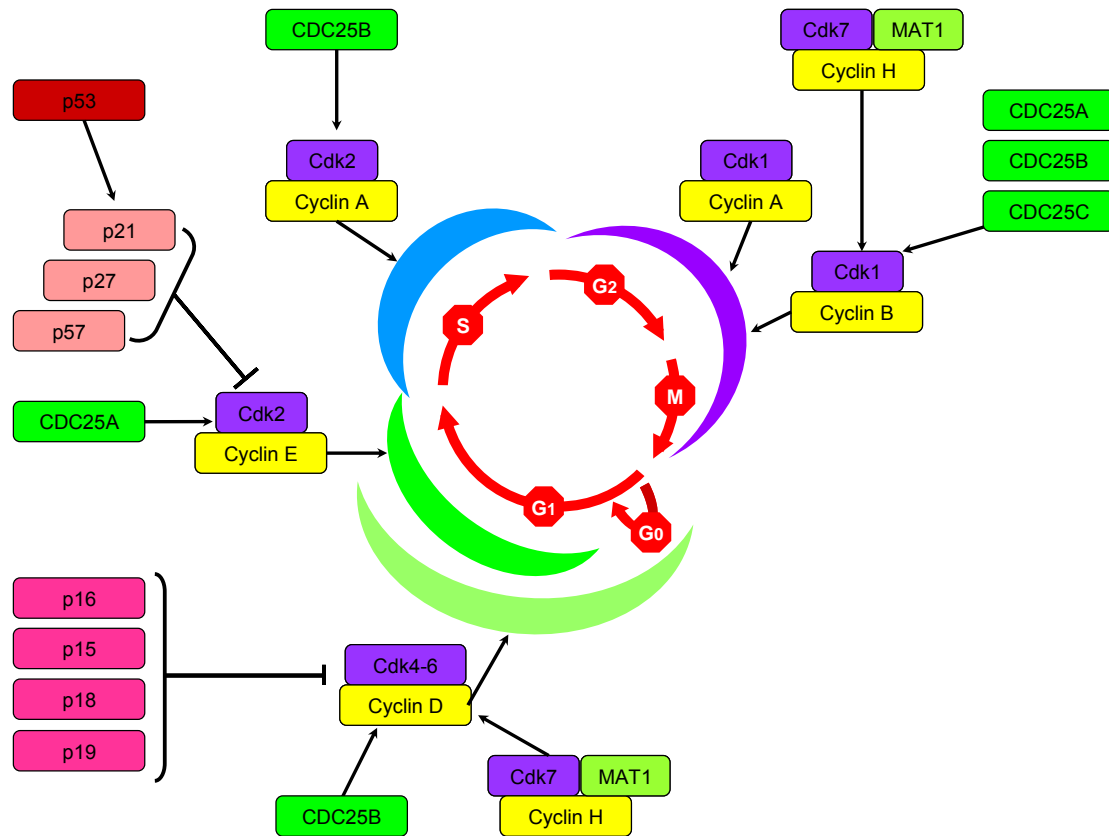


Fig. 1.6. The cell cycle control. The cell cycle is comprised of four phases: G1, S, G2 and M. Progression of the cell cycle is triggered by the activation of a series of cyclin-dependent kinases (Cdks), which form complexes with corresponding cyclins, and are regulated by the availability of the cyclin subunit, changes in phosphorylation state, and association with cellular Cdk inhibitors (CKIs), such as p21, p27, p57, and p16, whose expression is also tightly controlled.

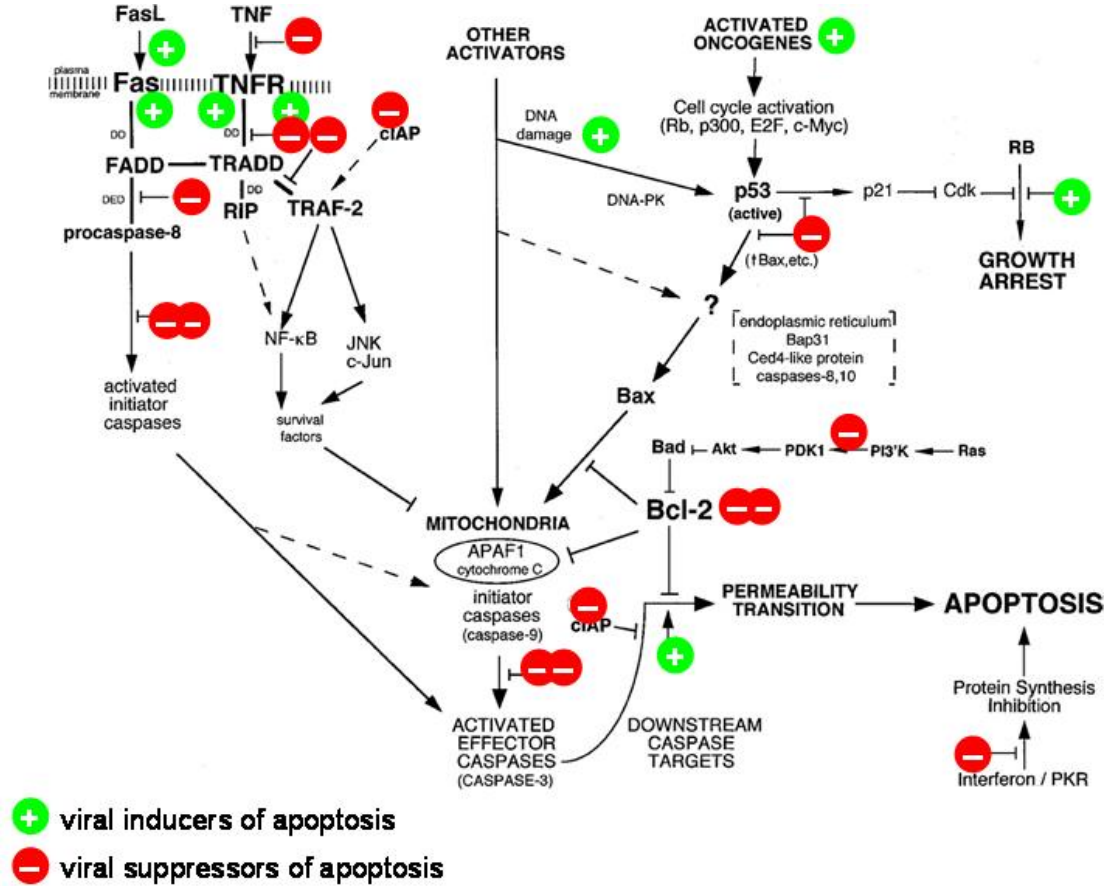


Fig. 1.7. Roles of viral proteins in the induction and suppression of apoptosis.

Modified from Roulston et al., 1999.

Table 1.1. Coronavirus groups, species, hosts, and principal associated diseases.

Antigenic group	Virus	Host	Diseases
I	Human coronavirus (HCoV)-229E	Human	Respiratory infection
	Transmissible gastroenteritis virus (TGEV)	Pig	Enteritis
	Porcine epidemic diarrhea virus (PEDV)	Pig	Enteritis
	Porcine respiratory coronavirus (PRCoV)	Pig	Respiratory infection
	Canine coronavirus (CCoV)	Dog	Enteritis
	Feline coronavirus (FCoV)	Cat	Respiratory infection / enteritis / peritonitis
	Human coronavirus (HCoV)-NL63	Human	Respiratory infection
	Bat coronavirus strain 61 (Bat-CoV-61)	Bat	?
	Bat coronavirus strain HKU2 (Bat-CoV-HKU2)	Bat	?
	Mouse hepatitis virus (MHV)	Mouse	Respiratory infection / enteritis / hepatitis / encephalitis
II	Bovine coronavirus (BCoV)	Cow	Respiratory infection / enteritis
	Rat coronavirus (RCoV)	Rat	Respiratory infection
	Hemagglutinating encephalomyelitis virus (HEV)	Pig	Enteritis
	Human coronavirus (HCoV)-OC43	Human	Respiratory infection
	SARS coronavirus (SARS-CoV)	Human	Respiratory infection / enteritis
	Human coronavirus (HCoV)-HKU1	Human	Respiratory infection
	Bat SARS coronavirus (Bat-SARS-CoV)	Bat	?
	Infectious bronchitis virus (IBV)	Chicken	Respiratory infection / enteritis
III	Turkey coronavirus (TCoV)	Turkey	Enteritis

Table 1.2. Summary of SARS-CoV proteins.

Protein	ORF	Protein Size (aa)	Main functions	Structure available?	Key references
<i>Main structural proteins</i>					
Spike (S) protein	ORF2	1255	Receptor binding; Inducing neutralizing antibodies	Yes (S protein fusion core)	Bartlam et al., 2005; Masters, 2006
Envelope (E) protein	ORF4	76	Viral assembly; Induce apoptosis; Viroporin activity	No	Liao et al., 2006; Masters, 2006
Membrane (M) protein	ORF5	221	Viral assembly	No	Masters, 2006
Nucleocapsid (N) protein	ORF9a	422	RNA binding; Form RNP; Disrupt host cell cytokinesis; Retard S-phase progression; Induce apoptosis; Stimulate humoral cellular response	Yes (N-terminal RBD and dimerization domain)	Huang et al., 2004a; Kim et al., 2004; Li et al., 2005a; Luo et al., 2006; Surjit et al., 2006; Surjit et al., 2006a; Yu et al., 2006
<i>Nonstructural proteins (NSPs)</i>					
NSP1	ORF1a	180	Suppresses host gene expression; Might facilitate SARS-CoV replication or block immune responses; Important in CCL5, CXCL10 and CCL3 expression via the activation of NF- κ B	Yes	Almeida et al., 2007; Connor and Roper, 2007; Kamitani et al., 2006; Law et al., 2006
NSP2	ORF1a	638	Dispensable for viral replication	No	Graham et al., 2005
NSP3	ORF1a	1922	PLP; ADP-ribose-1"-phosphatase	Yes	Ratia et al., 2006; Saikatendu et al., 2005
NSP4	ORF1a	500	Component of replicase-transcriptase complex	No	Tan et al., 2005
NSP5	ORF1a	306	3CL ^{pro}	Yes	Anand et al., 2003
NSP6	ORF1a	290	?	No	/
NSP7	ORF1a	83	NSP7-NSP8 hexadecamer	Yes	Peti et al., 2005; Zhai et al., 2005
NSP8	ORF1a	198	Second RdRp; NSP7-NSP8 hexadecamer	Yes	Imbert et al., 2006; Zhai et al., 2005
NSP9	ORF1a	113	ssRNA binding	Yes	Egloff et al., 2004; Sutton et al., 2004

NSP10	ORF1a	139	GFL; nucleic acid-binding; Transcription factor for coronavirus replication/transcription	Yes	Joseph et al., 2006; Su et al., 2006
NSP11	ORF1a	13	?	No	/
NSP12	ORF1b	932	RdRp	No	Xu et al., 2003
NSP13	ORF1b	601	Helicase	No	Ivanov et al., 2004
NSP14	ORF1b	527	3'-to-5' Exonuclease (ExoN homologue)	No	Minskaia et al., 2006; Snijder et al., 2003
NSP15	ORF1b	346	Endoribonuclease (XendoU homologue)	Yes	Bhardwaj et al., 2004; Ricagno et al., 2006
NSP16	ORF1b	298	2'-O-MT	No	von Grotthuss et al., 2003
<i>Accessory proteins</i>					
3a	ORF3a	274	A minor structural protein; Induces apoptosis; Ion channel	No	Ito et al., 2005; Law et al., 2005; Lu et al., 2006; Shen et al., 2005
3b	ORF3b	154	Interferon antagonist; Induce cell cycle arrest and apoptosis	No	Kopecky-Bromberg et al., 2007; Yuan et al., 2005
6	ORF6	63	Interferon antagonist; Enhance MHV virulence; Enhance DNA synthesis	No	Geng et al., 2005; Kopecky-Bromberg et al., 2007; Pewe et al., 2005
7a	ORF7a	122	A minor structural protein; Induces apoptosis; Inhibits cellular protein synthesis; Induce cell cycle arrest; Interacts with host SGT	Yes	Fielding et al., 2006; Huang et al., 2006; Kopecky-Bromberg et al., 2006; Tan et al., 2004; Yuan et al., 2006b
7b	ORF7b	44	?	No	/
8a	ORF8a	39	?	No	/
8b	ORF8b	84	Down-regulate E protein expression	No	Keng et al., 2006
9b	ORF9b	98	Lipid-binding	Yes	Meier et al., 2006

Chapter 2

Materials and Methods

2.1. Materials

2.1.1. Viruses

IBV

The Beaudette strain of IBV (ATCC VR-22) was obtained from the American Type Culture Collection (ATCC) and was adapted to Vero and H1299 cells as previously described (Liu et al., 2001).

Vaccinia virus recombinants

The recombinant vaccinia virus, vTF7-3 (Fuerst et al., 1986), expresses the bacteriophage T7 RNA polymerase. Briefly, DNA coding for bacteriophage T7 RNA polymerase was ligated to a vaccinia virus transcriptional promoter and integrated within the vaccinia virus genome. The recombinant vaccinia virus retained infectivity and could stably express T7 RNA polymerase in mammalian cells. When cells were infected with the recombinant vaccinia virus and transfected with plasmids containing the target gene under a T7 promoter, the target gene could be highly expressed. The recombinant vaccinia virus was propagated in HeLa cells.

2.1.2. Cells

The human epithelial cervical adenocarcinoma cell line HeLa, African green monkey kidney cell line Vero, and human lung carcinoma cell line H1299 were obtained from ATCC and cultured in complete Dulbecco's modified Eagle's medium (DMEM) or RPMI 1640 supplemented with 10% newborn calf serum and 1% penicillin/streptomycin and maintained at 37°C in humidified 5% CO₂.

2.1.3. Bacteria strains

Escherichia coli (*E. coli*) strain DH5 α (Invitrogen) was used in plasmid cloning and amplification unless otherwise noted. Strain BL21 (DE3) (Novagen) was specifically used to express GST fusion proteins since it lacks *lon* and *ompT* proteases and allows for IPTG-inducible expression of GST fusion proteins from pGEX plasmids.

2.1.4. Yeast

Saccharomyces cerevisiae Y187 and AH109 were used in yeast two-hybrid screen.

2.1.5. Chemicals, radiochemicals and reagents

The following is a list of chemicals, radiochemicals and reagents used in this study, and their suppliers.

Agarose	Bio-Rad
Ampicillin	Sigma-Aldrich
Carboxymethyl-cellulose (CMC)	Merck
Colchicine	Sigma-Aldrich
Crystal violet	BDH Chemicals
Cytomatin fluorescent mounting medium	DAKO
DMEM	Gibco
DMSO	Sigma-Aldrich
Effectene transfection reagent	Qiagen
Enhanced chemiluminescence (ECL) kit	Amersham
Ethidium bromide	Sigma-Aldrich
Glutathione-sepharose 4B	Amersham
Hoechst 33258	Fisher Scientific
Iodoacetamide (IAA)	Sigma-Aldrich

IPTG (isopropanol- β -D-thiogalactoside)	Calbiochem
Kanamycin	Sigma-Aldrich
Lactacystin	Merck
Methotrexate	Sigma-Aldrich
Molecular weight standards	
100bp DNA ladder	New England Biolabs
1kb DNA ladder	New England Biolabs
Precision plus protein standards	Bio-Rad
Precision plus protein prestained standards	Bio-Rad
Low-range rainbow molecular weight markers	Amersham
Mounting medium	Dako
<i>N</i> -ethylmaleimide (NEM)	Sigma-Aldrich
Newborn calf serum	Sterile
NIP-leu-leu-leu-vinylsulfone (NLVS)	Merck
Penicillin/streptomycin	Invitrogen
Propidium iodide	Sigma-Aldrich
Protease inhibitor cocktail	Sigma-Aldrich
Protein-A agarose	KPL
Q-VD-OPh, Non-O-methylated	Merck
RNase	Invitrogen
RPMI	Hyclone
³⁵ S-methionine (1000Ci/mmol) at 10 μ Ci/ μ l	Amersham
SuperSignal west pico chemiluminescence substrate kit	Pierce
Trypsin-EDTA	Gibco
Tris-saturated phenol	Gibco

2.1.6. Enzymes

Restriction endonucleases and modifying enzymes, unless otherwise mentioned, were purchased from New England Biolabs.

2.1.7. Antibodies

Flag M2 monoclonal antibody (Stratagene): Raised in mouse against a peptide containing the flag tag MDWKDDDDK. Used dilutions were 1:2000 for Western blotting and immunoprecipitation, and 1:200 for immunofluorescence in this study.

c-Myc monoclonal antibody (Clontech): Raised against a peptide containing a c-Myc tag. Used dilution was 1:2000 for Western blotting and immunoprecipitation in this study.

Penta-His biotin conjugate monoclonal antibody (Qiagen): For sensitive detection of 6×His-tagged proteins with HHHHHH epitopes. Used dilution was 1:1000 for immunoprecipitation in this study.

GMP-1 (SUMO-1) monoclonal antibody (Zymed): Specifically detects the unconjugated form of GMP-1 (SUMO-1), as well as proteins covalently ligated to GMP-1 (SUMO-1). Used dilution was 1:1000 for Western blotting and immunoprecipitation in this study.

SARS-CoV N polyclonal antibody (IMCB, Singapore): Raised in rabbit using the full-length SARS-CoV N protein as the antigen. Used dilutions were 1:2000 for immunoprecipitation and Western blotting, and 1:200 for immunofluorescence.

IBV N polyclonal antibody (IMCB, Singapore): Raised in rabbit using the full-length IBV N protein as the antigen. Used dilution was 1:2000 for Western blotting.

IBV S polyclonal antibody (IMCB, Singapore): Raised in rabbit using the full-length IBV S protein as the antigen. Used dilutions were 1:2000 for Western blotting.

Fibrillarin (H-140) rabbit polyclonal antibody (Santa Cruz): Fibrillarin is a widely occurring, basic, nonhistone nucleolar protein that localizes exclusively in the fibrillar region of the nucleolus, including both the dense fibrillar and fibrillar center regions. Used dilutions were 1:1000 for Western blotting, and 1:100 for immunofluorescence.

Cyclin A (H-432) rabbit polyclonal antibody (Santa Cruz): Raised against amino acids 1-432 representing full length cyclin A of human origin. Used dilution was 1:500 for Western blotting.

Cyclin E (E-4) mouse monoclonal antibody (Santa Cruz): Raised against amino acids 1-145 of cyclin E of human origin. Used dilution was 1:500 for Western blotting.

Cdc2 p34 (17) mouse monoclonal antibody (Santa Cruz): Raised against amino acids 224-230, mapping with a central region of Cdc2 of human origin. Used dilution was 1:500 for Western blotting.

Cdk2 (D-12) mouse monoclonal antibody (Santa Cruz): Raised against amino acids 1-298 representing full length Cdk2 of human origin. Used dilution was 1:500 for Western blotting.

p21 (F-5) mouse monoclonal antibody (Santa Cruz): Raised against amino acids 1-159 representing full length p21 of mouse origin. Used dilution was 1:500 for Western blotting.

p27 (F-8) mouse monoclonal antibody (Santa Cruz): Raised against amino acids 1-197 representing full length p27 of mouse origin. Used dilution was 1:500 for Western blotting.

Ub (FL-76) rabbit polyclonal antibody (Santa Cruz): Raised against amino acids 1-76 representing full length Ub of human origin. Used dilution was 1:1000 for Western blotting.

β -tubulin (H-235) rabbit polyclonal antibody (Santa Cruz): Raised against amino acids 210-444 mapping at the C-terminus of β -tubulin of human origin. Used dilution was 1:1000 for Western blotting.

Cyclin B1 (V152) mouse monoclonal antibody (Cell Signaling Technology): Produced by immunizing mice with a peptide corresponding to a sequence for hamster cyclin B1, and detects endogenous levels of cyclin B1 independent of phosphorylation. Used dilution was 1:2000 for Western blotting.

Cyclin D1 (DCS6) mouse monoclonal antibody (Cell Signaling Technology): Produced by immunizing mice with a recombinant cyclin D1 of human origin and maps to amino acids 151-170. This antibody detects endogenous levels of cyclin D1, and does not cross-react with cyclin D2 or D3. Used dilution was 1:2000 for Western blotting.

PE-conjugated mouse anti-human Rb monoclonal antibody (G3-245) (BD Pharmingen): Raised against amino acids 300-380 of the human retinoblastoma protein. A Trp-E-Rb fusion protein was used as the immunogen. Used dilution was 1:1000 for Western blotting.

p53 (Ab6) mouse monoclonal antibody (Calbiochem): Used dilution was 1:1000 for Western blotting.

Polyclonal Goat anti-Rabbit immunoglobulins HRP (DAKO): For Western blotting as the secondary antibody. Used dilution was 1:2000.

Polyclonal rabbit anti-Mouse immunoglobulins HRP (DAKO): For Western blotting as the secondary antibody. Used dilution was 1:1000.

Polyclonal Goat anti-Mouse immunoglobulins FITC (DAKO): For immunofluorescence as the secondary antibody. Used dilution was 1:100.

Polyclonal Swine anti-Rabbit immunoglobulins FITC (DAKO): For immunofluorescence as the secondary antibody. Used dilution was 1:100.

Polyclonal Rabbit anti-Mouse immunoglobulins TRITC (DAKO): For immunofluorescence as the secondary antibody. Used dilution was 1:100.

Polyclonal Swine anti-Rabbit immunoglobulins TRITC (DAKO): For immunofluorescence as the secondary antibody. Used dilution was 1:100.

2.1.8. Vectors

pET-24a(+) (Novagen): pET-24a(+) carries an N-terminal T7-Tag sequence plus an optional C-terminal His-Tag sequence. The vector is Kanamycin-resistant for selection in *E. coli*.

pGEX (Pharmacia Biotech): A bacterial vector that permits inducible protein expression with IPTG, used to express GST-fused proteins. A multiple cloning site (MCS) is present downstream of the GST coding region. The vector carries the Amp^r for selection in *E. coli*.

pGBKT7 (Clontech): The pGBKT7 vector expresses proteins fused to amino acids 1–147 of the GAL4 DNA binding domain (DNA-BD). In yeast, fusion proteins are expressed at high levels from the constitutive ADH1 promoter (PADH1); transcription is terminated by the T7 and ADH1 transcription termination signals (TT7 & ADH1). pGBKT7 also contains the T7 promoter, a c-Myc epitope tag, and a

MCS. pGBKT7 replicates autonomously in both *E. coli* and *S. cerevisiae* from the pUC and 2 m ori, respectively. The vector carries the Kan^r for selection in *E. coli* and the TRP1 nutritional marker for selection in yeast.

pcDNA3.1(+) (Invitrogen): pcDNA3.1(+) is a 5.4 kb vector derived from pcDNA3 and designed for high-level stable and transient expression in mammalian hosts. The vectors contain the following elements: Human cytomegalovirus immediate-early (CMV) promoter for high-level expression in a wide range of mammalian cells; multiple cloning sites in the forward (+) and reverse (-) orientations to facilitate cloning; neomycin resistance gene for selection of stable cell lines; episomal replication in cells lines that are latently infected with SV40 or that express the SV40 large T antigen.

pEGFP-N1 (Clontech): pEGFP-N1 encodes a red-shifted variant of wild-type GFP which has been optimized for brighter fluorescence and higher expression in mammalian cells. The MCS in pEGFP-N1 is between the immediate early promoter of CMV (PCMV IE) and the EGFP coding sequences. Genes cloned into the MCS will be expressed as fusions to the N-terminus of EGFP if they are in the same reading frame as EGFP and there are no intervening stop codons. A neomycin-resistance cassette (Neo^r) allows stably transfected eukaryotic cells to be selected using G418. A bacterial promoter upstream of this cassette expresses kanamycin resistance in *E. coli*.

pKT0-Flag: pKT0 is obtained from Department of Pathology, University of Cambridge, UK. It is a mammalian vector with a T7 promoter. pKT0-Flag is derived

from pKT0 by inserting a flag-tag (MDWKDDDDK) sequence between the T7 promoter and the first MCS. The vector carries the Amp^r for selection in *E. coli*.

2.2. Methods

2.2.1. DNA manipulations

2.2.1.1. Construction of plasmids

Plasmid pcDNA3.1-N, which covers the SARS-CoV N sequence, was constructed by cloning an *EcoRI/NotI* digested PCR fragment into *EcoRI/NotI* digested pcDNA3.1(+). The PCR fragment was generated using primers (5'-CGGAATTCCGATGTCTGATAATGGACCC-3') and (5'-AATAAATAGCGGCCGCTGCCTGAGTTGAATC-3'). pFlag-N was created by cloning a *PstI/EcoRI* digested PCR fragment into *PstI/EcoRI* digested pKT0-Flag. The PCR fragment was generated using primers (5'-AACTGCAGCATGTCTGATAATGGACCCC-3') and (5'-CGGAATTCCGTTATGCCTGAGTTGAATCAGC-3'). Plasmid pEGFP-N was generated by cloning an *EcoRI*- and *BamHI*-digested PCR fragment into *EcoRI/BamHI* digested pEGFP-N1. The two primers used to generate the PCR fragments are (5'-CGGAATTCCGATGTCTGATAATGGACCC-3') and (5'-CGGGATCCCGTGCCTGAGTTGAATCAGC-3'). Plasmid pGEX-N was made by cloning a *BamHI*- and *EcoRI*-digested PCR fragment into *BamHI/EcoRI* digested pGEX-5X-1. The two primers used are (5'-CGGGATCCCGATGTCTGATAATGGACCC-3') and (5'-CGGAATTCTGCCTGAGTTGAATCAGC-3'). The K62A mutant was introduced by two rounds of PCR. All constructs were confirmed by automated nucleotide sequencing.

Human Ubc9 cDNA was inserted into pKT0-Flag at the PstI/EcoRI cloning sites. Primers used were (5'-AACTGCAGCATGTCTCGGGGATCGCCCTCAGC-3') and (5'-CGGAATTCCGTTATGAGGGCGCAAACCTTCTT-3').

SUMO-1 was amplified from human cDNA derived from HeLa cells by PCR with primers (5'-TATCGGATCCCATGTCTGACCAGGCAAAACC-3') and (5'-CGGATCCTCGAGCTAAACTGTTGAATGACCCCCCGT-3'). The purified PCR product was digested with *Bam*HI and *Xho*I and cloned into *Bam*HI/*Xho*I digested pcDNA3.1(+) to generate pcDNA3.1-SUMO-1. The construct was confirmed by automated nucleotide sequencing.

2.2.1.2. Cloning techniques

(1) Polymerase chain reaction (PCR)

Specific primers were designed manually and synthesized. The melting temperature (T_m value) of primers were calculated according to the following equation: $T_m (^{\circ}\text{C}) = 4 \times (\text{G}+\text{C}) + 2 \times (\text{A}+\text{T})$. Conventional PCR reactions were carried out in 200 μl thin-wall Gene-Amp tubes (Axygen) containing a 50 μl mixture of $1\times$ *Pfu* DNA polymerase reaction buffer (Stratagene), 0.125 mM each of the deoxynucleoside triphosphate (dNTPs) (dATP, dCTP, dGTP, and dTTP) (Gibco), 20 μM of both forward and reverse primers, 5 U of *Pfu* DNA polymerase (Stratagene) and 50 ng of DNA template. The reaction tubes were subjected to PCR thermal cycling in a Applied Biosystems DNA Thermal Cycler, by denaturing at 94 $^{\circ}\text{C}$ for 45 sec, annealing at X $^{\circ}\text{C}$ for 45 sec, and extension at 72 $^{\circ}\text{C}$ for Y min, for 30 amplification cycles. X and Y refer to values for annealing temperature and extension

time, adjusted according to the T_m of the primers employed and length of the PCR fragments amplified, respectively.

(2) Site-directed mutagenesis by two rounds of PCR

Two pairs of primers were designed: the first pair being the cloning primers (primers 1 and 2), were used to amplify the full-length fragment, while the second pair carried the respective mutations (primers 3 and 4). The first round of PCR was performed in 2 separated reactions. Each tube contains the appropriate DNA template and primer combinations of primer 1 / primer 4 or primer 3 / primer 2. The two PCR fragments were subjected to electrophoresis before they were gel-purified. Equal amounts of PCR products were mixed and subjected to a second round of PCR using cloning primers 1 and 2.

(3) Agarose gel electrophoresis and gel purification of nucleic acid fragments

1% agarose gels containing 0.5 µg/ml ethidium bromide were prepared by dissolving agarose powder in 1×TAE buffer (40mM Tris base, 10mM EDTA, 20mM acetic acid, adjusted pH to 8.5). Gels were submerged in a running tank of TAE buffer and run horizontally at 120 V. Appropriate amounts of nucleic acids were mixed with 6×DNA loading buffer (0.25% bromophenol blue and 40% sucrose (w/v)), and loaded into preset agarose gels. Nucleic acid bands separated on agarose gels were visualized by UV transillumination, and fragment sizes were compared with that of 1 kb ladder DNA marker. If necessary, upon separating and viewing, the desired band was excised using a sterile razor blade before it was extracted by gel extraction kit according to protocols provided by the manufacturer.

(4) Restriction endonuclease digestion of PCR products and DNA fragments

In a reaction volume of 100 µl, up to 5 µg of plasmid DNA or half of the purified PCR products was digested with 5 U of the appropriate restriction endonuclease(s) for 2 h, using the buffer provided and conditions recommended by the manufacturer. Double digestion with two enzymes was performed either sequentially with intervening phenol/chloroform extraction and ethanol precipitation or simultaneously, if the condition of each reaction was compatible.

(5) Dephosphorylation of plasmid DNA

To prevent self-ligation of digested DNA vector with compatible ends, 5 µg of linearized plasmid was subjected to dephosphorylation in a 100 µl reaction containing 10 U of calf intestinal alkaline phosphatase (CIP) and a buffer recommended by the manufacturer. After incubating at 37°C for 1 h, the DNA was phenol/chloroform extracted and ethanol precipitated.

(6) Ligation reactions

Purified, dephosphorylated vector was mixed in 1:5 ratio with excised insert DNA and covalently joined by incubation with 5 U of T4 DNA ligase (Fermentas) in the presence of the ligation buffer provided. Ligation reactions were performed overnight at room temperature. For self-ligation of plasmids with compatible ends, 1 µg of restriction endonuclease-digested DNA was subjected to similar ligation conditions in a 20 µl reaction volume, as mentioned above.

(7) Preparation of competent *E. coli* cells

A single colony of *E. coli* cells on a LB plate was inoculated into 2 ml of LB medium (1% tryptone (w/v), 0.5% yeast extract (w/v), 1% NaCl (w/v), adjusted to pH 7.0) and grown overnight (approximately 16 h) at 37°C incubator, while shaking at 250 rpm. 150 µl of the overnight culture was diluted 100 folds into 15 ml of fresh LB medium, and incubated at 37°C, shaking at 250 rpm, till O.D.₅₉₅ reached 0.5. Upon cooling to 4 °C, the culture was centrifuged at 2,500 rpm for 5 min at 4 °C. The pellets were resuspended in 10 ml of sterile ice-cold 50 mM CaCl₂ and allowed to stand on ice for 30 min. Pelleted the cells again, resuspended in 1 ml of ice-cold 20% glycerol in 50 mM CaCl₂ and allowed to stand on ice for 5 min. Cells were then aliquoted in 100 µl volumes and stored at -80°C for future use.

(8) Transformation of competent *E. coli* cells by plasmid DNA by heat shock

Either 5 µl of ligated materials or 1 µg of circular DNA was added into 100 µl of fresh or frozen *E. coli* competent cells and cooled on ice for 30 min, after which cells were transferred to 42°C. After 90 sec, the transformed cells were immediately chilled on ice for 2 min and spread on LB agar plates containing the appropriate selective antibiotics, with either 100 µg/ml of Ampicillin or 50 µg/ml of Kanamycin.

2.2.1.3. Plasmid DNA purification

(1) Small scale preparation of plasmid DNA (Miniprep) – Alkaline lysis

Single bacterial colonies were inoculated into snap-capped test tubes (Falcon) containing 2 ml of LB medium with the appropriate selective antibiotics and grown overnight at 37°C. The cell pellet from each tube was resuspended in 100 µl of Solution I (1M Tris-HCl, pH 8.0, 0.5M EDTA, pH 8.0, 1M sucrose), and

subsequently lysed with 200 µl of Solution II (1% SDS, 0.2M NaOH) for 5 min at room temperature. 150 µl of Solution III (3M NaOAc, pH 5.2) was then added to the alkaline mixture, gently mixed and incubated on ice for 30 min. Precipitated proteins and chromosomal DNA were removed by microcentrifugation for 30 min at 4°C. The crude DNA was precipitated by adding 1 ml absolute ethanol to the 400 µl lysate. Air-dried the pellet briefly and resuspended it in 100 µl of sterile ddH₂O. Appropriate amount of DNA was then used for restriction endonuclease digestion in 20 µl volumes, followed by agarose gel electrophoresis.

(2) Phenol/chloroform extraction and ethanol precipitation

Half volumes of Tris-saturated phenol was added to 100 µl of aqueous solution of nucleic acids, vortex and centrifuged at 14,000 rpm for 1 min at room temperature (Eppendorf Centrifuge 5415D) to separate the two phases. The upper aqueous phase containing the deproteinized solution was transferred to a new 1.5 ml microfuge tube (Eppendorf). Equal volume of chloroform was then added, vortex and centrifuged, before the aqueous phase was once again transferred to a new tube. Plasmid DNA and PCR products were recovered by ethanol precipitation. 2.5 volumes of absolute ethanol and 2 M NaOAc (pH 5.2) were added to aqueous solutions containing the desired nucleic acids, and stored at -20°C for 20 min. The tube was centrifuged at 14,000 rpm for 5 min, before the supernatant was removed by aspiration. The pelleted DNA was air-dried, after which appropriate amount of sterile ddH₂O was added to resuspend DNA.

2.2.1.4. Automated DNA sequencing

Nucleotide sequencing of all constructs created was carried out by using 200 ng of the double-stranded templates and 10 ng of primers with the Big Dye terminator v3.1 cycle sequencing kit (Applied-Biosystems) and the automated DNA sequencer 373 from PE Applied Biosystems.

2.2.2. Preparation of RNA, cDNA and RT-PCR

2.2.2.1. Extraction of RNA from HeLa cells

Confluent monolayers of HeLa cells in 75 cm² flasks were lysed directly by adding 2 ml of TRIZOL Reagent (Invitrogen). The homogenized samples were incubated for 5 min at room temperature to permit the complete dissociation of nucleoprotein complexes. 0.4 ml of chloroform was added. Shake tubes vigorously by hand for 15 sec and incubated at room temperature for 2 min. Centrifuge the samples at 2,000 ×g for 15 min at 4°C. Transfer the aqueous phase to a fresh tube. The RNA was precipitated from the aqueous phase by mixing with 1 ml of isopropyl alcohol. Incubate samples at room temperature for 10 min and centrifuge at 2,000 ×g for 10 min at 4°C. Remove the supernatant, wash the RNA pellet once with 75% ethanol. Briefly dry the RNA pellet. RNA was dissolved in RNase-free water and stored at -80°C.

2.2.2.2. Reverse transcription – polymerase chain reaction (RT-PCR)

2.5 µl (approximately 1 µg) of total RNA was added to 1 µl of 10 µM of an appropriate reverse primer in a sterile 200 µl thin-wall Gene-Amp tubes. After denaturation at 65°C for 10 min, the tubes were immediately cooled on ice for 2 min. The denatured RNA-primer mixture were then added to a 20 µl of reaction mixture

containing 10 mM of each dNTPs, 200 mM of DTT, 1×expand reverse transcriptase buffer and 50 U of expand reverse transcriptase (Roche). The first strand cDNA was synthesized at 37°C for 1 h, and reaction was terminated by heating at 65°C for 10 min. Amplification of cDNA was achieved by PCR in a 50 µl reaction containing 20 µM of appropriate primers and 5 U of *Pfu* DNA polymerase.

2.2.3. Protein characterizations

2.2.3.1. SDS-polyacrylamide gel electrophoresis (SDS-PAGE)

Separating gels of various acrylamide concentrations and 3% stacking gels were cast between two glass plates. After protein samples were loaded into the wells, gels were run vertically in a reservoir filled with running buffer (2.88% glycine (w/v), 0.6% Tris (w/v), and 0.1% SDS (v/v)) at 30 mA, constant current. Electrophoresis was carried out for an appropriate length of time.

2.2.3.2. Expression of GST fusion protein

The SARS-CoV N protein was cloned into pGEX-5X-1 and expressed as GST-N fusion protein in *E. coli* BL21 cells. Both GST-N and GST alone were purified by affinity chromatography using glutathione-sepharose 4B according to protocols provided by the manufacturer.

2.2.3.3. GST pull-down assay

In vitro translation of Ubc9 was carried out using the T7-coupled rabbit reticulocyte lysate system in the presence of [³⁵S] methionine according to the manufacturer's instructions (Promega). For the binding assay, 2 µg of GST alone or

GST-Ubc9 fusion proteins were prebound to glutathione-sepharose beads by incubation with agitation for 1 h at room temperature in 0.5 ml of binding buffer (10 mM Tris-HCl, pH 7.4, 50 mM NaCl, 2% bovine serum albumin). 5 μ l of 35 S-labeled Ubc9 was then added, and incubation was continued for at least 2 h. The beads were washed five times with 0.5% NP-40 in 10 mM Tris-HCl, pH 8.0, 140 mM NaCl, and 0.025% NaN₃ buffer. Labeled protein bound on the beads was recovered by heating at 100°C in 10 μ l of SDS loading buffer and was analyzed by SDS-PAGE. Radiolabeled bands were visualized by autoradiography.

2.2.3.4. In vitro translation

In vitro translation assays were performed by using the TNT-coupled transcription/translation system (Promega). Plasmids with a T7 promoter were prepared. The reaction mixtures contained 2 μ g of DNA template in 12.5 μ l of rabbit reticulocyte lysate reaction mixture in the presence of [35 S]methionine. The reaction mixtures were incubated at 30°C for 90 min, after which the reactions were stopped by the addition of an equal volume of SDS loading buffer containing 100 mM Tris hydrochloride (pH 6.8), 200 mM dithiothreitol, 4% (w/v) SDS, 20% glycerol, and 0.2% bromphenol blue. The mixture was then heated at 100°C for 3 to 5 min and analyzed by SDS-PAGE, followed by autoradiography.

2.2.3.5. Autoradiography

After SDS-PAGE, gels were placed in a fixing solution containing 10% glacial acetic acid and 50% methanol for 40 min with shaking. Gels were dried down under vacuum at 64°C for 1 h before exposure to X-ray film (Kodak) at -70°C. The film was developed after an appropriate length of time using a Kodak developing machine.

2.2.3.6. Immunoprecipitation

Transiently transfected HeLa cells in 100-mm dishes were lysed in 1 ml of lysis buffer (150mM NaCl, 1% NP-40, and 50mM Tris-HCl, pH 8.0) with 0.5% protease inhibitor cocktail. The lysates were centrifuged at 12,000 rpm for 20 min at 4 °C. The supernatants were added with anti-His, anti-SUMO-1, anti-Flag M2, or anti-c-Myc antibodies at 4°C for 2 h. Protein-A agarose beads (40 μ l) were added to the lysates and incubated with shaking for 1 h at 4 °C. The beads were collected by centrifugation and washed for three times with RIPA buffer (150mM NaCl, 1% NP-40, 0.5% sodium deoxycholate, 0.05% SDS, and 50mM Tris-HCl, pH 8.0). Proteins binding to the beads were eluted by adding 2 \times SDS loading buffer and analyzed by Western blotting with anti-Flag antibody.

2.2.3.7. Western blot analysis

Whole cell lysates from infected or transfected cells were separated by SDS-PAGE. Protein was transferred to polyvinylidene difluoride (PVDF) membranes (Bio-Rad) by using a semi-dry transfer cell (Bio-Rad, Trans-blot SD), and blocked overnight at room temperature with 10% nonfat milk in PBS-T. The membrane was probed with primary antibodies followed by anti-mouse or anti-rabbit antibodies conjugated with horseradish peroxidase. Membrane-bound antibodies were detected with either an ECL kit or a SuperSignal west pico chemiluminescence substrate kit.

2.2.4. Yeast two-hybrid screen

Screening for interacting proteins for SAR-CoV N was carried out with the yeast two-hybrid system. SARS-CoV N, cloned into pGBKT7 vector, was used as the bait. Yeast strain AH109 containing pGBKT-N mated with Y187 containing a HeLa

cDNA library was incubated at 30 °C for 24 h with gently swirling (30 rpm). The library mating mixtures were selected on SD/-Trp/-Leu/-His plates. After 8 days, colonies with a diameter more than 2 mm were streaked out onto SD/-Trp/-Leu/-His/-Ade plates for another 3 days, and -gal colony-lift filter assay was performed.

2.2.5. Virus manipulations

2.2.5.1. Preparation of recombinant vaccinia virus-T7 (vTF7-3) working stock

Hela cells were grown to confluence in $4 \times 175 \text{ cm}^2$ and infected with 0.1 P.F.U./cell of a recombinant vaccinia virus (vTF7-3) for 24 h, before fresh medium was used to replace the inoculum. Prior to infection, the vTF7-3 virus stock was briefly sonicated using an ultrasonic processor (Misonik) for 1 min. After 48 h, when cytopathic effects (CPE) were observed, the infected cells were harvested together with the culture medium by scraping. The viruses were released from cells via three rounds of freeze-thaw (at -80 °C and room temperature respectively), before they were aliquoted in 1.5 ml screw-cap vials (IWAKI) and stored at -80 °C.

2.2.5.2. Preparation of working stock of IBV

Following 3 washes of the confluent Vero or H1299 cells with PBS, IBV was inoculated at a multiplicity of infection (MOI) of 1 P.F.U./cell. IBV was allowed to absorb to monolayer for 3 h, before the medium was replaced with fresh serum-free DMEM or RPMI that was sufficient to cover the monolayer. Cells were then incubated at 37°C in 5% humidified CO₂, until CPE was observed. Both culture medium and cells were harvested and aliquoted in appropriate amounts. The IBV stock was stored at -80°C.

2.2.5.3. Infection of mammalian cells by IBV

Confluent monolayers of Vero and H1299 cells in 60 mm diameter culture dishes were infected by IBV Beaudette strain at an MOI of 1. After 3 h, the inoculum was replaced by serum-free DMEM or RPMI and incubated at 37°C in 5% CO₂, before the cells were rinsed and incubated in fresh DMEM or RPMI for variable lengths of time. The cells were subsequently harvested and subjected to various analyses.

2.2.5.4. Virus titration assays

Plaque assay – Vero cells were seeded in six-well plates at 2×10^5 cells per well 48 h prior to infection. Serial dilutions (10-fold dilutions with serum-free DMEM) of IBV were incubated on Vero monolayer for 3 h. After absorption, cells were overlaid with 1% CMC in 2 ml of complete DMEM, concomitantly treated with either DMSO or cell cycle inhibitors. At 72 h p.i., cells were fixed by addition of 500 µl of 4% paraformaldehyde for 15 min at room temperature, and afterwards stained with 500 µl of crystal violet solution (0.5% crystal violet in 20% ethanol). Plaques were visualized and counted.

TCID₅₀ – H1299 cells were seeded in 48-well plates 48 h prior to infection. Serial dilutions (10-fold dilutions) of IBV were incubated on cell monolayer for 3 h. After absorption, cells were overlaid with complete DMEM containing either DMSO or cell cycle inhibitors. At 24 and 48 h p.i., the amount of virus was deduced by the 50% tissue culture infective dose (TCID₅₀), which was calculated from the cytopathic effect induced in cell culture by different dilutions of the virus. The data were analyzed by Student's *t* test.

2.2.6. Tissue culture

2.2.6.1. Passage of continuous cell line

Rinse the confluent cells in 75 cm² flasks with tissue culture grade phosphate buffered-saline (PBS, 0.8% NaCl (w/v), 0.02% KCl (w/v), 0.144% Na₂HPO₄ (w/v), and 0.024% KH₂PO₄ (w/v), adjusted to pH 7.4 by HCl). Detach the adherent cells from polystyrene surface by adding 1 ml of trypsin (0.05% trypsin, 0.02% EDTA) to the culture and incubation at room temperature for 5 min. 5 ml of complete DMEM or RPMI containing 10% newborn calf serum was added to stop the proteolytic process and the cells were subjected to low speed centrifugation for 5 min. The cell pellets were resuspended in 10 ml of fresh complete medium, and were plated onto flasks or dishes in appropriate density.

2.2.6.2. Preparation and resuscitation of frozen cell line stock

Cells cultured in 175 cm² flasks were subjected to trypsinization, and centrifugation as usual. 10 ml of freezing medium containing 5% DMSO and 95% newborn calf serum was used to resuspend the cell pellet. Cells were aliquoted into plastic cryogenic polypropylene vials (IWAKI) and were subjected to slowing freezing to -20°C and -80°C for 1 h each, prior to long term storage in liquid nitrogen.

To resuscitate the frozen cell line stock, a vial of frozen cells was thawed at 37°C and carefully transferred to a 25 cm² flask containing 8 ml of complete medium prewarmed to 37°C. Resuscitated cells were incubated at 37°C in humidified 5% CO₂, for 24 h, before the culture medium was replaced with fresh complete medium.

2.2.6.3. Cell transfection

Transfection experiments were performed using Effectene transfection reagent. Cells (1.5×10^5) were plated into six-well tissue culture plates 14-18 h before transfection. 1 μ g of plasmid DNA in 150 μ l EC buffer was mixed with 8 μ l of enhancer and the mixture was allowed to stand at room temperature for 2-5 min. 15 μ l of Effectene transfection reagent was added and the mixture was incubated at room temperature for another 5-10 min. Cells were washed once with PBS and the DNA-Effectene mixture diluted in 2 ml of complete growth medium was added. The cultures were incubated at 37°C in 5% CO₂ for 2-3 h, after which the medium was aspirated and the cells were washed again. Added 2 ml fresh complete medium and incubation was continued for another 30-72 h, after which cells were harvested for various assays.

2.2.6.4. Transient expression of viral proteins in mammalian cells

Constructs containing plasmid DNA under the control of a T7 promoter were transiently expressed in mammalian cells using a vaccinia virus-T7 system. Briefly, semiconfluent monolayers of HeLa cells were infected with 10 P.F.U./cell of recombinant vaccinia virus (vTF7-3), which expresses the T7 RNA polymerase gene, for 2 h at 37°C prior to transfection. The plasmid DNA was transfected into vTF7-3-infected cells using Effectene transfection reagent according to the manufacturer's instructions.

2.2.7. Cell cycle and apoptosis assays

2.2.7.1. Measurement of cell proliferation and viability

Vero and H1299 cells were seeded in six-well plates at 10^5 cells per well. After 24 h of incubation, cells were mock infected or infected with IBV at an MOI of 0.5 or 1 at 37°C for 3 h. After viral infection, 2 ml of fresh medium was added to each well. At various times postinfection (p.i.), cells were harvested, resuspended in 2 ml of PBS, and counted using a hemocytometer. Results are presented as percentage of cell numbers compared with that of mock infected cells at 0 h p.i.

MTT assay was carried out using the cell proliferation kit I (MTT) according to the manufacturer's recommended procedures (Roche Applied Science). Vero and H1299 cells plated in 96-well plates at approximately 50% confluence were mock infected or infected with IBV at an MOI of 1. At various times p.i., 20 μ l of MTT labeling reagent was added into each well and incubated at 37°C for 4 h. After 150 μ l of solubilization solution was added, the absorbance was measured at 550 nm in an enzyme-linked immunosorbent assay reader. Results are presented as percentage of live cell numbers compared with that of mock infected cells at 0 h p.i.

2.2.7.2. Determination of cell division

HeLa cells grown on coverslips were transfected with appropriate constructs expressing the N protein or SUMO-1, and fixed with 4% paraformaldehyde. The number of cells undergoing cell division was determined by counting a total of 300 cells that expressing the green fluorescence protein (GFP). Statistical analysis was performed using Student's *t* test, and *P* values less than 0.05 were considered to be statistically significant.

2.2.7.3. Cell cycle manipulation

Vero and H1299 cells were synchronized in the quiescent state by serum deprivation for 48 and 24 h, respectively. Approximately 3×10^5 cells were seeded into 6-mm dishes and maintained in medium without newborn calf serum for indicated hours. Synchronized cells were either mock-infected or infected with IBV at an MOI of 1 as described above. At various times p.i., cells were processed for flow cytometry analysis.

For analysis of IBV replication in the S-phase, asynchronously growing Vero and H1299 cells in 12- or 48-well plates were treated with either DMSO or 20 μ M of methotrexate for 20 h, and incubated in fresh medium for 6 h afterwards to release the cell cycle. Cells were then mock-infected or infected with IBV at an MOI of 1 and processed at various times p.i. for plaque assay, endpoint assay, analysis of cell cycle profiles, and assessment of virus protein expression. Vero and H1299 cells were synchronized at the G₁/S border using 20 μ M of methotrexate.

2.2.7.4. Cell cycle analysis by flow cytometry

To determine cell cycle status, nuclear DNA content was measured by using propidium iodide staining and fluorescence-activated cell sorting (FACS) analysis. Briefly, cells were detached with trypsin, and washed with PBS. The cell pellets were resuspended in 0.5 ml PBS containing 50 μ g/ml propidium iodide and 100 μ g/ml RNase, incubated at 4°C for 30 min, and then analyzed using a FACScan flow cytometer and ModFit LT Mac 3.0 software (BD Biosciences).

2.2.7.5. TUNEL assay

The terminal deoxynucleotidyltransferase-mediated dUTP-biotin nick end labeling (TUNEL) assay was performed with an *in situ* cell death detection kit,

fluorescein according to the protocol of the manufacturer (Roche). Briefly, cells were fixed with paraformaldehyde and permeabilized with Triton X-100 at room temperature. After equilibration, specimens were overlaid with 50 µl TUNEL reaction mixture and incubated in a humidified atmosphere for 60 min at 37°C in the dark. Then rinse slides 3 times with PBS. Samples with the incorporated fluorescein can directly be analyzed under a fluorescence microscope using an excitation wavelength of 488 nm.

2.2.8. IF and confocal microscopy

2.2.8.1. Indirect immunofluorescence (IF)

SARS-CoV N protein and Ubc9 were transiently expressed in HeLa cells grown on 4-well chamber slides (IWAKI). After rinsing with phosphate-buffered saline (PBS), cells were fixed with 4% paraformaldehyde for 15 min at room temperature and permeabilized with 0.2% Triton X-100, followed by incubation with specific antibodies diluted in fluorescence dilution buffer (PBS with 5% newborn calf serum) at room temperature for 2 h. Cells were then washed with PBS and incubated with FITC- or TRITC-conjugated anti-rabbit or anti-mouse secondary antibodies in fluorescence dilution buffer at 4 °C for 1 hour before mounting. All images were taken using a Zeiss LSM510 META laser scanning confocal microscope.

2.2.8.2. Confocal microscopy

Confocal microscopy was performed on a Zeiss LSM 510 META laser scanning system; featuring an Axiovert 100M inverted microscope connected to Windows NT based computer. The microscope is equipped with one argon and two

helium-neon lasers for fluorescence excitation of 458/488, 543, and 633 nm. The green (FITC) and red (Rhodamine, TRITC, and Texas red) fluorescence could be detected using respective filters at appropriate wavelengths according to the microscope settings. Dual labeled cells were viewed for co-localization by superimposing the green and red fluorescent images by the triple labeling method. The region of overlap in the merged image was displayed as yellow. Images were saved in the TIFF format and processed using the Adobe Photoshop 6.0.

2.2.9. Statistical analysis

P values were determined by Student's *t* test. A value of < 0.05 was considered significant. Data were reported as the mean \pm standard deviation (STDEV). Calculations of the means and STDEVs were carried out using Microsoft Excel software (Microsoft).

Chapter 3

Sumoylation of the Nucleocapsid Protein of Severe Acute Respiratory Syndrome Associated Coronavirus by Ubc9

3.1. Introduction

In this study, the SARS-CoV N protein was cloned and expressed in bacterial and mammalian cells. In *Escherichia coli* BL21 cells, the protein was expressed as a single protein species. However, multiple protein bands with a wide range of molecular masses were detected when the N protein was expressed in mammalian cells, indicating that it may have undergone other posttranslational modifications by host cells in addition to phosphorylation and it may form homo-oligomers. To address host factors that might affect the N protein, a yeast two-hybrid screen of a HeLa cDNA library was performed. We identified ubiquitin-conjugating enzyme 9 (Ubc9), which was found to interact specifically with the N protein both *in vitro* and *in vivo*.

Biochemical characterization and mutagenesis analyses demonstrated that the SARS-CoV N protein was posttranslationally modified by sumoylation. The sumoylation site was mapped to the 62nd lysine residue of the N protein. Further expression and characterization of wild-type N protein and K62A mutant revealed that sumoylation drastically promotes homo-oligomerization of the protein. Sumoylation of the N protein may also play certain roles in its subcellular localization and its interference of host cell division. As self-association and homo-oligomerization of the N protein are essential for the formation of viral ribonucleoprotein complex and nucleocapsid assembly, it suggests that sumoylation of this protein may play an important regulatory role in SARS-CoV replication cycles.

3.2. Results

3.2.1. Expression of SARS-CoV N protein in bacterial and mammalian cells

To study its biochemical properties and functions in viral replication, virion assembly and virus-host interaction, we cloned and expressed the SARS-CoV N protein in bacterial and mammalian cells. As seen in Fig. 3.1, expression of the protein in *E. coli* BL21 cells as a GST fusion protein showed the detection of a single band of approximately 70 kDa, representing the GST-N fusion protein (Fig. 3.1, lane 2). The protein could be purified by using the GST resin (Fig. 3.1, lane 2). Expression of the N protein tagged with the nine amino acid Flag tag at its N-terminus in mammalian cells showed the detection of multiple bands instead of a single protein band (Fig. 3.1, lane 4). Similar to the recently reported detection of three major isoforms (Leung et al., 2004), a major protein species of approximately 48 kDa together with two slightly less abundant species, which migrate more rapidly than the 48-kDa band, were detected (Fig. 3.1, lane 4). These three isoforms may represent the full-length and posttranslationally modified forms of the N protein. In addition, three other species with approximately molecular masses of 175, 85, and 82 kDa, which may represent oligomerization of the N protein, were sometimes detectable under reducing conditions (Fig. 3.1, lane 4).

3.2.2. Identification of Ubc9 as a SARS-CoV N-interacting protein

The detection of multiple protein species with a wide range of molecular masses when the N protein was expressed in mammalian cells indicates that the protein may undergo other posttranslational modification, in addition to the known phosphorylation. As N protein does not contain any cysteine residue, the detection of

potential oligomers suggests that it may form higher order structures through other interactions. To identify host proteins that interact with the N protein, a yeast two-hybrid screen of a HeLa cDNA library was performed. We obtained 20 independent clones corresponding to Ubc9 among a total of 24 positive clones (Fig. 3.2a).

To address whether Ubc9 also interacts with the N protein in a context other than in yeast, we performed GST pull-down assays with a bacterially expressed GST-N fusion protein and ³⁵S-labelled Ubc9 (Fig. 3.2b). An equal amount of ³⁵S-labelled Ubc9 was incubated with 2 µg each of GST alone or GST-N fusion proteins bound to glutathione-Sepharose beads. After extensive washing, the ³⁵S-labelled protein bound to the beads was extracted and analyzed by autoradiography. Ubc9 associated with GST-N but not with GST alone (Fig. 3.2b, lanes 3 and 4).

Further verification of Ubc9-N interaction was obtained by coimmunoprecipitation experiments. HeLa cells were transfected with His-tagged N, Flag-tagged Ubc9, or cotransfected with both plasmids (Fig. 3.2c). At 18 h after transfection, the cell lysate was prepared and subsequently analyzed by Western blotting using anti-Flag antibody or subjected to immunoprecipitation with anti-His antibody before analysis on SDS-PAGE. As shown in Fig. 3.2c (lanes 4-6), an 18-kDa band which represents the precipitated Ubc9 could only be detected when coexpressed the two proteins.

To investigate the subcellular localization of the N protein and Ubc9, HeLa cells were cotransfected with plasmids that express N (pcDNA3.1-N) and Flag-tagged Ubc9. Immunofluorescence analyses with a confocal microscope revealed that the N protein was distributed throughout the cytoplasm, and was also localized to the nucleolus (Fig. 3.2d). Ubc9 was present more abundantly in the nucleus than in the

cytoplasm (Fig. 3.2d). A merged picture revealed that Ubc9 colocalized with the N protein on the perinuclear region and the nucleolus (Fig. 3.2d).

3.2.3. Posttranslational modification of SARS-CoV N protein by sumoylation

The detection of multiple protein species with a wide range of molecular masses when the N protein was expressed in mammalian cells also indicates that the protein may undergo other posttranslational modification, in addition to the known phosphorylation. N protein does not contain any cysteine residue, the detection of potential oligomers suggests that it may form higher-order structures through other interactions. Above we described a novel interaction between the SARS-CoV N protein and Ubc9. As Ubc9 is known to mediate the conjugation of SUMO to target proteins (Desterro et al., 1997; Schwarz et al., 1998), we thus examined whether the N protein is modified by sumoylation. Cells transfected with pFlag-N were lysed either with a lysis buffer containing two isopeptidase inhibitors, iodoacetamide (IAA, 10 mM) and *N*-ethylmaleimide (NEM, 20mM), or with the Laemmli protein gel loading buffer preheated to 80⁰C, and subjected to Western blot analysis with anti-Flag antibody. As can be seen in Fig. 3.3a, in addition to the three major isoforms of N protein that were detected under all conditions, a protein species of approximately 65 kDa was detected in cell lysates prepared with lysis buffer containing IAA and NEM (Fig. 3.3a, lanes 2, 3, and 5). Occasionally, a band of approximately 55 kDa was also detected in cell lysates prepared with buffer containing IAA and NEM (Fig. 3.3a, lane 3). Co-expression of N protein with SUMO-1 led to the detection of significant more 65 kDa species (Fig. 3.3a, lanes 2 and 3). The 65-kDa band was also detected when cells were lysed directly with preheated SDS loading buffer (Fig. 3.3a, lane 6). During the course of this study, we noted that the 65-kDa band could also be

efficiently detected under non-reducing conditions (Fig. 3.3a, lanes 5 and 6). Under both reducing and non-reducing conditions, the three major isoforms and the 65-kDa band are migrating at the same positions. This would allow detection of N proteins in the subsequent co-immunoprecipitation experiments using SDS-PAGE under non-reducing conditions. The reason for choosing the non-reducing conditions in these assays is that the IgG heavy chain would mask the detection of the three major N isoforms under reducing conditions.

The molecular mass of 65 kDa and its biochemical properties suggest that this species may represent the sumoylation of the N protein. To confirm this possibility further, cell lysates were subjected to immunoprecipitation with either anti-Flag or anti-SUMO-1 antibody, and then analyzed by Western blotting with anti-Flag antibody. The results showed that anti-Flag antibody specifically precipitated the three major isoforms of N protein from cells transfected with pFlag-N (Fig. 3.3b, lanes 2 and 3). In addition, the 65-kDa species was also detected (Fig. 3.3b, lanes 2 and 3). Analysis of the anti-SUMO-1 precipitates by Western blotting with anti-Flag antibody showed that only the 65-kDa band was detected (Fig. 3.3b, lanes 5 and 6). Once again, co-expression of N protein with SUMO-1 greatly increased the detection of the 65 kDa species (Fig. 3.3b, lanes 3 and 6). No N protein bands were detected from cells transfected with SUMO-1 alone (Fig. 3.3b, lanes 1 and 4). These results confirmed that the 65 kDa band represents the sumoylated N protein.

3.2.4. Mapping of the sumoylation site on SARS-CoV N protein

The consensus motif for sumoylation has been defined as a tetrapeptide Ψ KXE (where Ψ is usually a hydrophobic residue with exceptions, and X is any amino acid) that surrounds the acceptor lysine in target proteins (Seeler and Dejean,

2003). Analysis of the N protein sequence showed that it contains 27 lysine residues. One lysine residue at amino acid position 62, K⁶², lies roughly within the consensus SUMO-1 modification sequence (GKEE) (Fig. 1.3). To determine whether this lysine was responsible for the modification of N protein by sumoylation, it was mutated to an Ala by site-directed mutagenesis. Proteins extracted from cells transfected with wild-type N and K62A mutant were immunoblotted with anti-Flag antibody. As shown in Fig. 3.4, similar amounts of the three isoforms of N protein were detected from cells transfected with either wild-type or mutant N constructs (Fig. 3.4, lanes 1 and 2). The 65 kDa sumoylated band was detected from cells transfected with wild-type N protein only (Fig. 3.4, lane 1); but not from cells expressing the K62A mutant (Fig. 3.4, lane 2). These results demonstrated that the K62 residue is the major sumoylation site of N protein.

3.2.5. Promotion of homo-oligomerization of SARS-CoV N protein by sumoylation

It has been well documented that the ability of viral nucleocapsid protein to interact with itself to form homo-oligomers is fundamental to the process of viral particle assembly and maturation. Recent studies showed that SARS-CoV N protein exhibits intrinsic properties of self-interaction (He et al., 2004; Surjit et al., 2004; Yu et al., 2005). Multimerization of N protein was observed both *in vitro* and *in vivo* (He et al., 2004; Surjit et al., 2004; Yu et al., 2005). To study the effects of sumoylation on the homo-oligomerization of N protein, cells expressing N protein alone or together with SUMO-1 were analyzed. As shown in Fig. 3.5, Western blot analysis of cells expressing wild-type N protein showed the detection of the three major isoforms of N protein and the 65-kDa sumoylated bands (Fig. 3.5a and b, lanes 1 and 2). In addition,

two bands of approximately 85 and 175 kDa were detected (Fig. 3.5a and b, lanes 1 and 2). Based on their apparent molecular masses, they may represent dimers and tetramers, respectively, of the N protein.

The effects of sumoylation on the formation of these oligomers were then analysed by expression of wild-type and K62A mutant constructs in cells in the presence of SUMO-1. The results showed that co-expression of wild-type N protein with SUMO-1 dramatically increased the detection of the 65-kDa sumoylated band and the 85-kDa/175-kDa oligomers (Fig. 3.5b, lanes 3 and 4). In contrast, co-expression of the K62A mutant with SUMO-1 showed no detection of the 65-kDa sumoylated N protein (Fig. 3.5b, lane 5). Interestingly, only a trace amount of the 85-kDa and 175-kDa species was detected (Fig. 3.5b, lane 5). These results suggest that abolishment of the sumoylation of N protein by mutating the K62 sumoylation site significantly decreases homo-oligomerization of the protein.

3.2.6. Further characterization of sumoylation-mediated homo-oligomerization of SARS-CoV N protein

The effect of sumoylation on homo-oligomerization of N protein was further characterized by two independent co-immunoprecipitation experiments. First, cells expressing wild-type and K62A mutant constructs were lysed with buffer containing IAA and NEM, immunoprecipitated with anti-Flag antibody. The immunoprecipitated proteins were separated in SDS-PAGE and analyzed by Western blotting with anti-Flag antibody. As shown in Fig. 3.6a, similar amounts of the three isoforms of N protein were detected from cells expressing the wild-type and mutant constructs (Fig. 3.6a, lanes 2 and 3). However, significantly more 85-kDa dimers were detected in

cells expressing the wild-type construct than did from cells expressing the mutant (Fig. 3.6a, lanes 2 and 3).

Second, the Flag-tagged wild-type and mutant N constructs were co-expressed with a c-Myc-tagged wild-type N construct. Cells were then lysed with buffer containing IAA and NEM, immunoprecipitated with anti-Myc antibody. The immunoprecipitated proteins were separated in SDS-PAGE and analyzed by Western blotting with anti-Flag antibody. As shown in Fig. 3.6b, the 85-kDa dimers were readily detected in cells co-expressing the Flag-tagged wild-type and Myc-tagged wild-type N protein (Fig. 3.6b, lane 3). Only a trace amount of the 85-kDa dimers was detected in cells co-expressing the Flag-tagged K62A mutant and Myc-tagged wild-type N protein (Fig. 3.6b, lane 4). It should be noted that no monomeric N protein was seen because different antibodies were used for IP and Western blotting, respectively (Fig. 3.6b, lines 1-4). A band migrating at approximately 50 kDa position was consistently detected (Fig. 3.6b, lines 1-4). It likely represents the heavy chain of the anti-Myc antibody used.

To make sure that similar levels of N protein were expressed in the transfected cells, total cell lysates were analyzed by Western blotting with anti-Flag (Fig. 3.6b, lanes 5-8) and anti-Myc (Fig. 3.6b, lanes 9-12) antibodies. The results showed that the expression levels of flag-tagged wild-type and mutant N protein and the Myc-tagged N protein are approximately the same (Fig. 3.6b, lanes 5-8 and 9-12). Interestingly, Western blot analysis of cells co-expressing Flag- and Myc-tagged wild type N protein with anti-Flag antibody showed readily detection of the 85- and 175-kDa oligomers (Fig. 3.6b, lane 7). Analysis of the same cell lysates with anti-Myc antibody, however, led to much less detection of the two forms (Fig. 3.6b, lane 11).

The two bands were only detectable after prolonged exposure of the gel (data not shown).

3.3.7. Nucleolar localization of SARS-CoV N protein

The nucleolar localization of SARS-CoV N protein was confirmed by its colocalization with fibrillarin in the nucleolus. As shown in Fig. 3.7, both cytoplasmic and nuclear localization pattern was observed in cells expressing the Flag-tagged N protein (Fig. 3.7a). Immunofluorescent staining with anti-fibrillarin antibodies showed typical nucleolar staining of both transfected and untransfected cells (Fig. 3.7b). Interestingly, strong cytoplasmic staining was also observed in cells expressing the N protein using the same antibodies (Fig. 3.7b). The staining patterns coaligned well with the patterns observed with anti-Flag antibodies (Fig. 3.7c). These results confirm the nucleolar localization of the N protein, and further demonstrate that N protein may physically interact with fibrillarin, resulting in the retention of fibrillarin in the cytoplasm of cells expressing the N protein.

3.2.8. Effects of sumoylation on the subcellular localization of SARS-CoV N protein

Subcellular distribution of N protein was further studied by cloning and expressing wild-type and K62A mutant N protein as a fusion protein with the enhanced green fluorescent protein (EGFP). The plasmid was transfected into HeLa cells and incubated at 37°C for 36 h. EGFP expression was then detected directly under the fluorescence microscope. The majority of the SARS-CoV N-EGFP fusion protein was observed to be distributed throughout the cytoplasm (Fig. 3.8b). A certain portion of the fusion protein was also observed to be localized to the nucleolus (Fig.

3.8b). Similar cytoplasmic localization was observed when K62A-EGFP fusion protein was expressed in HeLa cells (Fig. 3.8c). However, much less, if any, nucleolar localization was seen in cells expressing this mutant construct (Fig. 3.8c), suggesting that sumoylation may affect the subcellular localization of the N protein.

To further support this argument, the wild-type and K62A mutant N protein was then cloned into pcDNA3.1(+) and expressed in HeLa cells. After incubation at 37°C for 18 h, cells were analyzed by indirect immunofluorescence using rabbit anti-SARS-CoV N antiserum, followed by FITC-labeled goat anti-rabbit antibody. Similar cytoplasmic localization pattern to the N-EGFP fusion protein was observed in cells expressing wild-type and mutant N protein (Fig. 3.8e and f). In some cells, wild-type N protein exhibited typical nucleolar localization (Fig. 3.8e). Once again, less obvious nucleolar staining was observed in cells expressing the K62A mutant (Fig. 3.8f). These results suggest that sumoylation of the N protein might promote its nucleolar localization.

3.2.9. Effects of sumoylation on SARS-CoV N protein-mediated disruption of host cell division

Similar to other coronavirus N protein, overexpression of SARS-CoV N protein in mammalian cells disrupts the cell division, as certain proportion of cells expressing the protein at various time points posttransfection were apparently undergoing cell division (Fig. 3.8). Furthermore, much less multinucleated cells were observed in cells expressing the K62A mutant (Fig. 3.8). To quantitate the multinucleated cells, HeLa cells transfected with pEGFP, pEGFP-N, pEGFP-N + SUMO-1, and pEGFP-N(K62A) + SUMO-1 were examined under the fluorescence microscope at 24, 36, 48 and 60 h posttransfection, respectively, and the

multinucleated cells were counted among 300 cells expressing GFP. As shown in Fig. 3.9, over 25% of HeLa cells expressing pEGFP-N were observed to be undergoing cell division at all time points. The percentages of cells undergoing cell division increased to 31 – 36% among GFP-positive cells when pEGFP-N were co-expressed with SUMO-1. However, the percentages of cells undergoing cell division were markedly reduced to 11 – 15% in cells overexpressing the K62A mutant and SUMO-1 (Fig. 3.9), significantly less than ($P < 0.05$) the multinucleated cells observed when the wild-type construct was expressed. In a control experiment, the percentages of multinucleated cells that overexpress GFP only were between 2% and 3%. These results indicate that sumoylation of the N protein may play certain roles in its interference and disruption of host cell division.

3.3. Discussion

In this study, using the yeast two-hybrid system, we identified Ubc9, a SUMO-1-conjugating enzyme, as a host protein that interacts specifically with SARS-CoV N protein. The interaction between N and Ubc9 was verified both *in vivo* and *in vitro*. Furthermore, we showed that, in addition to phosphorylation, the N protein was modified by covalent attachment of SUMO to its 62nd lysine residue. Evidence provided demonstrated that sumoylation may promote homo-oligomerization of the protein. It may also play certain roles in the N protein-mediated interference of host cell division and its subcellular localization.

Coronavirus N protein is a multi-functional protein (Lai and Cavanagh, 1997; Wurm et al., 2001). Among them, the most prominent function of the protein is to wrap up the RNA genome to form RNP and assemble into the nucleocapsid core, due to its RNA-binding activities and self-association properties. Studies with other coronavirus N protein have mapped the RNA binding domain to the N-terminal one third region of the protein (Huang et al., 2004a). A basic amino acid stretch between amino acids 238 and 293 may be responsible for the RNA binding activities of the coronavirus infectious bronchitis virus N protein (Zhou et al., 1996). Interactions between N protein and RNA are generally required for encapsidation of viral genomic RNA. It is possible that RNA could promote N-N interactions by neutralizing charge repulsions between the two stretches of basic amino acids. As the K⁶² residue is located in the putative RNA-binding domain of the SARS-CoV N protein, is the reduced homooligomerization of the K62A mutant reported in this study due to its loss of the RNA binding activity? Although we do not know if this mutation could affect the RNA-binding activities of the protein, co-expression of the Flag-tagged K62A mutant with the Myc-tagged wild type N protein resulted in the detection of

remarkably less 85-kDa dimers than in cells co-expressing the Flag- and Myc-tagged wild type N protein. As two different antibodies were used in the immunoprecipitation and Western blot analyses, it virtually rules out the possibility that the detection of less 85- and 175- kDa oligomers in Western blot studies involving a single antibody is due to a weaker RNA binding activity of the mutant construct.

Self-association and homo-oligomerization are another essential property of the coronavirus N protein. Recent studies have shown that the S/R-rich motif and the C-terminal one-third region are essential for self-association and multimerization of the SARS-CoV N protein (He et al., 2004; Luo et al., 2005; Surjit et al., 2004b; Yu et al., 2005; Yu et al., 2006). The findings in this report indicate that the N protein is capable of forming dimers and higher order multimers. Similar to the equivalent protein of equine arteritis virus and simian hemorrhagic fever virus, SARS N protein does not contain any cysteine in its 422 amino acid residues. This excludes the possibility that disulfide bonds are the primary force that mediates the initial N-N interactions. In fact, disulfide bonds do not appear to be relevant until the virus enters the secretory pathway (ER and Golgi) and/or egresses from the cell, both events occurred following the core particle assembly. Data reported in this study demonstrate that sumoylation of the SARS-CoV N protein dramatically enhances the homo-oligomerization of the protein. Promotion of oligomerization of protein by sumoylation has been speculated for a pathogenic protein, Huntingtin (Steffan et al., 2004). Since self-association and homo-oligomerization of N protein are essential for the assembly of nucleocapsid core, it suggests that sumoylation would play an important role in the SARS-CoV replication cycle. Systematic testing this possibility would rely on the availability of an infectious cloning system, as developed by Yount et al. (Yount et al., 2003).

The apparent molecular weight of the dimer of the N protein detected in this report is 85 kDa, suggesting that it does not contain the SUMO conjugate. The failure to detect the sumoylated dimer in this study is unexpected, considering that sumoylation was shown to promote dimerization of the N protein. Two possibilities have been considered. First, sumoylation is a highly reversible process. The current data showed that only a small proportion of the N protein was dimerized compared to the monomers, and a certain proportion of the sumoylated dimer may be reversed during sample preparation and detection. The combination of these two factors would hamper the detection of the sumoylated dimers by the approaches used. The second possibility is that the sumoylated N protein may be not directly involved in the formation of dimers and other oligomers. Instead, it may target the N protein to different cellular compartments and facilitate the oligomerization of the N protein. Further studies are required to address these possibilities.

Site-directed mutagenesis studies mapped the ⁶²lysine residue as a major site for covalent attachment of SUMO to the protein, as the 65-kDa sumoylated band cannot be detected when the mutant construct was expressed in cells. We do not know whether other minor sumoylation sites may exist in the SARS-CoV N protein. Potential sumoylation at these minor positions would compensate the effect of K62A mutation, and complicate the interpretation of the data generating from functional studies, such as the partial interference of cell division by the K62A mutant N protein. Sumoylation of protein at multiple sites was recently reported for several viral and host proteins. For example, the EBV Rta protein was shown to be sumoylated at three alternating sites (Chang et al., 2004). As the SARS-CoV N protein contains a total of 27 lysine residues and no any other lysine residue is located in a consensus sequence

context for sumoylation, it would be difficult to further define these sites, if any, by a conventional mutagenesis approach.

SARS-CoV N protein has been found to be translocated to the nucleolus of host cells, resembling other coronavirus N proteins, such as IBV (Hiscox et al., 2001), MHV and TGEV (Wurm et al., 2001). This might be a common strategy for coronaviruses to control both host and viral RNA translation (Hiscox, 2003). However, the functional significance and the mechanism by which the N protein translocates to the nucleolus are yet to be determined. Systematic investigation of NuLS of the SARS-CoV N protein that might target it to the nucleolus will be carried out based on sequence comparison with other coronaviruses. An alternative possibility that may account for the nucleolar localization of a viral protein is its interaction with certain nucleolar antigens such as fibrillarin and nucleolin. This was demonstrated on IBV and MHV N proteins (Chen et al., 2002). Sumoylation of certain host proteins can regulate their nucleo-cytoplasmic shuttling (Salinas et al., 2004; Xiao et al., 2001). The K62A mutant exhibits much less nucleolus localization, indicating that sumoylation may regulate the subcellular localization of the SARS-CoV N protein.

Figures

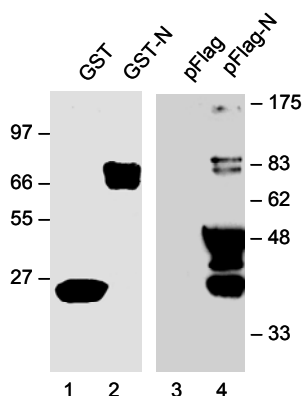


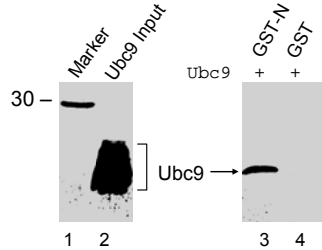
Fig. 3.1. Analysis of the expression of N protein in bacterial and mammalian cells. Plasmids pGEX-5X-1 and pGEX-N were transformed into *E. coli* BL21, and expressed by induction with IPTG. The GST (lane 1) and GST-N (lane 2) proteins were affinity-purified and separated on an SDS-10% polyacrylamide gel. The protein was visualized by staining the gel with Coomassie blue. Total cell lysates prepared from HeLa cells transfected with pKT0-Flag empty plasmid (lane 3) and Flag-tagged N protein (lane 4) were separated by SDS-PAGE and analyzed by Western blotting with anti-Flag antibody. Numbers on the left and right indicate molecular masses in kilodaltons.

a

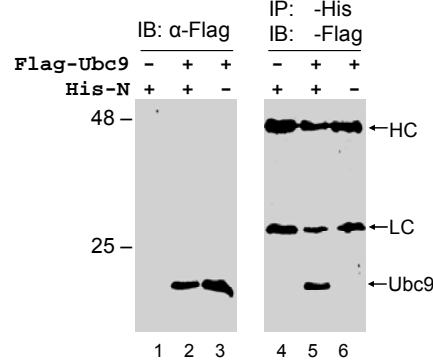
Summary of yeast two-hybrid experiments

Total positive clones	Ubc9	Cyclin A1	Others
24	20	2	2

b



c



d

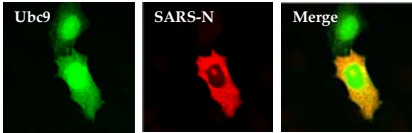


Fig. 3.2. Interaction of SARS-CoV N protein with Ubc9. a| Results of yeast two-hybrid screens using N as a bait. b| GST pull-down assays. *in vitro* translated and ^{35}S -labelled Ubc9 was incubated with GST alone or GST-N fusion proteins (lanes 3 and 4) bound to glutathione-sepharose beads. After extensive washing, the ^{35}S -labelled protein bound to the beads was extracted and analyzed by autoradiography. Lane 1 is the Rainbow [^{14}C] methylated protein molecular weight marker. c| Coimmunoprecipitation of N protein and Ubc9 from cellular extracts. HeLa cells expressing His-tagged N (lanes 1 and 4), Flag-tagged Ubc9 (lanes 3 and 6), or coexpressing both proteins (lanes 2 and 5) were lysed and analyzed by Western blotting using anti-Flag monoclonal antibody (Lanes 1-3) or subjected to immunoprecipitation with anti-His monoclonal antibody before analysis on SDS-10% polyacrylamide gel (Lanes 4-6). Numbers on the left indicate molecular masses in kilodaltons. d| Subcellular localization of N protein and Ubc9. HeLa cells were cotransfected with plasmids that express N (pcDNA3.1-N) and Flag-tagged Ubc9. Indirect immunofluorescent staining was carried out at 16 h posttransfection with mouse anti-Flag and rabbit anti-N antisera. The N protein was then detected by TRITC-conjugated anti-rabbit secondary antibody and Ubc9 was detected by FITC-conjugated anti-mouse secondary antibody. All images were taken using a Zeiss LSM510 META laser scanning confocal microscope. HC, Ig heavy chain. LC, Ig light chain.

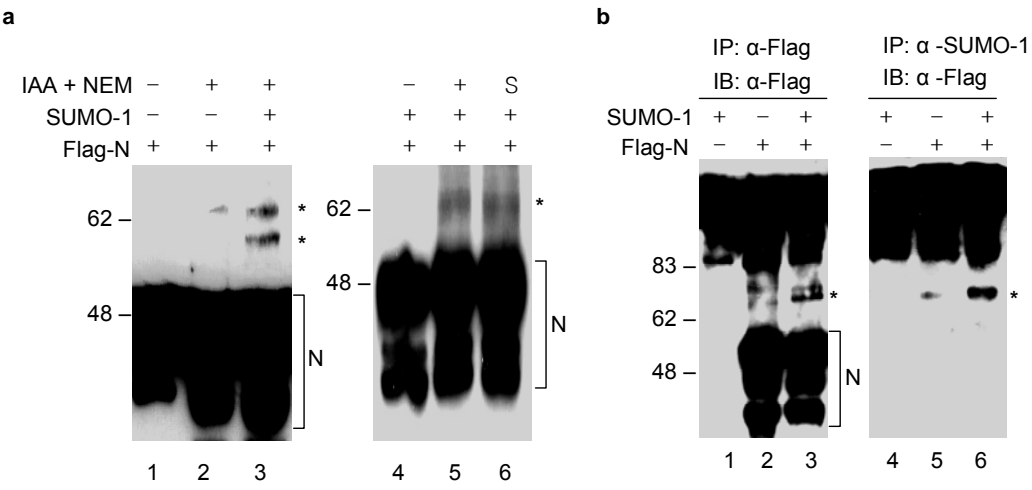


Fig. 3.3. Modification of SARS-CoV N protein by SUMO-1. a| Analysis of sumoylation of N protein by Western blotting. Cell lysates prepared from HeLa cells overexpressing either the Flag-tagged N protein alone (lanes 1 and 2) or together with SUMO-1 (lanes 3, 4, 5, and 6) were prepared either in the presence (lanes 2, 3 and 5) or absence (lanes 1 and 4) of the isopeptidase inhibitors IAA and NEM or by direct lysis in preheated SDS loading buffer (lane 6). The polypeptides were separated by SDS-PAGE under either reducing (lanes 1-3) or non-reducing (lanes 4-6) conditions and analyzed by Western blotting with anti-Flag antibody. The three major isoforms of N protein are indicated by brackets and the major SUMO-1 modified form of N protein is indicated by asterisks. Numbers on the left indicate molecular masses in kilodaltons. b| Analysis of sumoylation of N protein by immunoprecipitation and Western blotting. Total cell lysates were prepared, in the presence of the isopeptidase inhibitors IAA and NEM, from HeLa cells expressing SUMO-1 (lanes 1 and 4), Flag-N (lanes 2 and 5), and Flag-N + SUMO-1 (lanes 3 and 6), and immunoprecipitated with either anti-Flag (lanes 1, 2 and 3) or anti-SUMO-1 antibody (lanes 4, 5, and 6). The immunoprecipitated proteins were separated by SDS-PAGE under nonreducing conditions and analyzed by Western blotting with anti-Flag antibody. The major SUMO-1 modified forms of N protein are indicated by asterisks, and the immunoglobulin is indicated by Ig.

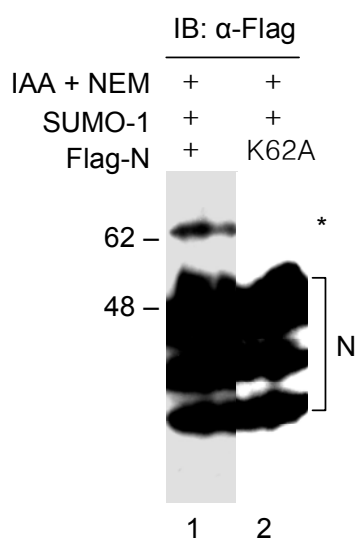


Fig. 3.4. Mapping of the major sumoylation site on SARS-CoV N protein. Cell lysates from HeLa cells overexpressing wild-type (lane 1) and K62A mutant N protein (lane 2) together with SUMO-1 were prepared in the presence of IAA and NEM. The polypeptides were separated by SDS-PAGE under non-reducing conditions and analyzed by Western blotting with anti-Flag antibody. The three major isoforms of N protein are indicated by brackets and the major SUMO-1 modified form of N protein is indicated by asterisks. Numbers on the left indicate molecular masses in kilodaltons.

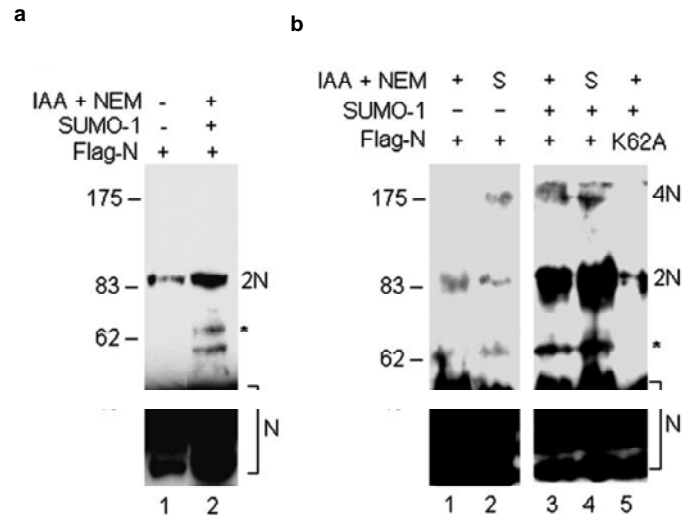
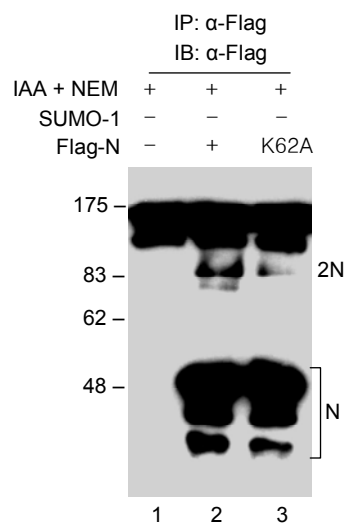


Fig. 3.5. Analysis of the homo-oligomerization of SARS-CoV N protein. a| HeLa cells overexpressing wild-type N protein only (lane 1) or together with SUMO-1 (lane 2) were lysed in the absence (lane 1) or presence of IAA and NEM (lane 2). The polypeptides were separated by SDS-PAGE under reducing conditions and analyzed by Western blotting with anti-Flag antibody. The three major isoforms of N protein are indicated by brackets and the major SUMO-1 modified form of N protein is indicated by asterisks. The dimers are also indicated. Numbers on the left indicate molecular masses in kilodaltons. b| HeLa cells overexpressing wild-type N protein only (lanes 1 and 2), wild-type + SUMO-1 (lanes 3 and 4) or the K62A mutant N protein + SUMO-1 (lane 5) were lysed in the presence of IAA and NEM (lanes 1, 3 and 5) or with preheated SDS loading buffer (lanes 2 and 4). The polypeptides were separated by SDS-PAGE under non-reducing conditions and analyzed by Western blotting with anti-Flag antibody. The three major isoforms of N protein are indicated by brackets and the major SUMO-1 modified form of N protein is indicated by asterisks. The dimers and tetramers are also indicated. Numbers on the left indicate molecular masses in kilodaltons.

a



b

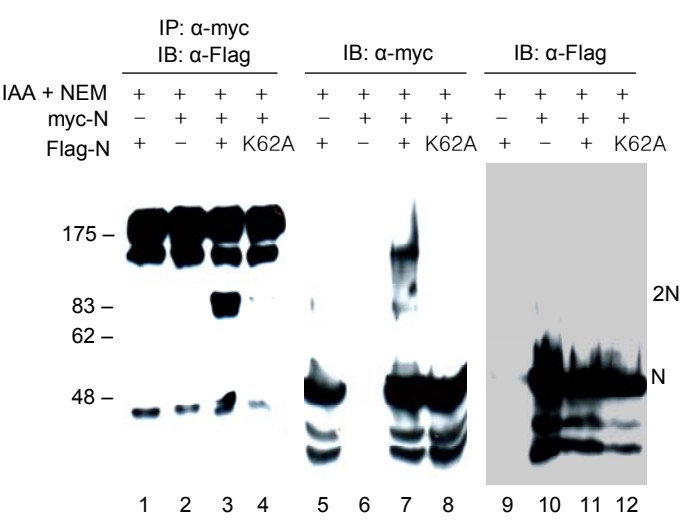


Fig. 3.6. Further analysis of the homo-oligomerization of SARS-C-V N protein. a| HeLa cells overexpressing the empty pKT0-Flag (lane 1), wild-type N protein (lane 2), or the K62A mutant N protein (lane 3) were lysed in the presence of IAA and NEM. The lysates were immunoprecipitated with anti-Flag antibody. The precipitated polypeptides were separated by SDS-PAGE under non-reducing conditions and analyzed by Western blotting with anti-Flag antibody. The three major isoforms of N protein, the N protein dimer, and the immunoglobulin are indicated. Numbers on the left indicate molecular masses in kilodaltons. b| HeLa cells overexpressing the Flag-tagged wild-type N protein alone (lane 1), the c-Myc-tagged wild-type N protein alone (lane 2), the Flag-tagged wild-type and c-Myc-tagged wild-type N protein (lane 3), and the Flag-tagged K62A mutant and c-Myc-tagged wild-type N protein (lane 4) were lysed in the presence of IAA and NEM. Polypeptides were immunoprecipitated with anti-Myc antibody, separated by SDS-PAGE under non-reducing conditions, and analyzed by Western blotting with anti-Flag antibody. The N protein dimer and the immunoglobulin are indicated. A band migrating at approximately 50 kDa, which may represent the antibody heavy chain, is also indicated. HeLa cells overexpressing the Flag-tagged wild-type N protein alone (lanes 5 and 9), the c-Myc-tagged wild-type N protein alone (lanes 6 and 10), the Flag-tagged wild-type and c-Myc-tagged wild-type N protein (lanes 7 and 11), and the Flag-tagged K62A mutant and c-Myc-tagged wild-type N protein (lanes 8 and 12) were lysed in the presence of IAA and NEM. Polypeptides were separated by SDS-PAGE under non-reducing conditions, and analyzed by Western blotting with either anti-Flag antibody (lanes 5-8), or anti-Myc antibody (lanes 9-12). The three major isoforms of N protein and the dimer are indicated.

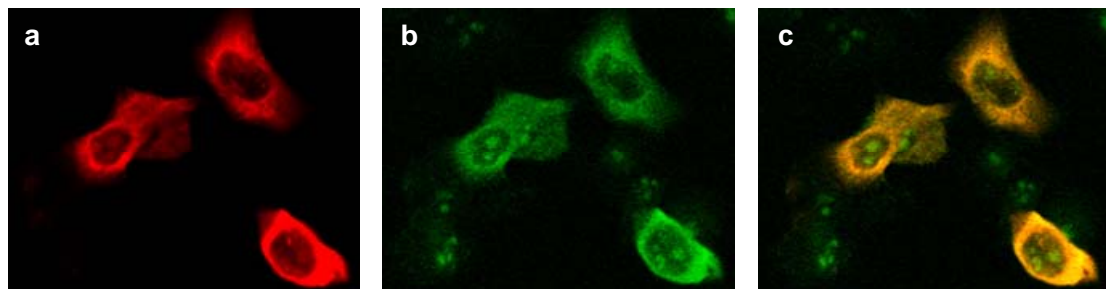


Fig. 3.7. Nucleolar localization of SARS-CoV N protein. Indirect immunofluorescent staining of HeLa cells expressing the Flag-tagged N protein was carried out at 18 h posttransfection with mouse anti-Flag (a) and rabbit anti-fibrillarin (b) antisera. The N protein was then detected by TRITC-conjugated anti-mouse secondary antibodies and fibrillarin was detected by FITC-labeled anti-rabbit antibodies. Panel c represents the merged images. All images were taken using a Zeiss LSM510 META laser scanning confocal microscope.

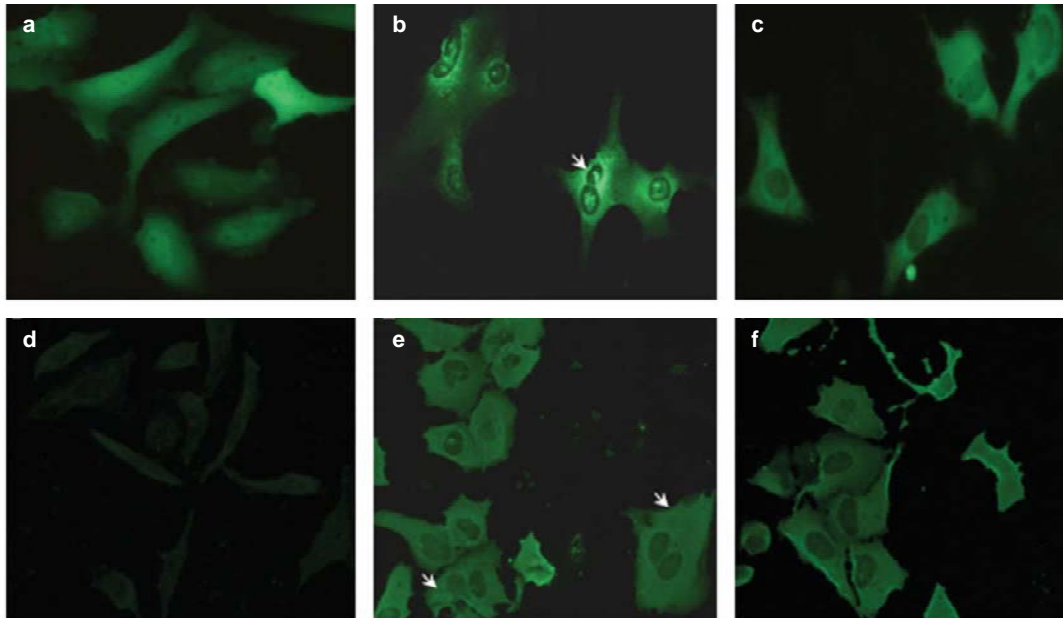


Fig. 3.8. Subcellular localization of SARS-CoV N protein constructs. HeLa cells expressing EGFP (a), N-EGFP (b) and K62A-EGFP fusion protein (c) were detected directly under the fluorescence microscope at 36 h posttransfection. Indirect immunofluorescent staining of HeLa cells transfected with empty plasmid (d), wild-type N protein (e) and K62A mutant (f), was carried out at 18 h posttransfection with rabbit anti-SARS N antisera and FITC-labeled goat anti-rabbit antibodies. The multinucleated cells are indicated by arrows.

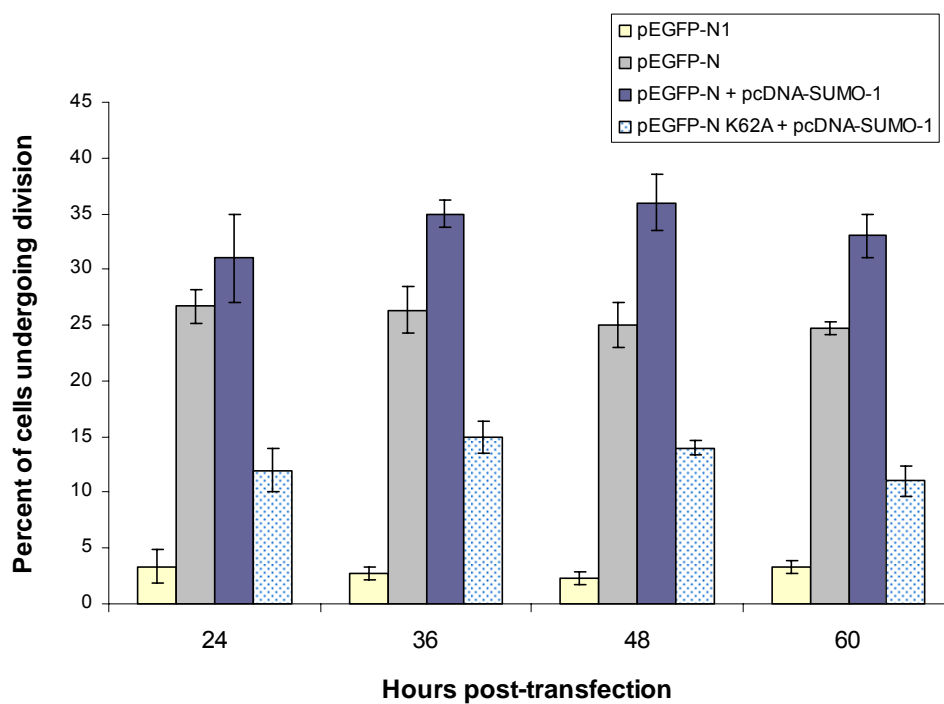


Fig. 3.9. Effects of sumoylation of SARS-CoV N protein on its interference of host cell division. Percentages of multinucleated cells among HeLa cells expressing EGFP, N-EGFP, N-EGFP + SUMO-1, and K62A-EGFP + SUMO-1 were calculated by counting the multinucleated cells among 300 green cells under the fluorescence microscope. The percentages and S.D. are results of three repeated experiments.

Chapter 4

Cell Cycle Arrest and Apoptosis Induced by the Coronavirus IBV in the Absence of p53

4.1. Introduction

Host factors participate in most steps of the viral replication cycle, including entry, viral gene expression, virion assembly, and release. Concomitantly, host gene expression and defenses are modulated by viruses to optimize viral replication (Ahlquist, 2003). One evidence the importance of which is increasingly emerging is the manipulation of host cell cycle progression (Op De Beeck and Caillet-Fauquet, 1997; Schang, 2003; Swanton and Jones, 2001).

A number of recent reports have highlighted the cell cycle perturbation properties of coronaviruses and their encoded proteins. Nevertheless, little is known about how these effects are brought out, and how the growth state of host cells influences coronavirus replication. In this study, we demonstrated that IBV infection imposed a growth-inhibitory effect on cultured cells by inducing cell cycle arrest at both S and G₂/M phases. The arrest was catalyzed by the modulation of various cell cycle regulatory genes and the accumulation of hypophosphorylated RB, but was independent of p53 status in host cells. Proteasome inhibitors such as lactacystin and NLVS could bypass the S-phase arrest by restoring the expression of corresponding cyclin-Cdk complexes. Moreover, our data showed that both S-phase and G₂/M-phase arrest were manipulated by IBV for the enhancement of viral replication.

Apoptosis constitutes part of the host cell defense against viral infection. For some viral gene products, apoptosis can also serve the purpose of releasing progeny virus and thus can play an important role in the viral life cycle during a lytic infection (Roulston et al., 1999). Various coronaviruses and their encoded proteins have been reported to be inducers of apoptosis. However, the involvement of p53, which is a key mediator of apoptosis, has never been reported. In this study, we examined the capability of IBV to induce caspase-dependent apoptosis in both p53-null H1299 cells

and wild-type p53-containing Vero cells and concluded that a p53-independent mechanism was recruited by IBV to induce apoptosis in cultured mammalian cells.

4.2. Results

4.2.1. IBV efficiently infects p53-null H1299 cells

IBV replication in wild-type p53-containing Vero cells (Shivakumar et al., 1995) resulted in typical cytopathic effects (CPE), i.e., rounding up and fusion of infected cells to form multinucleated giant syncytia, detachment of infected cells from the culture dish, and eventually cell lysis and death (Liu et al., 2001). Similar phenomena were observed in p53-null H1299 human lung carcinoma cells (Gjoerup et al., 2001) at 36 h post IBV infection (Fig. 4.1a). To address whether IBV could replicate efficiently in H1299 cells, we used the nucleocapsid protein as a marker and examined its expression at various times p.i. As can be seen in Fig. 4.1b, the protein was detected as early as 6 h post-infection (p.i.), and increased gradually to a relatively high level at 24 h p.i.

4.2.2. IBV replication inhibits cell proliferation

The observation of growth retardment in mammalian cells infected with IBV led us to speculate that IBV replication might inhibit host cell proliferation. H1299 and Vero cells were either mock-infected or infected with IBV at an MOI of 0.5 (IBV-I) or 1 (IBV-II). At various times p.i., determination of total cell number showed that IBV inhibited cell growth in an MOI- as well as time-dependent manner, and the reduction in cell number for H1299 cells was more significant than that of Vero cells (Fig. 4.2a). MTT assay was carried out to further examine the effect of IBV infection on growth viability of host cells. At an MOI of 1, IBV inhibited the growth of both cell lines efficiently, although H1299 cells were more sensitive to IBV infection (Fig. 4.2b). These results demonstrated that IBV infection inhibited cell proliferation, and

p53 status was not found to be a determinant of IBV-mediated growth inhibition. However, p53 might play a role in governing its efficiency, as the growth retardment was more obvious in cells that lack p53.

4.2.3. IBV infection induces cell cycle arrest in the S and G₂/M phases

We next investigated cell cycle profiles of mock-infected and IBV-infected cells, and deduced that the inhibitory effect on cell proliferation by IBV might be due to a perturbation of cell cycle progression. Asynchronously growing H1299 and Vero cells were mock-infected or infected with IBV. At various times p.i., cells were harvested and nuclear DNA was stained with propidium iodide (PI) before analysis by FACS. For both cell lines, slight increase (3%-10%) of S-phase cells was observed in IBV-infected cells at 6 and 12 h p.i. The increase of S-phase cells kept at levels of 7%-10% for Vero at 18 and 24 h p.i., but dramatically rose to 20% at 30 h p.i. Discrepantly, IBV-infected H1299 cells showed much higher increase (20%-30%) of S-phase cells starting from 18 h p.i. (Fig. 4.3 a and b, upper panel). We also observed the accumulation of G₂/M-phase cells from IBV-infected Vero cells at 18 and 24 h p.i. (15% and 6%, respectively). The accumulation of cells in the G₂/M phase was only observed at 30 h p.i. from IBV-infected H1299 cells (Fig. 4.3 a and b, upper panel).

To further investigate the cell cycle perturbation induced by IBV infection, we synchronized H1299 and Vero cells in the quiescent state by serum deprivation prior to infection. The cell cycle progression was re-started by serum stimulation and cells were subjected to FACS analysis. The cell cycle profiles of mock-infected and IBV-infected cells showed comparable levels of arrest in both the S phase (10%-30%) and the G₂/M phase (5%-15%) with those of asynchronously growing cells (Fig. 4.3b, lower panel).

The small proportion (less than 5%) of cells containing hypodiploid DNA in IBV-infected cells as shown by FACS analysis were demonstrated to be apoptotic cells (Fig. 4.13). However, the number is not commensurate with the reduction of cells after IBV infection, indicating that the IBV-induced cell growth suppression was not due to apoptotic cell death.

4.2.4. IBV infection stimulates cell cycle reentry in quiescent cells

FACS analysis also revealed that IBV infection selectively induced cell cycle entry. Quiescent H1299 cells were mock-infected or infected with IBV. After incubation for 3 h, fresh medium with 10% serum was added to stimulate cell cycle reentry. Cell cycle profiles showed that IBV infection remarkably decreased the proportion of G₀/G₁-phase cells and significantly increased the number of S-phase cells (Fig. 4.4a and b). Prior to infection, approximately 83% of serum-starved cells were arrested in the G₀/G₁ phase. At 12 and 18 h p.i., mock-infected cells showed 5% and 21% decrease of G₀/G₁-phase population and 12% and 24% increase of S-phase population. Much more dramatic decrease (15% and 45%, respectively) of G₀/G₁-phase cells and increase (17% and 48%, respectively) of S-phase cells were observed in IBV-infected cells at the two indicated time points (Fig. 4.4a and b). Similar phenomena could be seen in quiescent Vero cells as well (Fig. 4.3b, lower panel). Obviously, IBV infection in quiescent cells was sufficient to stimulate G₀/G₁-phase cell cycle progression.

4.2.5. IBV infection does not inhibit cytokinesis or mitotic exit

The exit from mitosis (M phase) or cytokinesis is the last critical decision during a cell-division cycle. Nucleocapsid proteins of coronaviruses have been

proposed to disrupt cytokinesis (Li et al., 2005a; Wurm et al., 2001). To explore the possibility that this N-protein-mediated cytokinesis impediment might be responsible for the accumulation of G₂/M-phase cells induced by IBV infection, we synchronized Vero cells with colchicine which blocks replicating cells at the metaphase. FACS analysis showed more than 85% of cells were arrested in the metaphase (Fig. 4.5a and b). Colchicine was removed to allow mitotic exit before the cells were either mock-infected or infected with IBV. The proportion of IBV-infected cells that passed mitosis was similar to that of mock-infected cells at 6 and 12 h p.i. (Fig. 4.5a and b). These data suggested that IBV infection did not block cytokinesis or mitotic exit. The cell cycle arrest in the G₂/M phase could be at an earlier stage, most probably the G₂/M boundary.

4.2.6. Quantitative analysis of cyclins and Cdks in IBV-infected cells

As progression through the cell cycle is mediated by Cdks complexed with corresponding cyclins (Morgan, 1995; Nurse, 2004; Sherr and Roberts, 1999), we analysed whether IBV infection would modulate the protein levels of such cell cycle regulators. Firstly, various Cdks and cyclins were detected in both Mock-infected (M) and IBV-infected (I) H1299 cells by Western blot analysis at various times p.i. At 12 h p.i., levels of cyclins B1 and E were 2-fold higher in IBV-infected cells compared to mock-infected cells. However, a marginal decrease of Cdk2 at the protein level was observed in IBV-infected cells, while levels of cyclins A and D1, as well as Cdk1 were unchanged (Fig. 4.6a). At 18 h p.i., the expression of Cdk2 and cyclin D1 began to decrease to 2- and 3-fold lower, respectively, in IBV-infected cells, and levels of cyclins A, B1 and E, as well as Cdk1 were almost identical between mock-infected and IBV-infected cells (Fig. 4.6a). A 3-fold reduction of cyclins A, B1 and D1 at

protein levels, and a 2-fold reduction of Cdk 1 and Cdk2 at protein levels were observed in IBV-infected cells at 24 h p.i. (Fig. 4.6a). At 30 h p.i., levels of cyclins A and D1 drastically dropped to 5- and 10-fold lower, respectively, in IBV-infected cells, and level of Cdk1 was 3-fold lower in IBV-infected cells compared to mock-infected cells (Fig. 4.6a). We also compared protein levels of these Cdks and cyclins among untreated (U), IBV-infected (I) and mock-infected (M) Vero cells. A noticeable drop (2-fold) of Cdk2 expression began at 12 h p.i. and became more prominent (5-fold) thereafter (Fig. 4.6b). At 24 h p.i., levels of cyclins A, B1 and D1, as well as Cdk1 appeared to be 2- or 3-fold lower in IBV-infected cells compared to untreated or mock-infected cells, while level of cyclin E remained unchanged (Fig. 4.6b). Flagged levels of cyclins A, B1 and D induced by IBV infection were more apparent at 36 h p.i., and all cyclins and Cdks detected were down-regulated in IBV-infected cells (Fig. 4.6b). However, in both H1299 and Vero cells, protein levels of nucleolar protein fibrillarin remained to be constant under all conditions indicated (Fig. 4.6a and b). IBV replication in both cell lines was monitored by detecting the expression of the nucleocapsid protein, and levels of the protein increased gradually throughout the infection (Fig. 4.6a and b). Reprobing of the membranes with anti- β -tubulin antibody confirmed equal protein loading in each case (Fig. 4.6a and b).

4.2.7. IBV infection causes the accumulation of hypophosphorylated RB

The RB protein plays a key role in cell cycle progression and the checkpoint pathways activate the protein to its hypophosphorylated form, leading to G₀/G₁, S or G₂/M cell cycle arrest (Harbour and Dean, 2000; Weinberg, 1995). It is well documented that the accumulation of active RB can be attributed to the reduced levels of Cdks and cyclins (Mittnacht, 1998). The modulation of cyclins A, B1, Cdk1 and

p107, which are all E2F target genes, was also reported to be a consequence of RB activation (Helin, 1998; Saudan et al., 2000). We therefore postulate that IBV infection might activate the hypophosphorylation of RB, which was responsible for, or alternatively, appeared as a downstream effect of the down-regulation of various Cdk's and cyclins we observed. To address this possibility, we examined the phosphorylation status of RB in IBV-infected H1299 cells by Western blot analysis at various times p.i. In mock-infected cells, only one slightly retarded band, which represented the hyperphosphorylated form of RB (ppRB) could be detected at 12, 18 and 24 h p.i., and at 30 h p.i. a minor fast-migrating band representing the hypophosphorylated RB (pRB) was seen (Fig. 4.7). In contrast, pRB was detectable in IBV-infected cells from as early as 18 h p.i., and was accumulated to a much higher level at 30 h p.i. (Fig. 4.7). We also noticed an obvious loss of ppRB in IBV-infected cells at 24 and 30 h p.i., indicating that the cells were not able to progress through the cell cycle smoothly (Fig. 4.7).

4.2.8. Effect of IBV infection on the expression of cellular p53 and p21

Modulation of the activity of p53 is a key event in the replication of many viruses (Collot-Teixeira et al., 2004; Nakamura et al., 2001). In cellular response to viral infection, p53 is generally activated to induce either cell cycle arrest or apoptosis. A major target for p53 is the p21 gene, which encodes a CKI of the Cip/Kip family, plays important roles in regulating cell cycle progression or arrest (Harper et al. 1995; Niculescu, 1998). To further explore the mechanisms of the IBV-induced cell cycle arrest, we examined whether IBV infection could induce p53 expression and accumulation of p21. Vero cells were mock-infected or infected with IBV, and the amounts of proteins were determined by Western blot analysis. The results showed

that there was no obvious difference in both the overall expression level and the post-translational modification state of p53 between mock- and IBV-infected cells throughout the infection (Fig. 4.8). The p21 expression was reduced by 3 and 4 folds in IBV-infected cells at 12 and 18 h p.i., respectively, but then went up and kept identical to that of mock-infected cells at 24 and 30 h p.i. (Fig. 4.8). Determination of β -tubulin levels confirmed equal protein loading (Fig. 4.8). These data suggested that IBV-induced cell cycle arrest was independent of the activation of p53 and p21.

4.2.9. Bypass of IBV-induced S-phase arrest by proteasome inhibitors

We have shown above that IBV infection induced concomitant inhibitions of S-phase progression and G₂/M transition through down-regulating various cell cycle regulatory proteins including cyclins A, B1, and D1, as well as Cdk1 and Cdk2. we next investigated the mechanisms of cyclins and Cdks regulation following IBV infection. Cyclin A, Cdk2 and cyclin D1 were reported to be degraded through a ubiquitin-dependent proteolysis pathway in tumor cells and coxsackievirus-infected cells (Chen et al., 2004b; Luo et al., 2003). We therefore performed a series of experiments where IBV-infected H1299 cells were exposed to proteasome inhibitors, lactacystin and NIP-leu-leu-leu-vinylsulfone (NLVS). As can be seen in Fig. 4.9a, IBV infection induced a 22% increase of S-phase cells at 24 h p.i. Both lactacystin and NLVS annulled the S-phase cell cycle arrest and restored cyclin A, Cdk2 and cyclin D1 protein expression in a dose-dependent manner (Fig. 4.9a and b). Lactacystin was shown to be more efficient than NLVS, except in the case of cyclin A stabilization (Fig. 4.9a and b). The effectiveness of the proteasome inhibitors was also proved by the accumulation of multiubiquitinated proteins (Fig. 4.9b). Protein levels of Cdk1 remained unchanged under identical experimental conditions (Fig. 4.9b). The

data suggested that IBV infection specifically facilitated the degradation of cyclin A, Cdk2 and cyclin D1 through a proteasome-dependent mechanism, leading to relevant cell cycle arrest, which was reversible, once the corresponding cell cycle regulatory genes were stabilized or restored.

4.2.10. IBV-induced cell cycle arrest is not catalyzed by the spike protein-mediated cell fusion

It has been discovered that viruses catalyze cell fusion as a means of cell-to-cell transmission, which appears to require either suppression of p53-dependent apoptosis or arrest of the cell cycle that would otherwise lead to cell death by “mitotic catastrophe” (Parris, 2005). One major biological activity of coronavirus S glycoprotein is to induce membrane fusion. This activity may be required for viral entry into cells or for cytopathic effects. And the S protein alone is sufficient to cause virus-host and cell-cell fusion (Lai and Cavanagh, 1997). To explore possible association between the IBV-induced cell cycle arrest and the S protein-mediated cell fusion, we examined cell cycle profiles of S protein-expressing cells. Vero cells were transiently transfected with a fusion-competent S protein (SP) or a fusion-incompetent S protein (EP3). Cell fusion could be observed under microscope in SP-expressing cells, but not in EP3-expressing cells (data not shown). At various times post-transfection, cells were harvested and subjected to FACS analysis. There was no significant difference in distributions of cell cycle phases among mock-, SP- and EP3-transfected cells at any given time post-transfection (Fig. 4.10a and b). SP and EP3 were efficiently expressed as demonstrated by Western bolt analysis (Fig. 4.10c). These data showed that the IBV-induced cell cycle arrest was not associated with the cell fusion mediated by S protein.

4.2.11. Cell cycle arrest in the S phase promotes IBV replication

Manipulation of cell cycle progression is an important strategy exploited by many viruses to create favorable cellular conditions for viral replication. To determine the influence of cell cycle status on IBV replication, we synchronized both H1299 and Vero cells with methotrexate to create an S-phase environment. If virus replication were more active during a certain phase, then the accumulation of cells in this phase should produce more virus than normally cycling cells. Virus production was determined by: i) virus titration assays, and ii) comparing expression levels of IBV N protein.

Asynchronously growing H1299 and Vero cells were treated with DMSO or methotrexate for 20 h, followed by incubation in fresh medium for 6 h to release the cell cycle progression. After release, more than 70% of the cells in the methotrexate group entered the S phase. Cells were then either mock-infected or infected with IBV and processed at various times p.i. for virus titration assays, analysis of cell cycle profiles, and assessment of N protein expression. At 24 h p.i., plaque assays showed an 8-fold ($P < 0.05$) increase of virus titers in the methotrexate-treated Vero cells, compared with DMSO-treated ones (Fig. 4.11d). In response to the methotrexate-imposed S-phase environment, titers of IBV were increased by approximately 7-fold ($P < 0.05$) and 11-fold ($P < 0.05$) at 24 and 48 h p.i., respectively, as revealed by TCID₅₀ in H1299 cells (Fig. 4.11c). Western blot analysis displayed higher expression levels of N protein at any time p.i. in both cell lines which were synchronized at the S phase by methotrexate treatment (Fig. 4.11e). Cells were stained with propidium iodide and analyzed by FACS to ensure that the cell cycle inhibitor was having the expected effects (Fig. 4.11a and b).

4.2.12. G₂/M-phase-dependent replication of IBV

Experiments were also carried to determine the effect of G₂/M-phase cell cycle arrest on IBV replication. Asynchronously growing H1299 and Vero cells were mock-infected or infected with IBV, followed by incubation with either DMSO as a control or methotrexate, which blocked replicating cells at the G₁/S border that led to a total loss of cells in the G₂/M phase, while percentage of cells in the S phase remained unchanged (Fig. 4.12 a and b). Plaque assays showed a 6-fold decrease ($P < 0.05$) of virus titers in methotrexate-treated Vero cells at 24 h p.i. (Fig. 4.12d). In H1299 cells, titers of IBV were decreased by approximately 7-fold ($P < 0.05$) and 10-fold ($P < 0.05$) at 24 and 48 h p.i., respectively, as a consequence of methotrexate-mediated G₁/S border stalling and loss of G₂/M-phase cells (Fig. 4.12c). Furthermore, reduced levels of IBV N protein were observed in the methotrexate group (Fig. 4.12e).

4.2.13. p53-independent apoptosis induced by IBV

Our previous studies showed that IBV infection induces caspase-dependent apoptosis in cultured cells (Liu et al., 2001). This conclusion was based on experiments showing that chromosomal condensation, DNA fragmentation, caspase-3 activation, and poly (ADP-ribose) polymerase degradation was detected in IBV-infected Vero cells. Addition of the general caspase inhibitor z-VAD-FMK to the culture media showed inhibition of the hallmarks of apoptosis.

To further elucidate the molecular mechanism by which IBV induces apoptosis, especially the requirement of p53 for induction of apoptosis by IBV, we studied the pro-apoptotic effects upon IBV infection in both p53-null H1299 cells and wild-type p53-containing Vero cells. The induction of apoptosis was measured by flow cytometry to determine the extent of genomic DNA fragmentation, i.e. the

occurrence of the characteristic nuclear hypodiploid DNA content. Interestingly, a substantial increase in the number of apoptotic cells was observed at 36 h p.i. in both cell lines. In contrast, only minor apoptosis was observed in mock-infected cells (Fig. 4.13a and b). Nuclear staining with Hoechst showed apparently distorted and fragmented nuclei in both H1299 and Vero cells from 36 h p.i. (Fig. 4.13c). As the TUNEL assay could distinguish apoptotic cells undergoing DNA fragmentation by adding labeled nucleotides to the fragmented DNA ends, cells even at early stages of apoptosis could be visualized by horseradish peroxidase colorimetric reaction. As shown in Fig. 4.13c, the number of TUNEL signal-positive cells drastically increased at 36 h p.i. in both cell lines. These data strongly suggest that IBV infection is capable of inducing apoptosis irrespective of the presence or absence of functional cellular p53.

4.3. Discussion

Cell cycle manipulation and apoptosis are two major biological events in virus-infected cells. In this study, we demonstrated that the avian coronavirus IBV infection imposes an early stage cell cycle arrest and a later stage apoptosis on cultured mammalian cells. The cell cycle arrest was at S and G₂/M phases, and was catalyzed by the modulation of various cell cycle regulatory genes and the accumulation of hypophosphorylated RB. Our data also showed that the cell cycle arrest manipulated by IBV was beneficial for viral replication. In addition, the IBV-induced cell cycle arrest and apoptosis were detected in both p53-null cell line (H1299) and wild-type p53-containing cell line (Vero), suggesting that p53 activation was not involved in these two events. Multiple overlapping p53-dependent and p53-independent pathways partake of the regulation of G₂/M transition and S phase progression in response to genotoxic stress, such as viral infection (Taylor and Stark, 2001). In the case of IBV infection, both p53-dependent and p53-independent pathways could be engaged by p53-positive cells for either cell cycle arrest or apoptosis. However, since neither p53 overall expression level nor its post-translational modification state was affected upon IBV infection, the participation of p53-dependent pathways could be ruled out.

Our results showed that expression of both S and G₂ cyclins (cyclins A and B1) was strongly down-regulated in IBV-infected cells. Interestingly, the levels of G₁ cyclins (cyclins D1 and E) were also reduced. Viral replication could affect cyclin levels through regulating their synthesis and degradation. Microarray analyses with several IBV-permissive cell lines revealed that there were no significant changes in cyclins A, B1, D1 and E mRNA levels in IBV-infected cells, suggesting that IBV

infection does not affect mRNA transcription or stability of these cyclins (data not shown).

Cyclins A and D1, and Cdk2 were proved to be destructed through ubiquitin-mediated proteolysis. The reduced levels of cyclin E, cyclin B1, and Cdk1, which are all E2F target genes, could be attributed to the accumulation of active RB. We therefore postulate that modulation of these cell cycle regulatory genes could be a consequence of the RB activation. RB may therefore play an important role in the cellular response to IBV. This speculation is supported by the fact that RB accumulated in its hypophosphorylated active form after IBV infection. RB is critical for regulating cell cycle progression at different phases (Chen and Makino, 2004; Niculescu et al., 1998; Weinberg, 1995). HPV E6 proteins induce proliferation by promoting activation of the Cdk complexes and consequently of RB hyperphosphorylation (Malanchi et al., 2004). Adeno-associated virus Rep78 induces a complete arrest within S phase by a mechanism involving the ectopic accumulation of active RB (Saudan et al., 2000). Inactivation of RB by viral proteins such as adenovirus E1a and human papillomavirus E7, or a complete lack of RB, as is the case with RB-null cells, results in the inability of Rep78 to induce the total S phase block (Berthet et al., 2005). There was other evidence based on over-expression of constitutively active RB mutants revealed that RB could interfere with S phase progression (Chew et al., 1998; Knudsen et al., 1998). In addition, RB can also regulate both p53-dependent and p53-independent apoptosis triggered by DNA damage through an unknown mechanism (Wang, 1997). Activated RB inhibits DNA synthesis. It is likely that this property of RB, when induced by IBV infection, inhibits the S phase progression.

Although p53 has been well documented to take part in the cellular response to DNA damage, the mechanism used by p53 to initiate apoptosis is controversial. In some cases, apoptosis is induced in a p53-independent manner. Several viral encoded proteins have been reported to induce p53-independent apoptosis. These include simian virus 40 small t antigen (Gjoerup et al., 2001), adeno-associated virus type 2 Rep78 (Schmidt et al., 2000), adenovirus E4orf4 protein (Kleinberger, 2000), HPV E6 (Fan et al., 2005b), papillomavirus E2 (Desaintes et al., 1999), and the chicken anemia virus protein apoptin (Teodoro et al., 2004). Our studies suggest that IBV infection results in a late stage apoptosis as measured by FACS, nuclear morphology, TUNEL staining, and suppression of cell death by the broad caspase inhibitor QVD. Induction of apoptosis by IBV was not restricted to the p53-null H1299 cells but was also observed in the wild-type p53-containing Vero cells. These results demonstrate that IBV infection induces apoptosis independently of p53.

Viruses must modulate apoptotic pathways to control the lifespan of their host in order to complete their replication cycle. IBV-induced apoptosis occurs at a late stage of virus infection in both H1299 and Vero cells. It is possible that apoptosis occurs at a time when IBV synthesis is complete and the progeny is released from the infected cells.

Crosstalk exists between cell cycle and apoptosis (Gil-Gomez et al., 1998; King and Cidlowski, 1998). Apoptosis is sometimes an end point of stalled cell cycle progression, but in other cases, it appears to require progression through the cell cycle (Santiago-Walker et al., 2005). One characteristic feature of DNA damage-induced apoptosis, especially in the absence of wild-type p53, is the activation of a G₂/M cell cycle checkpoint prior to cell death. However, G₂/M cell cycle arrest is not always a prerequisite for subsequent apoptosis. Moreover, it has been reported that apoptosis is

frequently associated with the G₁ phase of the cell cycle (King and Cidlowski, 1998) and arrest at the late G₁ or S phase may accelerate or potentiate apoptosis (Meikrantz et al., 1994). In addition, apoptosis was shown to be a consequence of the S-phase arrest imposed by IFN- β in human papilloma virus-infected cervical carcinoma cell line ME-180 (Vannucchi et al., 2005). The cell cycle arrest and apoptosis were shown to be independent of p53, but the apoptosis was mediated by the tumor necrosis factor-related apoptosis-inducing ligand (TRAIL) in a manner dependent on the S-phase deregulation (Vannucchi et al., 2005). In our study, apoptosis may mechanistically link to the cell cycle arrest induced by IBV infection, but it is unlikely that the former is merely a consequence of the later. However, it is possible that cell cycle arrest in IBV-infected cells prevents the induction and execution of early cell death in infected cells.

We demonstrated that IBV could manipulate cell cycle for the enhancement of viral replication. Cellular functions that are essential for virus replication can provide useful targets for antiviral agents. Increased understanding of the interactions between IBV infection and host cell cycle regulation may provide new insights into viral replication and viral pathogenicity and may lead to new avenues for therapeutic intervention in coronavirus-induced diseases.

It is not clear whether the three different IBV-induced phenomena, namely, growth suppression, cell cycle arrest, and apoptosis, might be regulated by same pathway? Furthermore, the question whether IBV-induced apoptosis is required for viral infection is unresolved yet. Further study is needed to clarify these points.

Figures

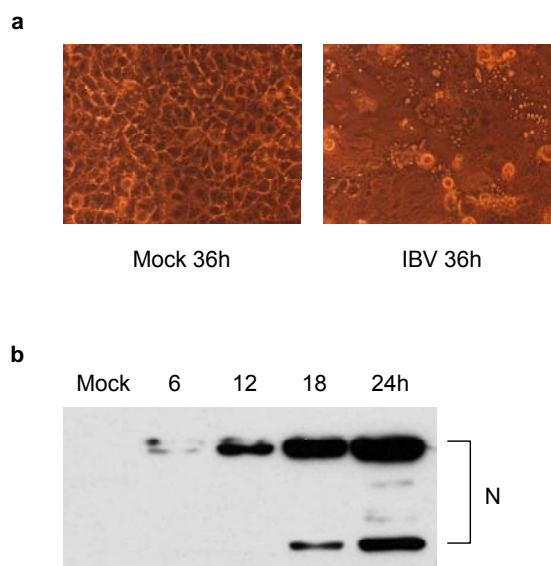


Fig. 4.1. IBV efficiently infects p53-null H1299 cells. H1299 cells were mock-infected (Mock) or infected with IBV at an MOI of 1 (IBV). a| At 36 h p.i., morphological characteristics of the cells were observed under a light microscope. b| At the indicated times p.i., cells were lysed with SDS sample buffer, and equal amounts of protein from the samples were tested by Western blot analysis against probes for IBV N protein. The data are representative of three independent experiments with similar results.

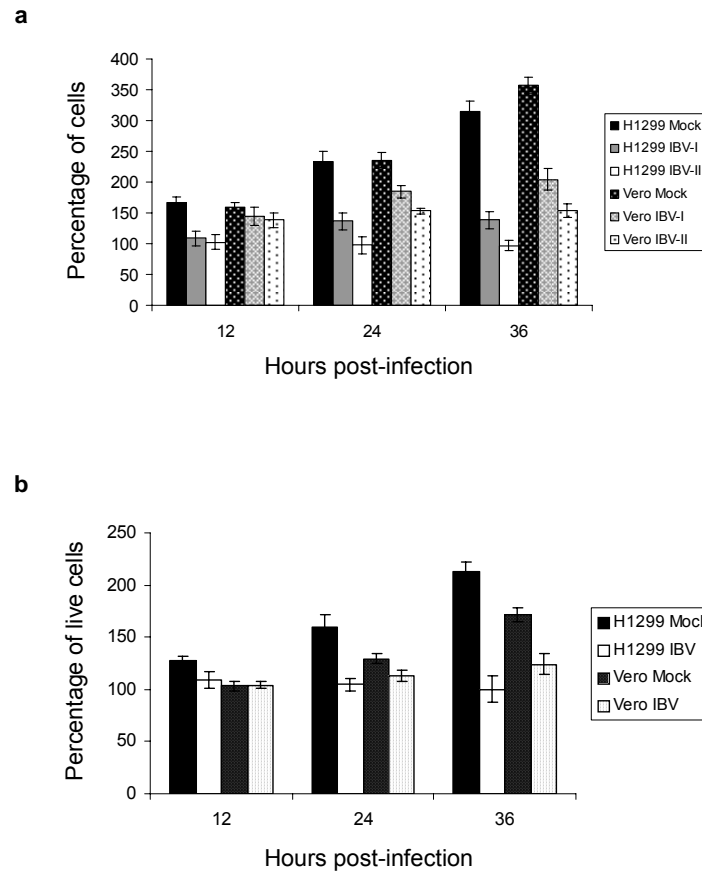


Fig. 4.2. IBV replication in both H1299 and Vero cells inhibits cell proliferation. a| H1299 and Vero cells at 50% confluence in six-well plates were mock-infected (Mock) or infected with IBV at an MOI of 0.5 (IBV-I) or 1 (IBV-II). At various times p.i., cell numbers were counted in a hemocytometer. The data are presented as percentage of cell numbers compared with that of mock-infected cells at 0 h p.i. The percentages and S.D. are results of five repeated experiments. b| MTT assay. H1299 and Vero cells at 50% confluence in 96-well plates were mock-infected (Mock) or infected with IBV at an MOI of 1 (IBV). At various times p.i., MTT assays were performed. The data are presented as percentage of live cell numbers compared with that of mock-infected cells at 0 h p.i. The percentages and S.D. are results of five repeated experiments.

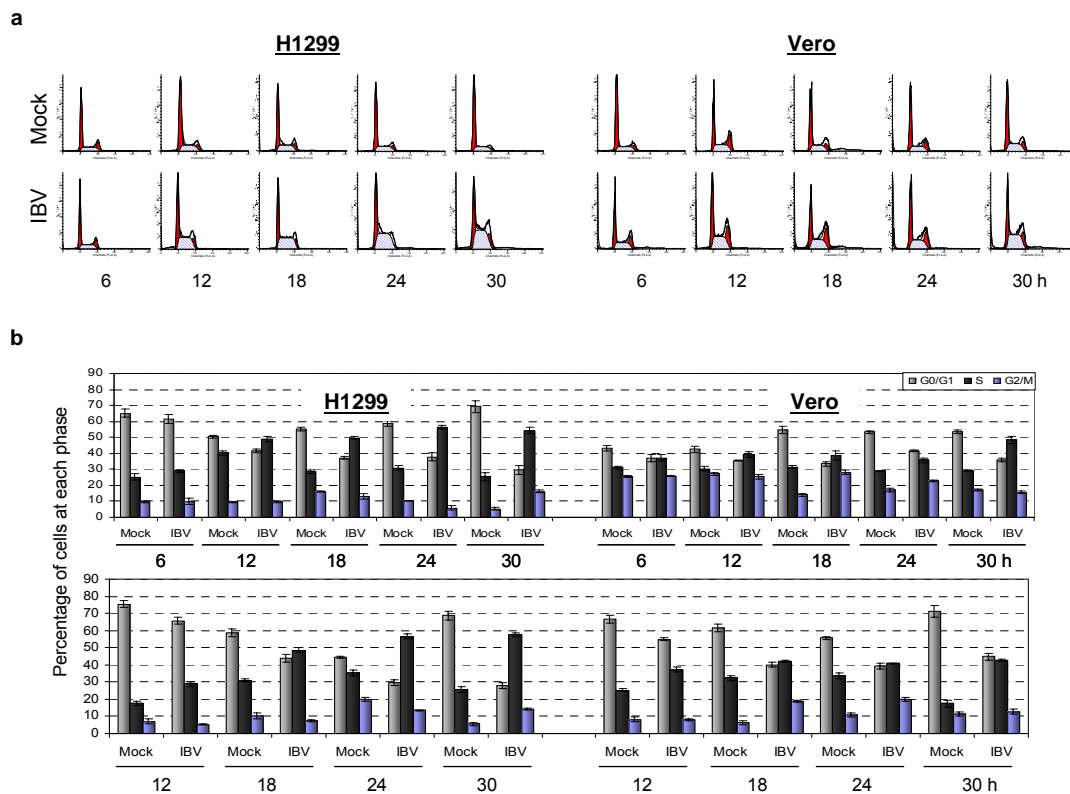


Fig. 4.3. IBV infection induces S and G₂/M arrest in both asynchronously growing and synchronized H1299 and Vero cells. a| H1299 and Vero cells were mock-infected (Mock) or infected with IBV at an MOI of 1 (IBV). At the indicated times p.i., cells were collected and stained with propidium iodide for FACS analysis. The data are from one of five repeated experiments with similar results. b| The histograms in panel a were analyzed by the ModFit LT Mac 3.0 software to determine the percentage of cells in each phase of the cell cycle in both asynchronously growing and synchronized H1299 and Vero cells. The data are presented as means and S.D. for five repeated experiments.

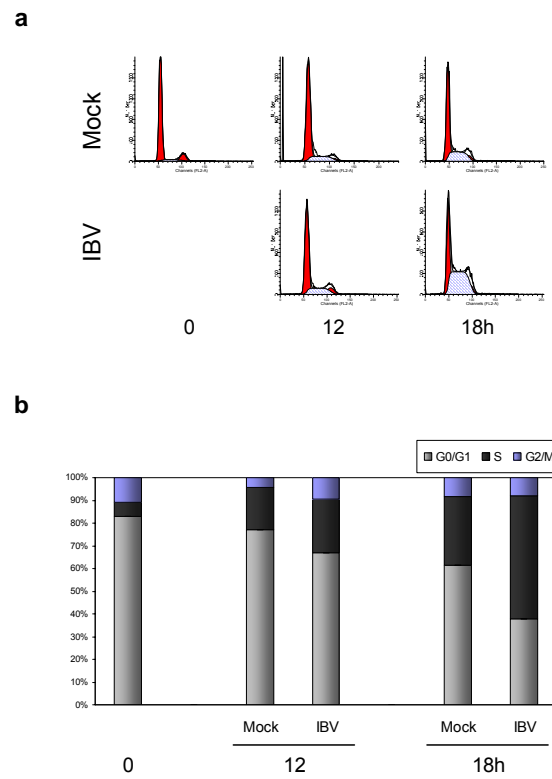


Fig. 4.4. IBV infection stimulates cell cycle reentry in quiescent cells. a| Serum-starved H1299 cells were mock-infected (Mock) or infected with IBV at an MOI of 1 (IBV). After 3 h of virus adsorption, fresh medium containing 10% newborn calf serum was added to the cells, and cell cycle profiles at the indicated times p.i. were determined by FACS analysis. The data are from one of five repeated experiments with similar results. b| The histograms in panel a were analyzed by the the ModFit LT Mac 3.0 software to determine the percentage of cells in each phase of the cell cycle.

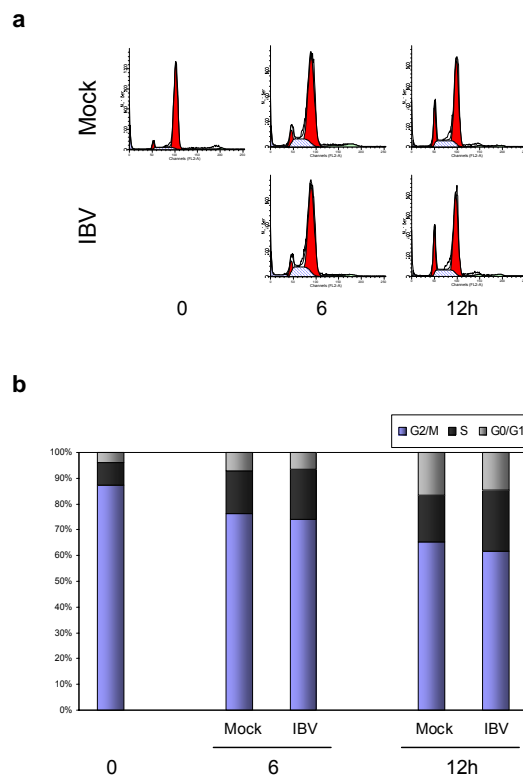


Fig. 4.5. IBV infection does not inhibit cytokinesis and mitotic exit. a| Colchicine-treated Vero cells were mock-infected (Mock) or infected with IBV at an MOI of 1 (IBV). After 3 h of virus adsorption, fresh medium was added to the cells, and cell cycle profiles at the indicated times p.i. were determined by FACS analysis. The data are from one of five repeated experiments with similar results. b| The histograms in panel a were analyzed by the the ModFit LT Mac 3.0 software to determine the percentage of cells in each phase of the cell cycle.

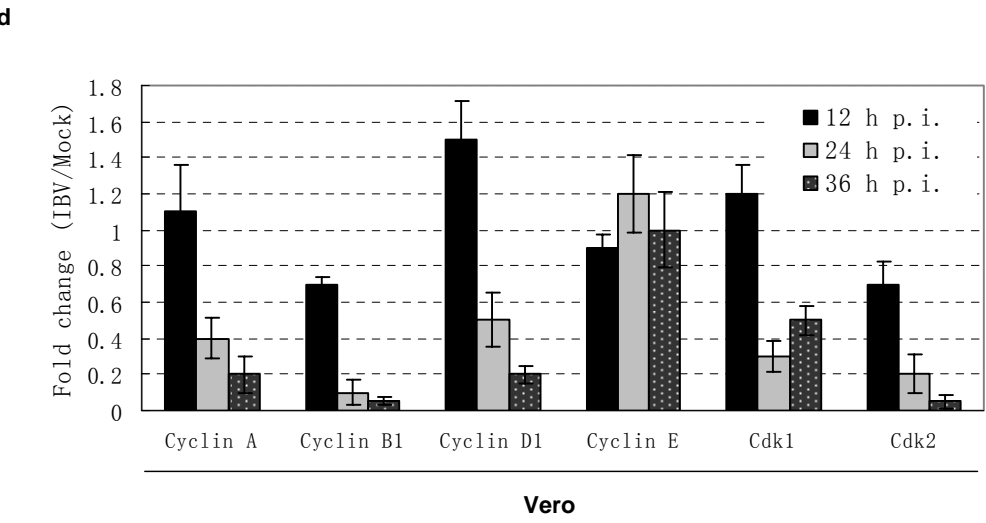
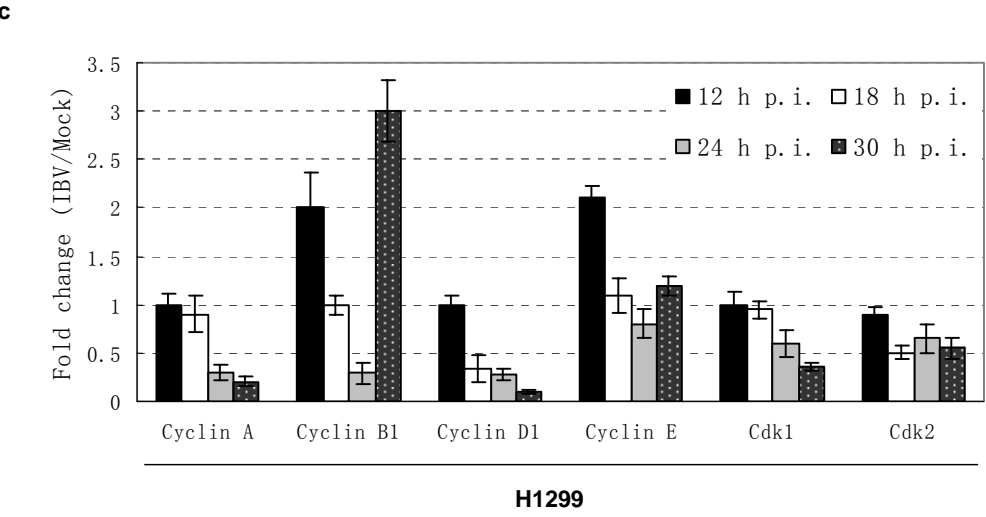
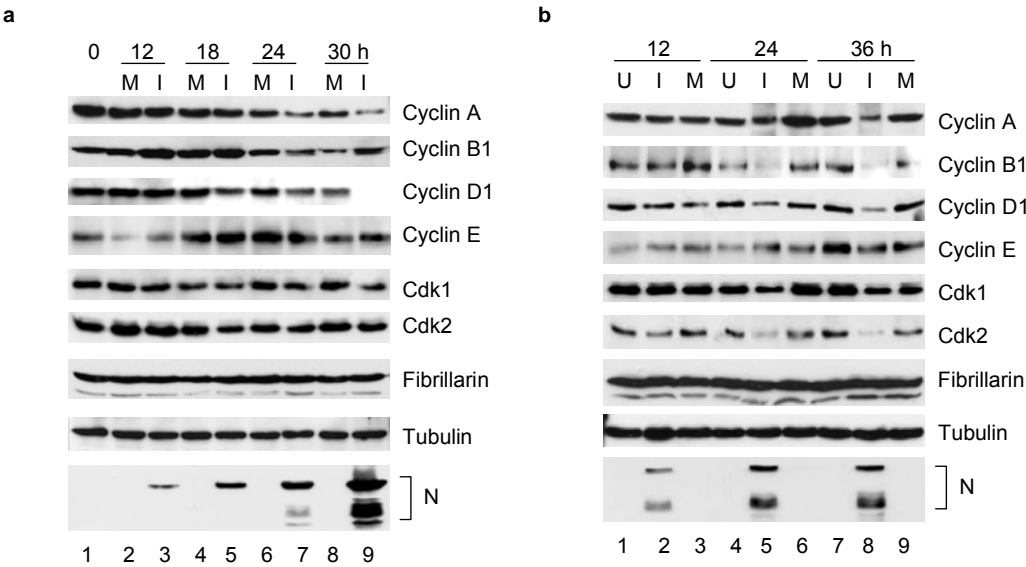


Fig. 4.6. Immunoblot analysis of cyclins and Cdks. a| H1299 cells were mock-infected (M) or infected with IBV (I). At the indicated times p.i., cells were lysed with SDS sample buffer, and equal amounts of protein from the samples were tested by Western blot analysis against probes for cyclins A, B1, D1, and E, Cdk1, Cdk2, as well as fibrillarin. Protein amounts were normalized as shown with tubulin. Viral replication was confirmed by the detection of the accumulation of N protein. The data were representatives of three repeated experiments with similar results. b| Vero cells were uninfected (U), IBV-infected (I) and mock-infected (M). At the indicated times p.i., cells were lysed, and various cell cycle regulatory proteins were tested by Western blot analysis, including cyclins A, B1, D1, and E, as well as Cdk1 and Cdk2. The expression of fibrillarin was also analyzed. Protein amounts were normalized as shown with tubulin. Viral replication was confirmed by the detection of the accumulation of N protein. The data are representative of three independent experiments with similar results. c| Cyclin and Cdk amounts in panel a were quantified by densitometric analysis and normalized against an internal control (tubulin). Bars indicate the ratio of cyclin and Cdk amounts in IBV-infected H1299 cells to those in mock-infected H1299 cells. The results are presented as means and SEs ($n=3$). d| Cyclin and Cdk amounts in panel b were quantified by densitometric analysis and normalized against an internal control (tubulin). Bars indicate the ratio of cyclin and Cdk amounts in IBV-infected Vero cells to those in mock-infected Vero cells. The results are presented as means and SEs ($n=3$).

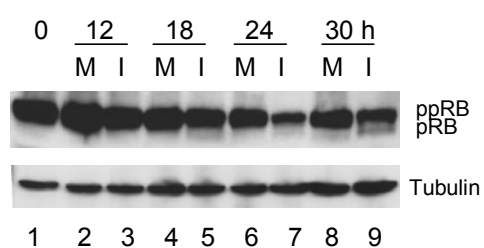


Fig. 4.7. Immunoblot analysis of RB. Asynchronously growing H1299 cells were mock-infected (M) or infected with IBV at an MOI of 1 (I). At the indicated times p.i., cells were lysed and subjected to Western blot analysis for RB and tubulin. Hypophosphorylated forms of RB (pRB) appeared as fast-migrating bands, and hyperphosphorylated RB (ppRB) appeared as slightly retarded bands. The data are representative of three independent experiments with similar results.

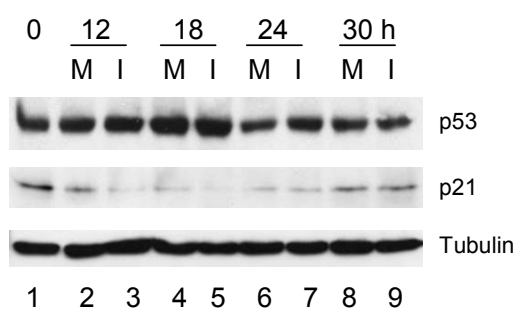


Fig. 4.8. Immunoblot analysis of p53 and p21. Vero cells were mock-infected (M) or infected with IBV (I). At the indicated times p.i., cell lysates were collected and subjected to Western blot analysis for p53, p21, and tubulin. The data are representative of three independent experiments with similar results.

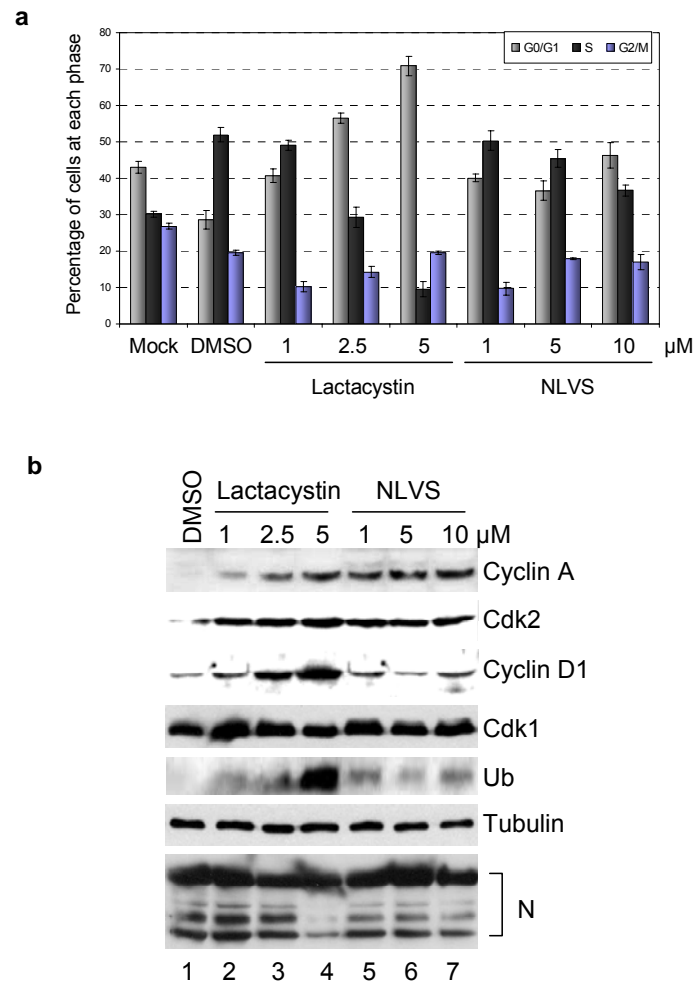


Fig. 4.9. Bypass of IBV-induced S-phase arrest by proteasome inhibitors. a| Vero cells were preincubated with increasing concentrations of proteasome inhibitors, lactacystin and NLVS, for 30 min and then infected with IBV. At 24 h p.i., the cells were collected and subjected to FACS analysis. The data are presented as means and S.D. for three repeated experiments. b| Cell lysates were analyzed for cyclin A, cyclin D1, Cdk1, Cdk2, ubiquitin, tubulin, and N protein expression by Western blotting. The data are representative of three independent experiments with similar results.

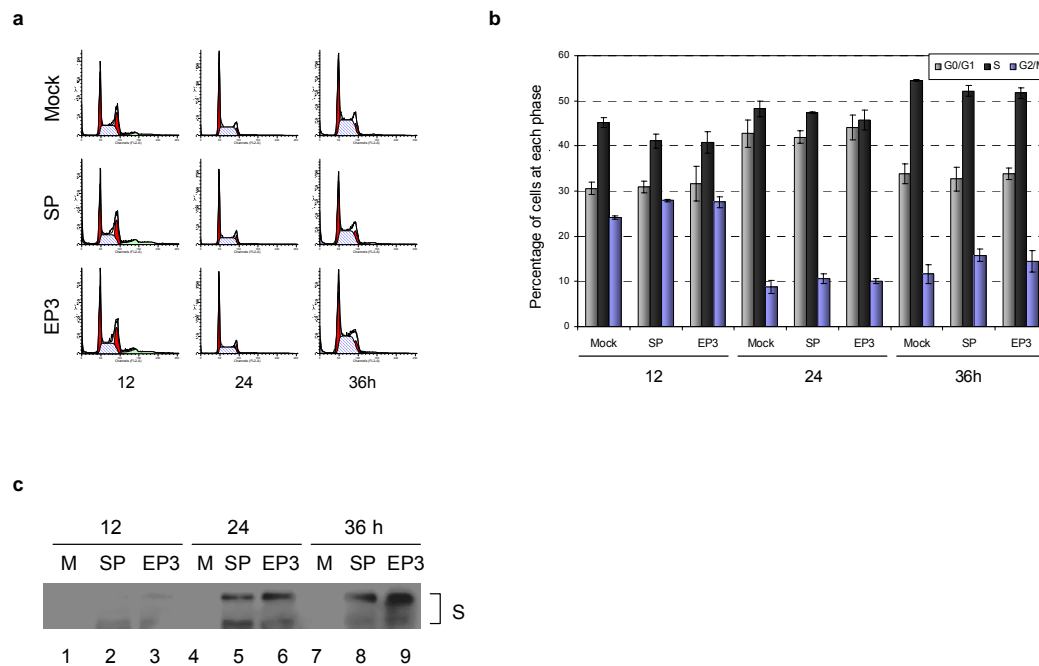


Fig. 4.10. IBV-induced cell cycle arrest is not catalyzed by the spike protein-mediated cell fusion. a| Vero cells were mock-transfected (Mock) or transiently transfected with a fusion-competent S protein (SP) or a fusion-incompetent S protein (EP3). At various times post-transfection, cells were harvested and subjected to FACS analysis. The data are from one of three repeated experiments with similar results. b| The histograms in panel a were analyzed by the the ModFit LT Mac 3.0 software to determine the percentage of cells in each phase of the cell cycle. The data are presented as means and S.D. for three repeated experiments. c| Cell lysates were analyzed for IBV S protein expression by Western blotting. The data are representative of three independent experiments.

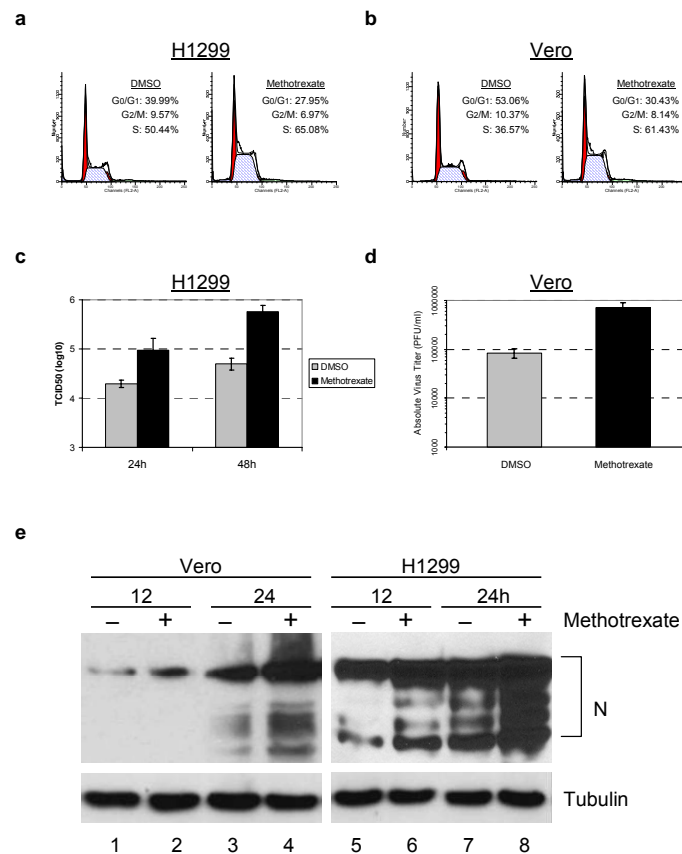


Fig. 4.11. S-phase arrest promotes IBV replication. Asynchronously growing H1299 and Vero cells were treated with DMSO or methotrexate for 20 h, followed by incubation in fresh medium for 6 h to release the cell cycle progression. Cells were then infected with IBV at an MOI of 1 and processed at various times p.i. for different assays. a| Cell cycle profiles of H1299 cells at 24 h p.i. were obtained by FACS analysis. b| Cell cycle profiles of Vero cells at 24 h p.i. were obtained by FACS analysis. Representative profiles are shown. c| TCID₅₀ in H1299 cells. d| Plaque assay in Vero cells. The data are presented as means and S.D. for three repeated experiments. e| Cell lysates were subjected to Western blot analysis for IBV N protein and tubulin expression. The data are representative of three independent experiments with similar results.

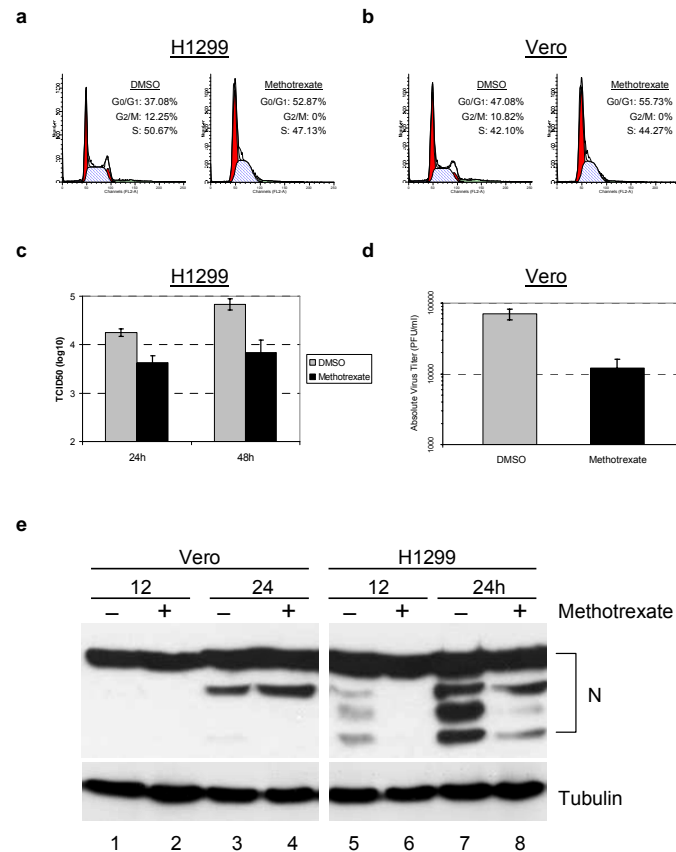
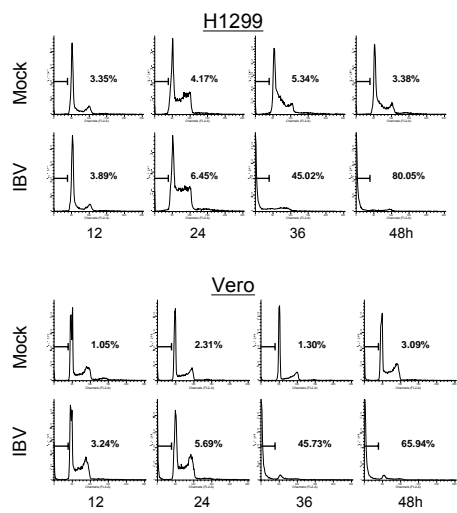
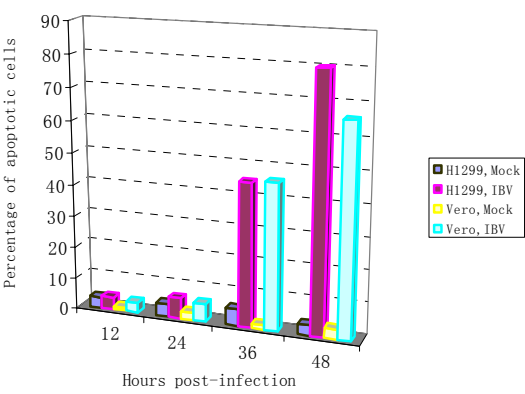


Fig. 4.12. G₂/M-phase-dependent replication of IBV. Asynchronously growing H1299 and Vero cells were mock-infected or infected with IBV at an MOI of 1, followed by incubation with either DMSO or methotrexate. Cells were then processed at various times p.i. for different assays. a| Cell cycle profiles of H1299 cells at 24 h p.i. were obtained by FACS analysis. b| Cell cycle profiles of Vero cells at 24 h p.i. were obtained by FACS analysis. Representative profiles are shown. c| TCID₅₀ in H1299 cells. d| Plaque assay in Vero cells. The data are presented as means and S.D. for three repeated experiments. e| Cell lysates were subjected to Western blot analysis for IBV N protein and tubulin expression. The data are representative of three independent experiments with similar results.

a



b



c

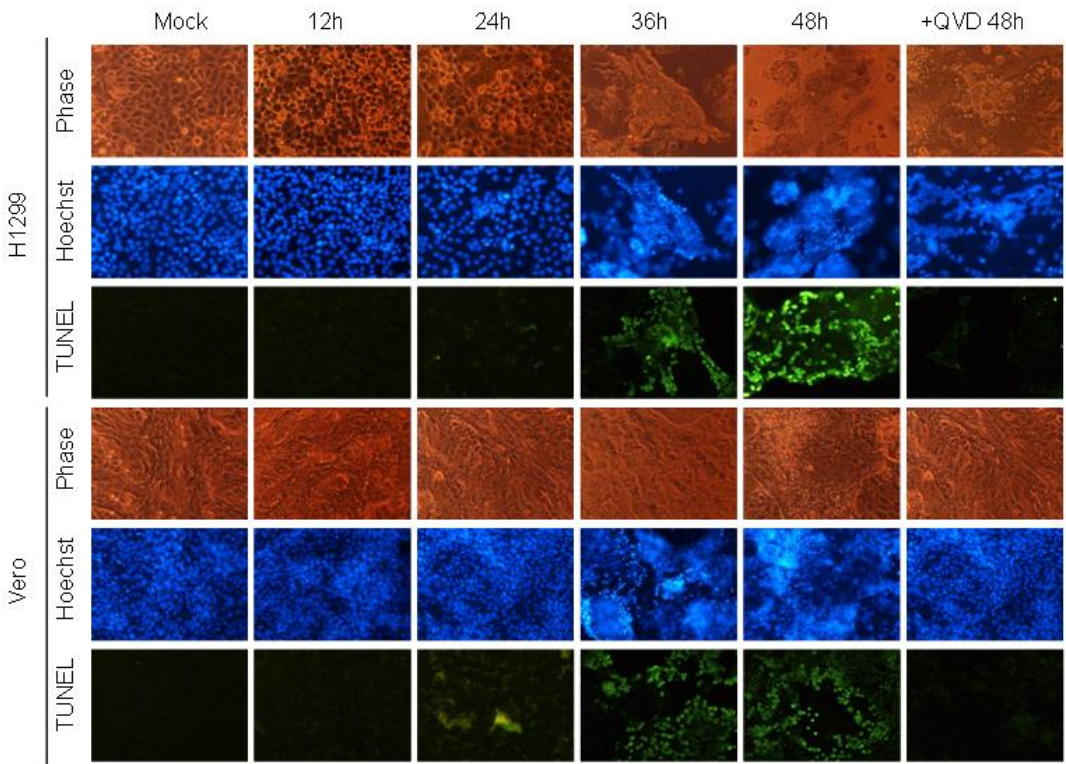


Fig. 4.13. IBV infection induces apoptotic cell death in both H1299 and Vero cells. a| H1299 and Vero cells were mock-infected (Mock) or infected with IBV at an MOI of 1 (IBV). At the indicated times p.i., total cells were collected and stained with propidium iodide for flow cytometric analysis. The bar in each graph represents cells with sub-G₀/G₁ (hypodiploid) DNA content (indicated as a percentage). The data are representative of three independent experiments with similar results. b| The histograms in panel a were analyzed to determine the percentage of sub-G₀/G₁ cells. c| Morphological characteristics and TUNEL assays of mock- and IBV-infected H1299 and Vero cells at 12, 24, 36, and 48 h p.i. Cells were mock-infected (Mock) or IBV-infected, stained with Hoechst 33342 or performed TUNEL assay with an *in situ* cell death detection kit, fluorescein at the indicated times p.i., and viewed in a fluorescence microscope. At 48 h p.i., QVD was added, and the effects of QVD on morphological changes of nuclei and TUNEL assay of IBV-infected cells were detected. The data are representative of three independent experiments with similar results. Phase, phase-contrast images; Hoechst, nuclear staining; TUNEL, TUNEL assay.

Chapter 5

General Discussion and Future Directions

5.1. Virus-host interactions

Understanding virus-host interactions is very important, since they constitute the basis of viral pathogenesis. Upon virus infection, the host responds by activating immune mechanisms, cell cycle control machinery, and apoptosis through different cellular signaling pathways. Whether an infection becomes persistent or is cleared depends largely on how effectively the virus is able to modulate these host responses. Concomitantly, host factors participate in most steps of virus life cycle, including entry, viral gene expression, virion assembly, and release (Ahlquist et al., 2003). Identification of such host factors and virus-host interactions can help define mechanisms of viral pathogenesis within the host cell as well as the roles of individual viral protein during infection.

Through various genetic and biochemical approaches, many host factors have been identified to interact with viral genomic RNAs or replication proteins, and, in some cases, they have been functionally linked to viral replication. Recent data show that host factors play important roles in assembling the viral RNA replication complex, selecting and recruiting viral RNA replication templates, activating the complex for RNA synthesis, and other steps of virus life cycle. Each of such virus-host interactions may contribute to the host and tissue specificity, or pathogenesis of infections, and may represent a potential target for virus control. While significant progress has been made, crucial details remain to be elucidated. For example, it remains unclear exactly if and how viral proteins interact with many factors of host cells. Progress in these areas could be reached due to the many advances, such as the availability of RNA interference approaches, microarray techniques, and other improved molecular biology tools.

Coronaviruses are representatives of enveloped, positive-strand RNA viruses which encompass almost one-third of all virus genera. They are unique in many aspects of viral structure and replication, such as their exceptionally large RNA genomes, nested subgenomic mRNAs, discontinuous transcription mechanism, high-frequency RNA recombination, and the unusually large number of gene products associated with RNA synthesis (Lai and Holmes, 2001). Although coronaviruses have been much more actively studied since the occurrence of the SARS epidemic in 2003, many questions regarding the molecular mechanisms of replication as well as the pathogenesis remain unresolved. One of these unresolved questions which call for ardent research needs is to reevaluate the role of host factors in coronavirus replication. Research in our lab has been focused on the molecular cell biology of virus-host interactions and on replication mechanisms and pathogenesis of coronaviruses. And data reported in this dissertation are from the work I have done during the period of my Ph.D. study.

5.2. Interaction of SARS-CoV N protein with Ubc9

In a yeast two-hybrid screen for cellular proteins that interact with the SARS-CoV N protein, several potentially interesting interactions have been found that were not reported by others at the time. In particular, we identified human Ubc9, an E2 SUMO-conjugating enzyme and an essential protein in mammalian cells. As yeast two-hybrid screen often recognizes proteins that interact non-specifically with the “bait” protein, we further characterized the N-Ubc9 interaction both *in vitro* by GST-N fusion protein binding experiment and *in vivo* by coimmunoprecipitation and colocalization of the two proteins.

Ubc9 is structurally very similar to E2 enzymes in the ubiquitination pathway, and binds, along with SUMO-1, to the SUMO consensus motif on the target protein. It plays a central role in sumoylation-mediated cellular pathways and regulating target protein functions.

It should be noted that although SUMO-1 conjugation is the principal known activity of Ubc9, there was also evidence that it would interact with proteins without leading to sumoylation. For example, Ubc9 interaction with TNF- α receptor 1 and kinase MEKK1 leads to upregulation of signal transduction to NF- κ B (Saltzman et al., 1998). In both cases, no SUMO-1 conjugation was detected, suggesting that Ubc9 is involved in ways other than through SUMO-1 association. Interaction between Ubc9 and importin 13, an importin β -related receptor primarily involved in nuclear import, suggests an involvement for Ubc9 in nuclear translocation of cytoplasmic targets (Mingot et al., 2001). Ubc9 has equally been shown to interact with an NLS sequence of homeobox protein Vsx-1, thus mediating Vsx-1 nuclear localization (Kurtzman and Schechter, 2001). Vsx-1 does not appear to be sumoylated, and a C93S mutant of Ubc9 is still able to restore Vsx-1 nuclear localization in a cell line with a low level of endogenous Ubc9 (Kurtzman and Schechter, 2001). Finally, Ubc9 interaction influences human herpesvirus 6 IE2 protein's function in the absence of sumoylation (Tomoiu et al., 2006).

Although many Ubc9-interacting proteins have been described already, especially assuming that all SUMO-1 conjugated proteins would interact with Ubc9, no simple motif on Ubc9 has yet been defined as the interacting region. Even though a SUMO-interacting motif has been brought to light (Song et al., 2004), it can not account for sumoylation-independent interactions, as just described. Further work is needed to characterize the putative consensus binding motif, if any, on Ubc9.

5.3. Sumoylation of the SARS-CoV N protein promotes its homo-oligomerization

We demonstrated that SARS-CoV N protein is a sumoylated protein. The major sumoylation site was mapped to the ⁶²lysine residue. Further expression and characterization of wild-type N protein and K62A mutant revealed that sumoylation of the N protein drastically promotes its homo-oligomerization, and plays certain roles in its subcellular localization and the N protein-mediated interference of host cell division.

Self-association of N protein has been well studied and suggested to be essential for the formation of viral nucleocapsid core, and maturation in viral replication. Although very little is known about coronaviruses regarding protein-protein interactions involved in the assembly of viral nucleocapsids, the coronavirus N proteins examined so far all possess cysteine residues which can potentially establish disulfide linkages. However, the SARS-CoV N protein does not contain any cysteine, suggesting a non-covalent interaction between N proteins may be necessary and sufficient for nucleocapsid assembly in SARS-CoV. Our most interesting finding in this study showed that sumoylation of the SARS-CoV N protein enhances its homo-oligomerization. It is possible that host factors involved in the sumoylation system play an important role in the SARS-CoV replication cycle. Systematic testing this possibility would rely on the availability of an infectious cloning system, as developed on IBV in our lab (Fang et al., 2006; Tan et al., 2006).

5.4. Aberrant cell cycle progression induced by IBV infection enhances viral replication

In the second part of this study, using IBV as the model, we characterized the two major cellular responses, cell cycle arrest and apoptosis upon coronavirus infection. Our results demonstrated that IBV infection induces cell cycle arrest at both S and G₂/M phases by modulating the expression of various host genes, including cyclins, Cdks, and RB protein. Proteasome inhibitors, such as lactacystin and NLVS, could bypass the S-phase arrest by restoring the expression of corresponding cyclin/Cdk complexes, indicating that the ubiquitination-mediated proteasomal degradation system plays a vital role in controlling the levels of cellular proteins in IBV-infected cells and thus regulates cell cycle progression. Most interestingly, our data showed that both S-phase and G₂/M-phase arrest are manipulated by IBV for the enhancement of viral replication.

Viral replication is governed by cellular characteristics, such as species, cell type, differentiation state, cell cycle status, and immune status, as well as by viral genetics. For successful propagation, viruses may manipulate cell cycle progression to create a more favorable environment (Op De Beeck and Caillet-Fauquet, 1997; Schang, 2003; Swanton and Jones, 2001). As cellular components fluctuate during the cell cycle, these manipulations can force the cell into a phase that is favorable for virus replication. For example, with DNA viruses, viral genome replication may require coordination with host cell DNA replication in S phase (Schang, 2003). The S phase is important because it involves precise duplication of the whole genome, which carries all genetic messages for the next generation. S-phase-dependent enhancement of viral replication or viral RNA synthesis has been elucidated for dengue virus 2, human cytomegalovirus, and hepatitis C virus (Helt and Harris, 2005; Petrik et al., 2006; Scholle et al., 2004). EBV skillfully blocks the host response and actively promotes an S-phase-like environment advantageous for viral lytic replication (Kudoh

et al., 2004; Kudoh et al., 2005). Furthermore, cell cycle dependence for retroviruses may include both S phase and mitosis (Katz et al., 2005).

It seems that G₂/M arrest may also be a common strategy employed by viruses to optimize virion production. For instance, cell cycle arrest in G₂/M boosts both early and late steps of HIV infection (Goh et al., 1998; Groshel and Bushman, 2005). Coxsackievirus, however, replicates more slowly in cells arrested in G₂/M when compared with cells arrested either in G₁ or at the G₁/S boundary (Feuer et al., 2002). The G₂/M arrest results in a change in cellular physiology that is more conducive to HIV infection, but it is also possible that a simple increase in cell surface area due to arrest would promote viral entry. Moreover, protein synthesis is greater in G₂/M phase, which most likely has a knock-on effect for virus assembly and hence increases virus output.

5.5. Cell cycle arrest and apoptosis in IBV-infected cells are p53-independent

The IBV-induced cell cycle arrest and apoptosis were shown to be p53-independent, since both events could occur in p53-null H1299 cells, as well as in wild-type p53-containing Vero cells, and IBV infection did not affect the expression of p53 in host cells.

In cellular responses to DNA damage or viral infection, an important role of p53 is to maintain the integrity of the genome by inducing cell cycle arrest until damage has been repaired or by inducing apoptosis in cells constituting a risk for the organism (Vogelstein et al., 2000). Nevertheless, p53-independent pathways also regulate the G₂/M transition and S phase completion upon these genotoxic stresses (Taylor et al., 1999). The different pathways engaged are cell type-dependent. It was shown that inhibitory phosphorylation of Cdk1 is essential for the p53-independent G₂

arrest, and is dependent on the protein kinases Chk1 and Chk2 (Taylor and Stark, 2001). The mechanism of p53-independent S phase arrest, however, is still not clear.

A few viral proteins have been reported to induce p53-independent apoptosis. The mechanism how p53-defective cells are sensitized to apoptosis is still not clear. Since the cell death is p53 independent, it may involve other p53 family members, such as p73. Recent studies have revealed that substantial components of the p53-independent pathway are mediated by p73. Overexpression of both p53 and p73 leads to apoptosis through activation of apoptotic machinery (Kaelin, 1999). They can also transactivate downstream effectors such as p21, MDM2, and GADD45 to regulate cell cycle progression. Further investigations have demonstrated that p73 but not p53 is the downstream effector and target of the nuclear tyrosine kinase c-Abl (Agami et al., 1999; Gong et al., 1999; Yuan et al., 1999), the activation of which by DNA damage induces cell apoptosis. It will be of interest to investigate whether p73 plays a role in IBV-induced apoptosis.

Although p21 has been considered an important p53 target in response to DNA damage, its expression by the p53-independent pathways has been observed in many cell types. It has also been shown in several systems that down-regulation of p21 leads to apoptosis (Fan et al., 2005b). Consistent with these observations, up-regulation of p21 inhibited apoptosis (Gorospe et al., 1996). p21 might inhibit the Cdk1 activity, whose aberrant activation induced apoptosis in a variety of cell types (Shi et al., 1994).

5.6. Novelty and significance of our work

We, for the first time, reported that a coronavirus structural protein (N) undergoes posttranslational modification by sumoylation, and the functional

implication of this modification in the formation of coronavirus ribonucleoprotein complex, virion assembly and virus-host interactions. This finding broadens our understanding of the potential mechanisms involved in regulating the coronavirus functions. In terms of its putative role in viral replication cycle, we also think that sumoylation of the N protein represents a promising target for developing anti-SARS-CoV inhibitors.

The key observations in our second part of study have several implications for understanding the coronavirus-induced cell cycle arrest and more specifically, the effect of cell cycle manipulation on viral replication, and roles of cellular growth regulatory proteins p53 and RB, and the ubiquitination-mediated proteasomal degradation system play in the IBV-induced arrest. Studies of coronaviruses in the context of cellular growth state would shed light on mechanisms governing viral replication, dissemination and pathogenesis *in vivo*. A better understanding of coronavirus-host interactions will ultimately lead to the development of anti-viral approaches, such as vaccines and drugs.

5.7. Future directions

5.7.1. Systematic characterization of coronavirus-host interactions

Using RNA interference and microarray techniques, we would be able to map the global regulation of host cell gene expression by coronavirus infection, thus identifying interesting interactions which might be involved in coronavirus replication cycles and pathogenesis. These techniques will also facilitate our efforts to characterize host antiviral mechanisms, as well as viral modulation of host antiviral defense mechanisms.

5.7.2. Post-translational modifications of coronavirus N proteins

5.7.2.1. Phosphorylation

Multifunctional proteins are often regulated by phosphorylation, and this phenomenon is particularly common to positively charged, nucleic acid binding proteins that make up viral nucleocapsids. The consequence of viral N protein phosphorylation in general falls into one of three categories: modulation of nucleic acid binding activity, regulation of nuclear localization, or mediation of protein-protein interactions such as oligomerization (Wootton et al., 2002). In some cases, viral transcription and replication are regulated by phosphorylation of N protein (Law et al., 2003; Wu et al., 2002), but it still needs to determine whether this is a general mechanism for other positive-strand RNA viruses.

Coronavirus N proteins are known to be phosphorylated, although the mechanism by which phosphorylation of the N protein plays a role in the coronavirus life cycle is not well understood. The project will focus on this molecular aspect of the IBV N protein, including: (i) to determine the precise phosphorylation sites on the N protein; and (ii) to investigate the influence of N protein phosphorylation on the virus life cycle.

As our lab has succeeded in constructing the infectious full-length genomic cDNA of IBV (Fang et al., 2006; Tan et al., 2006), once the phosphorylation sites are identified, we could use this approach to introduce the mutations into the IBV genome to determine the role of N protein phosphorylation in modulating viral replication.

In addition, kinase inhibitors can be used. Kinases affect various cellular functions and hence the use of kinase inhibitors is likely to have either a direct or indirect effect on the virus life cycle.

5.7.2.2. Sumoylation

SUMO conjugation of virus-encoded proteins has been linked to virus life cycle. We wonder whether sumoylation of the SARS-CoV N protein would affect SARS-CoV replication. To verify this hypothesis, we will use reverse genetic approaches to introduce a K62A mutant of the N protein into the SARS-CoV genome, and then observe the infectivity of the recombinant viruses.

5.7.3. Crosstalk between IBV-induced cell cycle arrest and apoptosis

Deregulation of the cell cycle has been frequently associated with apoptosis induction (King and Cidlowski, 1998). In some models, apoptosis may be viewed as a consequence of conflicting growth signals. FACS analysis in our study suggests a possible correlation between the ability of IBV to modulate cell cycle progression and apoptosis. This possibility will be further addressed through the manipulation of cell cycle and induction/suppression of apoptosis.

5.7.4. Further characterization of IBV-induced apoptosis

It is possible that IBV would regulate the expression of certain genes to induce apoptosis. RNA microarray technology can be used to compare gene expression in the presence or absence of IBV. Genes whose expression is found to be significantly altered in the presence of IBV will have to be investigated for their role in IBV-induced apoptosis.

The elucidation of evasion strategies directed at apoptotic mechanisms can provide deeper insight into virus-host interactions that hopefully will yield better vaccine strategies.

5.7.5. Other questions remain to be elucidated

- (1) What is the biological significance of IBV-induced cell cycle arrest?
- (2) How IBV manages to accomplish its maximum replication prior to cell death?

References

- Adamson, A. L., and Kenney, S. (2001) Epstein-Barr virus immediate-early protein BZLF1 is SUMO-1 modified and disrupts promyelocytic leukemia bodies. *J. Virol.* **75**, 2388–2399.
- Agami, R., Blandino, G., Oren, M., and Shaul, Y. (1999) Interaction of c-Abl and p73alpha and their collaboration to induce apoptosis. *Nature*, **399**, 809–813.
- Ahlquist, P., Noueiry, A. O., Lee, W-M, Kushner, D. B., and Dye, B. T. (2003) Host factors in positive-strand RNA virus genome replication. *J. Virol.* **77**, 8181–8186.
- Almazan, F., Galan, C., and Enjuanes, L. (2004) The nucleoprotein is required for efficient coronavirus genome replication. *J. Virol.* **78**, 12683–12688.
- Almeida, M. S., Johnson, M. A., Herrmann, T., Geralt, M., and Wuthrich, K. (2007) Novel beta-barrel fold in the nuclear magnetic resonance structure of the replicase nonstructural protein 1 from the severe acute respiratory syndrome coronavirus. *J. Virol.* **81**, 3151–3161.
- An, S., Chen, C-J., Yu, X., Leibowitz, J. L., and Markino, S. (1999) Induction of apoptosis in murine coronavirus-infected cultured cells and demonstration of E protein as an apoptosis inducer. *J. Virol.* **73**, 7853–7859.
- Anand, K., Ziebuhr, J., Wadhwani, P., Mesters, J. R., and Hilgenfeld, R. (2003) Coronavirus main proteinase (3CLpro) structure: basis for design of anti-SARS drugs. *Science* **300**, 1763–1767.
- Arbely, E., Khattari, Z., Brotons, G., Akkawi, M., Salditt, T., and Arkin, I. T. (2004) A highly unusual palindromic transmembrane helical hairpin formed by SARS coronavirus E protein. *J. Mol. Biol.* **341**, 769–779.
- Arima, N., Kao, C. Y., Licht, T., Padmanabhan, R., and Sasaguri, Y. (2001) Modulation of cell growth by the hepatitis C virus nonstructural protein NS5A. *J. Biol. Chem.* **276**, 12675–12684.
- Asada, M., Yamada, T., Ichijo, H., Delia, D., Miyazono, K., Fukumuro, K., and Mizutani, S. (1999) Apoptosis inhibitory activity of cytoplasmic p21^{CIP1/WAF1} in monocytic differentiation. *EMBO J.* **18**, 1223–1234.
- Ashraf, H. (2003) WHO declares Beijing to be free of SARS. *Lancet* **361**, 2212.
- Bacon, L. D., Hunter, D. B., Zhang, H. M., Brand, K., and Etches, R. (2004) Retrospective evidence that the MHC (B haplotype) of chickens influences genetic resistance to attenuated infectious bronchitis vaccine strains in chickens. *Avian Pathology* **33**, 605–609.

- Banerjee, S., Narayanan, K., Mizutani, T., and Makino, S. (2002) Murine coronavirus replication-induced p38 mitogenactivated protein kinase activation promotes interleukin-6 production and virus replication in cultured cells. *J. Virol.* **76**, 5937–5948.
- Barber, G. N. (2001) Host defense, viruses and apoptosis. *Cell Death Diff.* **8**, 113–126.
- Baric, R. S., Nelson, G. W., Fleming, J. O., Deans, R. J., Keck, J. G., Casteel, N., and Stohlman, S. A. (1988) Interactions between coronavirus nucleocapsid protein and viral RNAs: implications for viral transcription. *J. Virol.* **62**, 4280–4287.
- Bartlam, M., Yang, H., and Rao, Z. (2005) Structural insights into SARS coronavirus proteins. *Curr. Opin. Struct. Biol.* **15**, 664–672.
- Baudoux, P., Carrat, C., Besnardeau, L., Charley, B., and Laude, H. (1998) Coronavirus pseudoparticles formed with recombinant M and E proteins induce alpha interferon synthesis by leukocytes. *J. Virol.* **72**, 8636–8643.
- Beaudette, F. R., and Hudson, C. B. (1937) Cultivation of the virus of infectious bronchitis. *J. Am. Vet. Med. Assoc.* **90**, 51–60.
- Benedict, C. A., Norris, P. S., and Ware, C. F. (2002) To kill or be killed: viral evasion of apoptosis. *Nature Immunol.* **3**, 1013–1018.
- Bergmann, C. C., Lane, T. E., and Stohlman, S. A. (2006) Coronavirus infection of the central nervous system: host-virus stand-off. *Nat. Rev. Microb.* **4**, 121–132.
- Berthet, C., Raj, K., Saudan, P., and Beard, P. (2005) How adeno-associated virus Rep78 protein arrests cells completely in S phase. *Proc. Natl. Acad. Sci. USA* **102**, 13634–13639.
- Bhardwaj, K., Guarino, L., and Kao, C. C. (2004) The severe acute respiratory syndrome coronavirus Nsp15 protein is an endoribonuclease that prefers manganese as a cofactor. *J. Virol.* **78**, 12218–12224.
- Bijlenga, G., Cook, J. K. A., Gelb, J., Jr., and de Wit, J. J. (2004) Development and use of the H strain of avian infectious bronchitis virus from the Netherlands as a vaccine: a review. *Avian Pathology* **33**, 550–557.
- Boggio, R., Colombo, R., Hay, R. T., Draetta, G. F., Chiocca, S. (2004) A mechanism for inhibiting the SUMO pathway. *Mol. Cell* **16**, 549–561.
- Boggio, R. and Chiocca, S. (2006) Viruses and sumoylation: recent highlights. *Curr. Opin. Microbiol.* **9**, 1–7.
- Bohren, K.M., Nadkarni, V., Song, J.H., Gabbay, K.H., and Owerbach, D. (2004) A M55V polymorphism in a novel SUMO gene (SUMO-4) differentially activates heat shock transcription factors and is associated with susceptibility to type I diabetes mellitus. *J. Biol. Chem.* **279**, 27233–27238.

- Booth, C. M., Matukas, L. M., Tomlinson, G. A., Rachlis, A. R., Rose, D. B., Dwosh, H. A., Walmsley, S. L., Mazzulli, T., Avendano, M., Derkach, P., Ephtimios, I. E., Kitai, I., Mederski, B. D., Shadowitz, S. B., Gold, W. L., Hawryluck, L. A., Rea, E., Chenkin, J. S., Cescon, D. W., Poutanen, S. M., and Detsky, A. S. (2003) Clinical features and short-term outcomes of 144 patients with SARS in the greater Toronto area. *JAMA* **289**, 2801–2809.
- Boursnell, M. E. G., Binns, M. M., and Brown, T. D. K. (1985) Sequencing of coronavirus IBV genomic RNA: Three open reading frames in the 5' 'unique' region of mRNA. *J. Gen. Virol.* **66**, 2253–2258.
- Bredenbeek, P. J., Pachuk, C. J., Noten, A. F., Charite, J., Luytjes, W., Weiss, S. R., and Spaan, W. J. (1990) The primary structure and expression of the second open reading frame of the polymerase gene of the coronavirus MHV-A59; a highly conserved polymerase is expressed by an efficient ribosomal frameshifting mechanism. *Nucleic Acids Res.* **18**, 1825–1832.
- Brian, D. A., Hogue, B. G., and Kienzle, T. E. (1995) The coronavirus hemagglutinin esterase glycoprotein. In “The Coronaviridae” (S. G. Siddell, ed.), pp. 165–179. Plenum Press, New York, N. Y.
- Brierley, I., Digard, P., and Inglis, S. C. (1989) Characterization of an efficient coronavirus ribosomal frameshifting signal: Requirement for an RNA pseudoknot. *Cell* **57**, 537–547.
- Bushell, M., and Sarnow, P. (2002) Hijacking the translation apparatus by RNA viruses. *J. Cell Biol.* **158**, 395–399.
- Calvo, E., Escors, D., Lopez, J. A., Gonzalez, J. M., Alvarez, A., Arza, E., and Enjuanes, L. (2005) Phosphorylation and subcellular localization of transmissible gastroenteritis virus nucleocapsid protein in infected cells. *J. Gen. Virol.* **86**, 2255–2267.
- Casais, R., Davies, M., Cavanagh, D., and Britton, P. (2005) Gene 5 of the avian coronavirus infectious bronchitis virus is not essential for replication. *J. Virol.* **79**, 8065–8078.
- Casais, R., Dove, B., Cavanagh, D., and Britton, P. (2003) Recombinant avian infectious bronchitis virus expressing a heterologous spike gene demonstrates that the spike protein is a determinant of cell tropism. *J. Virol.* **77**, 9084–9089.
- Cavanagh, D. (1997) Nidovirales: A new order comprising Coronaviridae and Arteriviridae. *Arch. Virol.* **142**, 629–633.
- Cavanagh, D. (2005) Coronaviruses in poultry and other birds. *Avian Pathol.* **34**, 439–448.
- Cavanagh, D., and Horzinek, M. C. (1993) Genus Torovirus assigned to the Coronaviridae. *Arch. Virol.* **128**, 395–396.

- Cavanagh, D., Mawditt, K., Welchman Dde, B., Britton, P., and Gough, R. E. (2002) Coronaviruses from pheasants (*Phasianus colchicus*) are genetically closely related to coronaviruses of domestic fowl (infectious bronchitis virus) and turkeys. *Avian Pathol.* **31**, 81–93.
- Cavanagh, D., and Naqi, S. (2003) Infectious bronchitis. In H.J. Barnes, A.M. Fadly, J.R. Glisson, L.R. McDougald & D.E. Swayne (Eds.), *Diseases of Poultry*, 11th edn (pp. 101–119). Ames: Iowa State University Press.
- Chang, L. K., Lee, Y. H., Cheng, T. S., Hong, Y. R., Lu, P. J., Wang, J. J., Wang, W. H., Kuo, C. W., Li, S. S., Liu, S. T. (2004) Post-translational modification of Rta of Epstein-Barr virus by SUMO-1. *J. Biol. Chem.* **279**, 38803–38812.
- Chang, R.-Y., and Brian, D. A. (1996) cis requirement for N-specific protein sequence in bovine coronavirus defective interfering RNA replication. *J. Virol.* **70**, 2210–2217.
- Charley, B., and Laude, H. (1988) Induction of alpha interferon by transmissible gastroenteritis coronavirus: Role of transmembrane glycoprotein E1. *J. Virol.* **62**, 8–11.
- Chau, T. N., Lee, K. C., Yao, H., Tsang, T. Y., Chow, T. C., Yeung, Y. C., Choi, K. W., Tso, Y. K., Lau, T., Lai, S. T., and Lai, C. L. (2004) SARS-associated viral hepatitis caused by a novel coronavirus: report of three cases. *Hepatology* **39**, 302–310.
- Chellappan, S. P., Hiebert, S., Mudryj, M., Horowitz, J. M., and Nevins, J. R. (1991) The E2F transcription factor is a cellular target for the RB protein. *Cell* **65**, 1053–1061.
- Chen, C-J., and Makino, S. (2002) Murine coronavirus-induced apoptosis in 17Cl-1 cells involves a mitochondria-mediated pathway and its downstream caspase-8 activation and bid cleavage. *Virology*. **302**, 321–332.
- Chen, C-J., and Makino, S. (2004) Murine coronavirus replication induces cell cycle arrest in G₀/G₁ phase. *J. Virol.* **78**, 5658–5669.
- Chen, C-J., Sugiyama, K., Kubo, H., Huang, H., and Makino, S. (2004a) Murine coronavirus nonstructural protein p28 arrests cell cycle in G₀/G₁ phase. *J. Virol.* **78**, 10410–10419.
- Chen, H., Gill, A., Dove, B. K., Emmett, S. R., Kemp, C. F., Ritchie, M. A., Dee, M., and Hiscox, J. A. (2005) Mass spectroscopic characterization of the coronavirus infectious bronchitis virus nucleoprotein and elucidation of the role of phosphorylation in RNA binding by using surface plasmon resonance. *J. Virol.* **79**, 1164–1179.
- Chen, H., Wurm, T., Britton, P., Brooks, G., and Hiscox, J. A. (2002) Interaction of the coronavirus nucleocapsid with nucleolar antigens and the host cell. *J. Virol.* **76**, 5233–5250.

- Chen, W., Lee, J., Cho, S. Y., and Fine, H. A. (2004b) Proteasome-mediated destruction of the cyclin A/cyclin-dependent kinase 2 complex suppresses tumor cell growth *in vitro* and *in vivo*. *Cancer Res.* **64**, 3949–3957.
- Chew, Y. P., Ellis, M., Wilkie, S., and Mittnacht, S. (1998) pRb phosphorylation mutants reveal roles of pRb in regulating S-phase completion by a mechanism independent of E2F. *Oncogene* **17**, 2177–2186.
- Chinese SARS Molecular Epidemiology Consortium. (2004) Molecular evolution of the SARS coronavirus during the course of the SARS epidemic in China. *Science* **303**, 1666–1669.
- Chow, K. Y. C., Yeung, Y. S., Hon, C. C., Zeng, F., Law, K. M., and Leung, F. C. C. (2005) Adenovirus-mediated expression of the C-terminal domain of SARS-CoV spike protein is sufficient to induce apoptosis in Vero E6 cells. *FEBS Letters* **579**, 6699–6704.
- Col, E., Caron, C., Chable-Bessia, C., Legube, G., Gazzeri, S., Komatsu, Y., Yoshida, M., Benkirane, M., Trouche, D., and Khochbin, S. (2005) HIV-1 Tat targets Tip60 to impair the apoptotic cell response to genotoxic stresses. *EMBO J.* **24**, 2634–2645.
- Collisson, E. W., Parr, R. L., Wang, L., and Williams, A. K. (1992) An overview of the molecular characteristics of avian infectious bronchitis virus. *Poultry Sci. Rev.* **4**, 41–55.
- Collot-Teixeira, S., Bass, J., Denis, F., and Ranger-Rogez, S. (2004) Human tumor suppressor p53 and DNA viruses. *Rev. Med. Virol.* **14**, 301–319.
- Cologna, R., and Hogue, B. G. (2000) Identification of a bovine coronavirus packaging signal. *J. Virol.* **74**, 580–583.
- Cologna, R., Spagnolo, J. F., and Hogue, B. G. (2000) Identification of nucleocapsid binding sites within coronavirus-defective genomes. *Virology* **277**, 235–249.
- Connor, R. F., and Roper, R. L. (2007) Unique SARS-CoV protein nsp1: bioinformatics, biochemistry and potential effects on virulence. *Trends Microbiol.* **15**, 51–53.
- Corse, E., and Machamer, C. E. (2000) Infectious bronchitis virus E protein is targeted to the Golgi complex and directs release of virus-like particles. *J. Virol.* **74**, 4319–4326.
- Corse, E., and Machamer, C. E. (2002) The cytoplasmic tail of infectious bronchitis virus E protein directs Golgi targeting. *J. Virol.* **76**, 1273–1284.
- Corse, E., and Machamer, C. E. (2003) The cytoplasmic tails of infectious bronchitis virus E and M proteins mediate their interaction. *Virology* **312**, 25–34.

- Cuconati, A., and White, E. (2002) Viral homologs of BCL-2: role of apoptosis in the regulation of virus infection. *Genes & Dev.* **16**, 2465–2478.
- Dahl, J., You, J., and Benjamin, T. L. (2005) Induction and utilization of an ATM signaling pathway by polyomavirus. *J. Virol.* **79**, 13007–13017.
- Davies, H. A., Dourmashkin, R. R., and MacNaughton, R. (1981) Ribonucleoprotein of avian infectious bronchitis virus. *J. Gen. Virol.* **53**, 67–74.
- de Groot-Mijnes, J. D., van Dun, J. M., van der Most, R. G. & de Groot, R. J. (2005) Natural history of a recurrent feline coronavirus infection and the role of cellular immunity in survival and disease. *J. Virol.* **79**, 1036–1044.
- de Haan, C. A. M., de Wit, M., Kuo, L., Montalto-Morrison, C., Haagmans, B. L., Weiss, S. R., Masters, P. S., and Rottier, P. J. M. (2003) The glycosylation status of the murine hepatitis coronavirus M protein affects the interferogenic capacity of the virus in vitro and its ability to replicate in the liver but not the brain. *Virology* **312**, 395–406.
- de Haan, C. A. M., and Rottier, P. J. M. (2006) Hosting the severe acute respiratory syndrome coronavirus: specific cell factors required for infection. *Cell Microbiol.* **8**, 1211–1218.
- DeCaprio, J. A., Ludlow, J. W., Figge, J., Shew, J. Y., Huang, C. M., Lee, W. H., Marsilio, E., Paucha, E., and Livingston, D. M. (1988) SV40 large tumor antigen forms a specific complex with the product of the retinoblastoma susceptibility gene. *Cell* **54**, 275–283.
- DeCaprio, J. A., Ludlow, J. W., Lynch, D., Furukawa, Y., Griffin, J., Piwnicka-Worms, H., Huang, C. M., and Livingston, D. M. (1989) The product of the retinoblastoma susceptibility gene has properties of a cell cycle regulatory element. *Cell* **58**, 1085–1095.
- Delmas, B., Gelfi, J., L'Haridon, R., Vogel, L. K., Sjostrom, H., Noren, O., and Laude, H. (1992) Aminopeptidase N is a major receptor for the entero-pathogenic coronavirus TGEV. *Nature* **357**, 417–420.
- Der, S. D., Yang, Y. L., Weissmann, C., and Williams, B. R. (1997) A double-stranded RNA-activated protein kinase-dependent pathway mediating stress-induced apoptosis. *Proc. Natl. Acad. Sci. USA.* **94**, 3279–3283.
- Desaintes, C., Goyat, S., Garbay, S., Yaniv, M., and Thierry, F. (1999) Papillomavirus E2 induces p53-independent apoptosis in HeLa cells. *Oncogene* **18**, 4538–4545.
- Desterro, J. M., Thomson, J. and Hay, R. T. (1997) Ubch9 conjugates SUMO but not ubiquitin. *FEBS Lett.* **417**, 297–300.

- Dieckhoff, P., Bolte, M., Sancak, Y., Braus, G.H., and Irniger, S. (2004) Smt3/SUMO and Ubc9 are required for efficient APC/C-mediated proteolysis in budding yeast. *Mol. Microbiol.* **51**, 1375–1387.
- Dove, B., Brooks, G., Bicknell, K., Wurm, T., and Hiscox, J. A. (2006) Cell cycle perturbations induced by infection with the coronavirus infectious bronchitis virus and their effect on viral replication. *J. Virol.* **80**, 4147–4156.
- Drosten, C., Gunther, S., Preiser, W., van der Werf, S., Brodt, H. R., Becker, S., Rabenau, H., Panning, M., Kolesnikova, L., Fouchier, R. A., Berger, A., Burguiere, A. M., Cinatl, J., Eickmann, M., Escriou, N., Grywna, K., Kramme, S., Manuguerra, J. C., Muller, S., Rickerts, V., Sturmer, M., Vieth, S., Klenk, H. D., Osterhaus, A. D., Schmitz, H., and Doerr, H. W. (2003a) Identification of a novel coronavirus in patients with severe acute respiratory syndrome. *N. Engl. J. Med.* **348**, 1967–1976.
- Drosten, C., Preiser, W., Gunther, S., Schmitz, H., and Doerr, H. W. (2003b) Severe acute respiratory syndrome: identification of the etiological agent. *Trends Mol. Med.* **9**, 325–327.
- Dyson, N. (1998) The regulation of E2F by pRB-family proteins. *Genes Dev.* **12**, 2245–2262.
- Egloff, M. P., Ferron, F., Campanacci, V., Longhi, S., Rancurel, C., Dutartre, H., Snijder, E. J., Gorbalenya, A. E., Cambillau, C., and Canard, B. (2004) The severe acute respiratory syndrome-coronavirus replicative protein nsp9 is a single-stranded RNA-binding subunit unique in the RNA virus world. *Proc. Natl. Acad. Sci. USA* **101**, 3792–3796.
- el-Deiry, W.S., Tokino, T., Velculescu, V.E., Levy, D.B., Parsons, R., Trent, J.M., Lin, D., Mercer, W.E., Kinzler, K.W., and Vogelstein, B. (1993) WAF1, a potential mediator of p53 tumor suppression. *Cell* **75**, 817–825.
- Eleouet, J. F., Chilmonczyk, S., Besnardeau, L., and Laude, H. (1998) Transmissible gastroenteritis coronavirus induces programmed cell death in infected cells through a caspase-dependent pathway. *J. Virol.* **72**, 4918–4924.
- Eleouet, J. F., Rasschaert, D., Lambert, P., Levy, L., Vende, P., and Laude, H. (1995) Complete sequence (20 kilobases) of the polyprotein-encoding gene 1 of transmissible gastroenteritis virus. *Virology* **206**, 817–822.
- Eleouet, J. F., Slee, E. A., Saurini, F., Castagne, N., Poncet, D., Garrido, C., Solary, E., and Martin, S. J. (2000) The Viral nucleocapsid protein of transmissible gastroenteritis coronavirus (TGEV) is cleaved by caspase-6 and -7 during TGEV-induced Apoptosis. *J. Virol.* **74**, 3975–3983.
- Enjuanes, L., Almazan, F., Sola, I., and Zuniga, S. (2006) Biochemical aspects of coronavirus replication and virus-host interaction. *Annu. Rev. Microbiol.* **60**, 211–230.

- Enjuanes, L., Sola, I., Alonso, S., Escors, D., and Zuniga, S. (2005) Coronavirus reverse genetics and development of vectors for gene expression. *Curr. Top. Microbiol. Immunol.* **287**, 161–197.
- Enjuanes, L., and van der Zeijst, B. A. M. (1995) Molecular basis of transmissible gastroenteritis virus, p. 337–376. *In* S. G. Siddell (ed.), *The Coronaviridae*. Plenum Press, New York, N.Y.
- Escors, D., Ortego, J., Laude, H., and Enjuanes, L. (2001) The membrane M protein carboxy terminus binds to transmissible gastroenteritis coronavirus core and contributes to core stability. *J. Virol.* **75**, 1312–1324.
- Fan, H., Ooi, A., Tan, Y. W., Wang, S., Fang, S., Liu, D. X., and Lescar, J. (2005a) The nucleocapsid protein of coronavirus infectious bronchitis virus: crystal structure of its N-terminal domain and multimerization properties. *Structure* **13**, 1859–1868.
- Fan, X., Liu, Y., and Chen, J. J. (2005b) Down-regulation of p21 contributes to apoptosis induced by HPV E6 in human mammary epithelial cells. *Apoptosis* **10**, 63–73.
- Fang, S., Chen, B., Tay, F. P., Ng, B. S., and Liu, D. X. (2006) An arginine-to-proline mutation in a domain with undefined functions within the helicase protein (Nsp13) is lethal to the coronavirus infectious bronchitis virus in cultured cells. *Virology* 2006 Sep 15; [Epub ahead of print]
- Farsang, A., Ros, C., Renström, L.H.M., Baule, C., Soós, T., and Belák, S. (2002) Molecular epizootiology of infectious bronchitis virus in Sweden indicating the involvement of a vaccine strain. *Avian Pathology* **31**, 229–236.
- Feuer, R., Mena, I., Pagarigan, R., Slifka, M. K., and Whitton, J. L. (2002) Cell cycle status affects coxsackievirus replication, persistence, and reactivation in vitro. *J. Virol.* **76**, 4430–4440.
- Fielding, B.C., Gunalan, V., Tan, T.H.P., Chou, C.-F., Shen, S., Khan, S., Lim, S.G., Hong, W., and Tan, Y.-J. (2006) Severe acute respiratory syndrome coronavirus protein 7a interacts with hGST. *Biochem. Biophys. Res. Commun.* **343**, 1201–1208.
- Fischer, F., Peng, D., Hingley, S. T., Weiss, S. R., and Masters, P. S. (1997). The internal open reading frame within the nucleocapsid gene of mouse hepatitis virus encodes a structural protein that is not essential for viral replication. *J. Virol.* **71**, 996–1003.
- Fisman, D. N. (2000) Hemophagocytic syndromes and infection. *Emerg. Infect. Dis.* **6**, 601–608.
- Flemington, E. K. (2001) Herpesvirus lytic replication and the cell cycle: arresting new developments. *J. Virol.* **75**, 4475–4481.

- Fouchier, R. A., Hartwig, N. G., Bestebroer, T. M., Niemeyer, B., de Jong, J. C., Simon, J. H., and Osterhaus, A. D. (2004) A previously undescribed coronavirus associated with respiratory disease in humans. *Proc. Natl. Acad. Sci. USA* **101**, 6212–6216.
- Fouchier, R. A., Kuiken, T., Schutten, M., Van Amerongen, G., Van Doornum, G. J., Van Den Hoogen, B. G., Peiris, M., Lim, W., Stohr, K., and Osterhaus, A. D. (2003) Aetiology: Koch's postulates fulfilled for SARS virus. *Nature* **423**, 240.
- Fournier, N., Raj, K., Saudan, P., Utzig, S., Sahli, R., Simanis, V., and Beard, P. (1999) Expression of human papillomavirus 16 E2 protein in *Schizosaccharomyces pombe* delays the initiation of mitosis. *Oncogene* **18**, 4015–4021.
- Frana, M. F., Behnke, J. N., Sturman, L. S., and Holmes, K. V. (1985) Proteolytic cleavage of the E2 glycoprotein of murine coronavirus: host- dependent differences in proteolytic cleavage and cell fusion. *J. Virol.* **56**, 912–920.
- Freiman, R. N., and Tjian, R. (2003) Regulating the regulators: lysine modifications make their mark. *Cell* **112**, 11–17.
- Fuerst, T. R., Niles, E. G., Studier, F. W., and Moss, B. (1986) Eukaryotic transient-expression system based on recombinant vaccinia virus that synthesizes bacteriophage T7 RNA polymerase. *Proc. Natl. Acad. Sci. USA* **83**, 8122–8126.
- Gelb, J., Jr., Weisman, Y., Ladman, B. S., and Meir, R. (2005) S1 gene characteristics and efficacy of vaccination against infectious bronchitis virus field isolates from the United States and Israel (1996 to 2000). *Avian Pathology* **34**, 194–203.
- Geng, H., Liu, Y.M., Chan, W.S., Lo, A.W., Au, D.M., Waye, M.M., and Ho, Y.Y. (2005) The putative protein 6 of the severe acute respiratory syndrome-associated coronavirus: expression and functional characterization. *FEBS Lett.* **579**, 6763–6768.
- Gil-Gomez, G., Berns, A., and Brady, H. J. (1998) A link between cell cycle and cell death: Bax and Bcl-2 modulate Cdk2 activation during thymocyte apoptosis. *EMBO J.* **17**, 7209–7218.
- Gill, G. (2003) Post-translational modification by the small ubiquitin-related modifier SUMO has big effects on transcription factor activity. *Curr. Opin. Genet. Dev.* **13**, 108–113.
- Gjoerup, O., Zaveri, D., and Roberts, T. M. (2001) Induction of p53-independent apoptosis by simian virus 40 small t antigen. *J. Virol.* **75**, 9142–9155.
- Godet, M., L'haridon, R., Vautherot, J.-F., and Laude, H. (1992) TGEV coronavirus ORF4 encodes a membrane protein that is incorporated into virions. *Virology* **188**, 666–675.

- Goebel, S. J., Taylor, J., and Masters, P. S. (2004) The 3' *cis*-acting genomic replication element of the severe acute respiratory syndrome coronavirus can function in the murine coronavirus genome. *J. Virol.* **78**, 7846–7851.
- Goh, W. C., Rogel, M. E., Kinsey, C. M., Michael, S. F., Fultz, P. N., Nowak, M. A., Hahn, B. H., and Emerman, M. (1998) HIV-1 Vpr increases viral expression by manipulation of the cell cycle: a mechanism for selection of Vpr in vivo. *Nat. Med.* **4**, 65–71.
- Gong, J. G., Costanzo, A., Yang, H. Q., Melino, G., Kaelin, W. G. Jr., Levvero, M., Wang, J. Y. (1999) The tyrosine kinase c-Abl regulates p73 in apoptotic response to cisplatin-induced DNA damage. *Nature* **399**, 806–809.
- Gorbalenya, A. E., Snijder, E. J., and Spaan, W. J. (2004) Severe acute respiratory syndrome coronavirus phylogeny: toward consensus. *J. Virol.* **78**, 7863–7866.
- Gorospe, M., Cirielli, C., Wang, X., Seth, P., Capogrossi, M. P., Holbrook, N. J. (1997) p21(Waf1/Cip1) protects against p53-mediated apoptosis of human melanoma cells. *Oncogene* **14**, 929–935.
- Graham, R. L., Sims, A. C., Brockway, S. M., Baric, R. S., and Denison, M. R. (2005) The nsp2 replicase proteins of murine hepatitis virus and severe acute respiratory syndrome coronavirus are dispensable for viral replication. *J. Virol.* **79**, 13399–13411.
- Gravel, A., Dion, V., Cloutier, N., Gosselin, J., and Flamand, L. (2004) Characterization of human herpesvirus 6 variant B immediate-early 1 protein modifications by small ubiquitin-related modifiers. *J. Gen. Virol.* **85**, 1319–1328.
- Groschel, B., and Bushman, F. (2005) Cell cycle arrest in G₂/M promotes early steps of infection by human immunodeficiency virus. *J. Virol.* **79**, 5695–5704.
- Guan, Y., Zheng, B. J., He, Y. Q., Liu, X. L., Zhuang, Z. X., Cheung, C. L., Luo, S. W., Li, P. H., Zhang, L. J., Guan, Y. J., Butt, K. M., Wong, K. L., Chan, K. W., Lim, W., Shortridge, K. F., Yuen, K. Y., Peiris, J. S., and Poon, L. L. (2003) Isolation and characterization of viruses related to the SARS coronavirus from animals in southern China. *Science* **302**, 276–278.
- Gurer, C., Berthoux, L., and Luban, J. (2005) Covalent modification of human immunodeficiency virus type 1 p6 by SUMO-1. *J. Virol.* **79**, 910–917.
- Harbour, J. W., and Dean, D. C. (2000) The Rb/E2F pathway: expanding roles and emerging paradigms. *Genes Dev.* **14**, 2393–2409.
- Harper, J.W., Adami, G.R., Wei, N., Keyomarsi, K., and Elledge, S.J. (1993) The p21 Cdk-interacting protein Cip1 is a potent inhibitor of G1 cyclin-dependent kinases. *Cell* **75**, 805–816.

- Harper, J. W., Elledge, S. J., Keyomarsi, K., Dynlacht, B., Tsai, L. H., Zhang, P., Dobrowolski, S., Bai, C., Connell-Crowley, L., Swindell, E., et al. (1995) Inhibition of cyclin-dependent kinases by p21. *Mol. Biol. Cell* **6**, 387–400.
- Hay, R. T. (2005) SUMO: a history of modification. *Mol. Cell* **18**, 1–12.
- Hay, S., and Kannourakis, G. (2002) A time to kill: viral manipulation of the cell death program. *J. Gen. Virol.* **83**, 1547–1564.
- He, B. (2006) Viruses, endoplasmic reticulum stress, and interferon responses. *Cell Death Diff.* **13**, 393–403.
- He, J., Choe, S., Walker, R., Di Marzio, P., Morgan, D. O., and Landau, N. R. (1995) Human immunodeficiency virus type 1 viral protein R (Vpr) arrests cells in the G2 phase of the cell cycle by inhibiting p34^{cdc2} activity. *J. Virol.* **69**, 6705–6711.
- He, R., Dobie, F., Ballantine, M., Leeson, A., Li, Y., Bastien, N., Cutts, T., Andonov, A., Cao, J., Booth, T. F., Plummer, F. A., Tyler, S., Baker, L. and Li, X. (2004) Analysis of multimerization of the SARS coronavirus nucleocapsid protein. *Biochem. Biophys. Res. Commun.* **316**, 476–483.
- He, Y., Li, J., Heck, S., Lustigman, S., and Jiang, S. (2006) Antigenic and immunogenic characterization of recombinant baculovirus-expressed severe acute respiratory syndrome coronavirus spike protein: implication for vaccine design. *J. Virol.* **80**, 5757–5767.
- Helin, K. (1998) Regulation of cell proliferation by the E2F transcription factors. *Curr. Opin. Genet. Dev.* **8**, 28–35.
- Helt, A. M., and Harris, E. (2005) S-phase-dependent enhancement of dengue virus 2 replication in mosquito cells, but not in human cells. *J. Virol.* **79**, 13218–13230.
- Hershko, A., and Ciechanover, A. (1998) The ubiquitin system. *Annu. Rev. Biochem.* **67**, 425–479.
- Hilton, A., Mizzen, L., MacIntyre, G., Cheley, S., and Anderson, R. (1986) Translational control in murine hepatitis virus infection. *J. Gen. Virol.* **67**, 923–932.
- Hiscox, J. A. (2003) The interaction of animal cytoplasmic RNA viruses with the nucleus to facilitate replication. *Virus Res.* **95**, 13–22.
- Hiscox, J. A., Wurm, T., Wilson, L., Cavanagh, D., Britton, P., and Brooks, G. (2001) The coronavirus infectious bronchitis virus nucleoprotein localizes to the nucleolus. *J. Virol.* **75**, 506–512.
- Holmes, K. V. (2003a) SARS-associated coronavirus. *N. Engl. J. Med.* **348**, 1948–1950.

- Holmes, K. V. (2003b) SARS coronavirus: a new challenge for prevention and therapy. *J. Clin. Investig.* **111**, 1605–1609.
- Holmes, K. V., Dollar, E. W., and Sturman, L. S. (1981) Tunicamycin resistant glycosylation of a coronavirus glycoprotein: Demonstration of a novel type of viral glycoprotein. *Virology* **115**, 334–344.
- Holmes, K. V., and Enjuanes, L. (2003) The SARS coronavirus: a postgenomic era. *Science* **300**, 1377–1378.
- Honda, M., Kaneko, S., Matsushita, E., Kobayashi, K., Abell, G. A., and Lemon, S. M. (2000) Cell cycle regulation of hepatitis C virus internal ribosomal entry site-directed translation. *Gastroenterology* **118**, 152–162.
- Howe, J. A., Mymryk, J. S., Egan, C., Branton, P. E., and Bayley, S. T. (1990) Retinoblastoma growth suppressor and a 300-kDa protein appear to regulate cellular DNA synthesis. *Proc. Natl. Acad. Sci. USA* **87**, 5883–5887.
- Hsieh, P. K., Chang, S. C., Huang, C. C., Lee, T. T., Hsiao, C. W., Kou, Y. H., Chen, I. Y., Chang, C. K., Huang, T. H., and Chang, M. F. (2005) Assembly of severe acute respiratory syndrome coronavirus RNA packaging signal into virus-like particles is nucleocapsid dependent. *J. Virol.* **79**, 13848–13855.
- Huang, C., Ito, N., Tseng, C. T., and Makino, S. (2006) Severe acute respiratory syndrome coronavirus 7a accessory protein is a viral structural protein. *J. Virol.* **80**, 7287–7294.
- Huang, Q., Yu, L., Petros, A. M., Gunasekera, A., Liu, Z., Xu, N., Hajduk, P., Mack, J., Fesik, S. W. and Olejniczak, E. T. (2004a) Structure of the N-terminal RNA-binding domain of the SARS-CoV nucleocapsid protein. *Biochemistry* **43**, 6059–6063.
- Huang, Y., Yang, Z. Y., Kong, W. P., and Nabel, G. J. (2004b) Generation of synthetic severe acute respiratory syndrome coronavirus pseudoparticles: Implications for assembly and vaccine production. *J. Virol.* **78**, 12557–12565.
- Hurst, K. R., Kuo, L., Koetzner, C. A., Ye, R., Hsue, B., and Masters, P. S. (2005) A major determinant for membrane protein interaction localizes to the carboxy-terminal domain of the mouse coronavirus nucleocapsid protein. *J. Virol.* **79**, 13285–13297.
- Imbert, I., Guillemot, J. C., Bourhis, J. M., Bussetta, C., Coutard, B., Egloff, M. P., Ferron, F., Gorbalenya, A. E., and Canard, B. (2006) A second, non-canonical RNA-dependent RNA polymerase in SARS coronavirus. *EMBO J.* **25**, 4933–4942.
- Ito, N., Mossel, E. C., Narayanan, K., Popov, V. L., Huang, C., Inoue, T., Peters, C. J., and Makino, S. (2005) Severe acute respiratory syndrome coronavirus 3a protein is a viral structural protein. *J. Virol.* **79**, 3182–3186.

Ivanov, K. A., Thiel, V., Dobbe, J. C., van der Meer, Y., Snijder, E. J., and Ziebuhr, J. (2004) Multiple enzymatic activities associated with severe acute respiratory syndrome coronavirus helicase. *J. Virol.* **78**, 5619–5632.

Izumiya, Y., Ellison, T. J., Yeh, E. T., Jung, J. U., Luciw, P. A., Kung, H. J. (2005) Kaposi's sarcoma-associated herpesvirus K-bZIP represses gene transcription via SUMO modification. *J. Virol.* **79**, 9912–9925.

Izumiya, Y., Lin, S. F., Ellison, T. J., Levy, A. M., Mayeur, G. L., Izumiya, C., and Kung, H. J. (2003) Cell Cycle Regulation by Kaposi's Sarcoma-Associated Herpesvirus K-bZIP: Direct Interaction with Cyclin-CDK2 and Induction of G1 Growth Arrest. *J. Virol.* **77**, 9652–9661.

Jayaram, H., Fan, H., Bowman, B. R., Ooi, A., Jayaram, J., Collisson, E. W., Lescar, J., and Prasad, B. V. (2006) X-ray structures of the N- and C-terminal domains of a coronavirus nucleocapsid protein: implications for nucleocapsid formation. *J. Virol.* **80**, 6612–6620.

Jeffers, S. A., Tusell, S. M., Gillim-Ross, L., Hemmila, E. M., Achenbach, J. E., Babcock, G. J., Thomas, W. D., Jr., Thackray, L. B., Young, M. D., Mason, R. J., Ambrosino, D. M., Wentworth, D. E. et al. (2004) CD209L (L-SIGN) is a receptor for severe acute respiratory syndrome coronavirus. *Proc. Natl. Acad. Sci. USA* **101**, 15748–15753.

Jonassen, C. M., Kofstad, T., Larsen, I.-L., Lovland, A., Handeland, K., Follestad, A., and Lillehaug, A. (2005) Molecular identification and characterization of novel coronaviruses infecting graylag geese (*Anser anser*), feral pigeons (*Columbia livia*) and mallards (*Anas platyrhynchos*). *J. Gen. Virol.* **86**, 1597–1607.

Jordan, R., Wang, L., Graczyk, T. M., Block, T. M. and Romano, P. R. (2002) Replication of a cytopathic strain of

Riductdsilcresticul]TJ07.64 0 Td[(oumstrass)-e dated

- Katz, R. A., Greger, J. G., and Skalka, A. M. (2005) Effects of cell cycle status on early events in retroviral replication. *J. Cell. Biochem.* **94**, 880–889.
- Kawakami, T., Chiba, T., Suzuki, T., Iwai, K., Yamanaka, K., Minato, N., Suzuki, H., Shimbara, N., Hidaka, Y., Osaka, F., Omata, M., and Tanaka, K. (2001) NEDD8 recruits E2-ubiquitin to SCF E3 ligase. *EMBO J.* **20**, 4003–4012.
- Keng, C. T., Choi, Y. W., Welkers, M. R., Chan, D. Z., Shen, S., Lim, S. G., Hong, W., and Tan, Y. J. (2006) The human severe acute respiratory syndrome coronavirus (SARS-CoV) 8b protein is distinct from its counterpart in animal SARS-CoV and down-regulates the expression of the envelope protein in infected cells. *Virology.* **354**, 132–142.
- Khattari, Z., Brotons, G., Akkawi, M., Arbely, E., Arkin, I. T., and Salditt, T. (2005) SARS coronavirus E protein in phospholipid bilayers: an x-ray study. *Biophys. J.* **90**, 2038–50.
- Kim, T. W., Lee, J. H., Hung, C. F., Peng, S., Roden, R., Wang, M. C., Viscidi, R., Tsai, Y. C., He, L., Chen, P. P., Boyd, D. A. K., and Wu, T.C. (2004) Generation and Characterization of DNA vaccines targeting the nucleocapsid protein of severe acute respiratory syndrome coronavirus. *J. Virol.* **78**, 4638 – 4645.
- King, D. J., and Cavanagh, D. (1991) Infectious bronchitis, p. 471–484. *In* B. W. Calnek, H. J. Barnes, C. W. Beard, W. M. Reid, and H. W. Yoder, Jr. (ed.), *Disease of poultry*, 9th ed. Iowa State University Press, Ames, Iowa.
- King, K. L., and Cidlowski, J. A. (1998) Cell cycle regulation and apoptosis. *Annu. Rev. Physiol.* **60**, 601–617.
- Kleinberger, T. (2000) Induction of apoptosis by adenovirus E4orf4 protein. *Apoptosis* **5**, 211–215.
- Knudsen, E. S., Buckmaster, C., Chen, T. T., Feramisco, J. R., Wang, J. Y. (1998) Inhibition of DNA synthesis by RB: effects on G₁/S transition and S-phase progression. *Genes Dev.* **12**, 2278–2292.
- Koepp, D. M., Harper, J. W., and Elledge, S. J. (1999) How the cyclin became a cyclin: regulated proteolysis in the cell cycle. *Cell* **97**, 431–434.
- Kopecky-Bromberg, S. A., Martinez-Sobrido, L., Frieman, M., Baric, R. A., and Palese, P. (2007) Severe acute respiratory syndrome coronavirus open reading frame (ORF) 3b, ORF 6, and nucleocapsid proteins function as interferon antagonists. *J. Virol.* **81**, 548–557.
- Kopecky-Bromberg, S.A., Martinez-Sobrido, L., and Palese, P. (2006) 7a protein of severe acute respiratory syndrome coronavirus inhibits cellular protein synthesis and activates p38 mitogen-activated protein kinase. *J. Virol.* **80**, 785–793.

- Ksiazek, T. G., Erdman, D., Goldsmith, C. S., Zaki, S. R., Peret, T., Emery, S., Tong, S., Urbani, C., Comer, J. A., Lim, W., Rollin, P. E., Dowell, S. F., Ling, A. E., Humphrey, C. D., Shieh, W. J., Guarner, J., Paddock, C. D., Rota, P., Fields, B., DeRisi, J., Yang, J. Y., Cox, N., Hughes, J. M., LeDuc, J. W., Bellini, W. J., Anderson, L. J., SARS Working Group (2003) A novel coronavirus associated with severe acute respiratory syndrome. *N. Engl. J. Med.* **348**, 1953–1966.
- Kudoh, A., Daikoku, T., Sugaya, Y., Isomura, H., Fujita, M., Kiyono, T., Nishiyama, Y., and Tsurumi, T. (2004) Inhibition of S-phase cyclin-dependent kinase activity blocks expression of Epstein-Barr Virus immediate-early and early genes, preventing viral lytic replication. *J. Virol.* **78**, 104–115.
- Kudoh, A., Fujita, M., Zhang, L., Shirata, N., Daikoku, T., Sugaya, Y., Isomura, H., Nishiyama, Y., and Tsurumi, T. (2005) Epstein-Barr Virus Lytic Replication Elicits ATM Checkpoint Signal Transduction While Providing an S-phase-like Cellular Environment. *J. Biol. Chem.* **280**, 8156–8163.
- Kurtzman, A. L., and Schechter, N. (2001) Ubc9 interacts with a nuclear localization signal and mediates nuclear localization of the paired-like homeobox protein Vsx-1 independent of SUMO-1 modification. *Proc. Natl. Acad. Sci. USA* **98**, 5602–5607.
- Ladman, B. S., Pope, C. R., Ziegler, A. F., Swieczkowski, T., Callahan, C. J., Davison, S., and Gelb, J., Jr. (2002) Protection of chickens after live and inactivated virus vaccination against challenge with nephropathogenic infectious bronchitis virus PA/Wolgemuth/98. *Avian Dis.* **46**, 938–944.
- Lai, M. M., Baric, R. S., Brayton, P. R., and Stohlman, S. A. (1984) Characterization of leader RNA sequences on the virion and mRNAs of mouse hepatitis virus, a cytoplasmic RNA virus. *Proc. Natl. Acad. Sci. USA* **81**, 3626–3630.
- Lai, M. M., and Cavanagh, D. (1997) The molecular biology of coronaviruses. *Adv. Virus Res.* **48**, 1–100.
- Lai, M. M. C., and Stohlman, S. A. (1978) RNA of mouse hepatitis virus. *J. Virol.* **26**, 236–242.
- Lai, M. M., and Stohlman, S. A. (1981) Comparative analysis of RNA genomes of mouse hepatitis viruses. *J. Virol.* **38**, 661–670.
- Lai, M. M. C., and Holmes, K. V. (2001) Coronaviridae: The Viruses and Their Replication. In: *Fields Virology* (Knipe, D. M., and Howley, P. M., eds) Vol. 1, 4th Ed., pp. 1163–1203. (Lippincott, Williams & Wilkins, Philadelphia)
- Lau, S. K. P., Woo, P. C. Y., Li, K. S. M., Huang, Y., Tsoi, H.-W., Wong, B. H. L., Wong, S. S. Y., Leung, S.-Y., Chan, K.-H., and Yuen, K.-Y. (2005) Severe acute respiratory syndrome coronavirus-like virus in Chinese horseshoe bats. *Proc. Natl. Acad. Sci. USA* **102**, 14040–14045.

- Law, A. H., Lee, D. C., Cheung, B. K., Yim, H. C., and Lau, A. S. (2006) A Role for the non-structural protein-1 of SARS-Coronavirus in chemokine dysregulation. *J. Virol.* 2006 Oct 11; [Epub ahead of print]
- Law, L. M. J., Everitt, J., Beatch, M. D., Holmes, C. F. B., and Hobman, T. C. (2003) Phosphorylation of rubella virus capsid regulates its RNA binding activity and virus replication. *J. Virol.* **77**, 1764–1171.
- Law, P. T. W., Wong, C-H., Au, T. C. C., Chuck, C. P., Kong, S. K., Chan, P. K. S., To, K-F., Lo, A. W. I., Chan, J. Y. W., Suen, Y-K., Chan, H. Y. E., Fung, K. P., Wayne, M. M. Y., Sung, J. J. Y., Lo, Y. M. D., and Tsui, S. K. W. (2005) The 3a protein of severe acute respiratory syndrome-associated coronavirus induces apoptosis in Vero E6 cells. *J. Gen. Virol.* **86**, 1921–1930.
- Lee, H. J., Shieh, C. K., Gorbalenya, A. E., Koonin, E. V., La Monica, N., Tuler, J., Bagdzhadzhyan, A., and Lai, M. M. (1991) The complete sequence (22 kilobases) of murine coronavirus gene 1 encoding the putative proteases and RNA polymerase. *Virology* **180**, 567–582.
- Lee, N., Hui, D., Wu, A., Chan, P., Cameron, P., Joynt, G. M., Ahuja, A., Yung, M. Y., Leung, C. B., To, K. F., Lui, S. F., Szeto, C. C., Chung, S., and Sung, J. J. (2003) A major outbreak of severe acute respiratory syndrome in Hong Kong. *N. Engl. J. Med.* **348**, 1986–1994.
- Lehman, J. M., Laffin, J., and Friedrich, T. D. (2000) Simian virus 40 induces multiple S phases with the majority of viral DNA replication in the G₂ and second S phase in CV-1 cells. *Exp. Cell Res.* **258**, 215–222.
- Leong, W. F., Tan, H. C., Ooi, E. E., Koh, D. R., and Chow, V. T. (2005) Microarray and real-time RTPCR analyses of differential human gene expression patterns induced by severe acute respiratory syndrome (SARS) coronavirus infection of Vero cells. *Microbes Infect.* **7**, 248–59.
- Leung, D. T. M., Tam, F. C. H., Ma, C. H., Chan, P. K. S., Cheung, J. L. K., Niu, H., Tam, J. S. L., and Lim, P. L. (2004) Antibody response of patients with severe acute respiratory syndrome (SARS) targets the viral nucleocapsid. *J. Infect. Dis.* **190**, 379–86.
- Leung, W. K., To, K. F., Chan, P. K., Chan, H. L., Wu, A. K., Lee, N., Yuen, K. Y., and Sung, J. J. (2003) Enteric involvement of severe acute respiratory syndrome-associated coronavirus infection. *Gastroenterology* **125**, 1011–1017.
- Li, F. Q., Xiao, H., Tam, J. P., and Liu, D. X. (2005a) Sumoylation of the nucleocapsid protein of severe acute respiratory syndrome coronavirus. *FEBS Letters* **579**, 2387–2396.
- Li, W., Moore, M. J., Vasilieva, N., Sui, J., Wong, S. K., Berne, M. A., Somasundaran, M., Sullivan, J. L., Luzuriaga, K., Greenough, T. C., Choe, H., and Farzan, M.

- (2003) Angiotensin-converting enzyme 2 is a functional receptor for the SARS coronavirus. *Nature* **426**, 450–454.
- Li, W., Shi, Z., Yu, M., Ren, W., Smith, C., Epstein, J. H., Wang, H., Crameri, G., Hu, Z., Zhang, H., Zhang, J., McEachern, J., Field, H., Daszak, P., Eaton, B. T., Zhang, S., and Wang, L. F. (2005b). Bats are natural reservoirs of SARS-like coronaviruses. *Science* **310**, 676–679.
- Li, X. D., Lankinen, H., Putkuri, N., Vapalahti, O., and Vaheri, A. (2005c) Tula hantavirus triggers pro-apoptotic signals of ER stress in Vero E6 cells. *Virology* **333**, 180–189.
- Liao, Y., Lescar, J., Tam, J. P., and Liu, D. X. (2004) Expression of SARS-coronavirus envelope protein in *Escherichia coli* cells alters membrane permeability. *Biochem Biophys Res Commun.* **325**, 374–380.
- Liao, Y., Yuan, Q., Torres, J., Tam, J. P., and Liu, D. X. (2006) Biochemical and functional characterization of the membrane association and membrane permeabilizing activity of the severe acute respiratory syndrome coronavirus envelope protein. *Virology*. **349**, 264–275.
- Lim, K. P., and Liu, D. X. (2001) The missing link in coronavirus assembly. Retention of the avian coronavirus infectious bronchitis virus envelope protein in the pre-Golgi compartments and physical interaction between the envelope and membrane proteins. *J. Biol. Chem.* **276**, 17515–17523.
- Lim, K. P., Ng, L. F., and Liu, D. X. (2000) Identification of a novel cleavage activity of the first papain-like proteinase domain encoded by open reading frame 1a of the coronavirus avian infectious bronchitis virus and characterization of the cleavage products. *J. Virol.* **74**, 1674–1685.
- Lin, C-W., Lin, K-H., Hsieh, T-H., Shiu, S-Y., and Li, J-Y. (2006) Severe acute respiratory syndrome coronavirus 3C-like protease-induced apoptosis. *FEMS Immunol. Med. Microbiol.* **46**, 375–380.
- Lin, G. Y., and Lamb, R. A. (2000) The paramyxovirus simian virus 5 V protein slows progression of the cell cycle. *J. Virol.* **74**, 9152–9166.
- Liu, C., Xu, H. Y., and Liu, D. X. (2001) Induction of caspase-dependent apoptosis in cultured cells by the avian coronavirus infectious bronchitis virus. *J. Virol.* **75**, 6402–6409.
- Liu, D. X., Brierley, I., Tibbles, K. W., and Brown, T. D. (1994) A 100-kilodalton polypeptide encoded by open reading frame (ORF) 1b of the coronavirus infectious bronchitis virus is processed by ORF 1a products. *J. Virol.* **68**, 5772–5780.
- Liu, D. X., and Inglis, S. C. (1991) Association of the infectious bronchitis virus 3c protein with the virion envelope. *Virology* **185**, 911–917.

- Liu, D. X., and Inglis, S. C. (1992) Internal entry of ribosomes on a tricistronic mRNA encoded by infectious bronchitis virus. *J. Virol.* **66**, 6143–6154.
- Liu, D. X., Shen, S., Xu, H. Y., and Wang, S. F. (1998) Proteolytic mapping of the coronavirus infectious bronchitis virus 1b polyprotein: evidence for the presence of four cleavage sites of the 3C-like proteinase and identification of two novel cleavage products. *Virology* **246**, 288–297.
- Liu, D. X., Xu, H. Y., and Brown, T. D. (1997) Proteolytic processing of the coronavirus infectious bronchitis virus 1a polyprotein: identification of a 10-kilodalton polypeptide and determination of its cleavage sites. *J. Virol.* **71**, 1814–1820.
- Liu, G., and Lozano, G. (2005) p21 stability: linking chaperones to a cell cycle checkpoint. *Cancer Cell* **7**, 113–114.
- Liu, Y., Cai, Y., and Zhang, X. (2003) Induction of caspase-dependent apoptosis in cultured rRat oligodendrocytes by murine coronavirus is mediated during cell entry and does not require virus replication. *J. Virol.* **77**, 11952–11963.
- Liu, Y., Pu, Y., and Zhang, X. (2006) Role of the mitochondrial signaling pathway in murine coronavirus-induced oligodendrocyte apoptosis. *J. Virol.* **80**, 395–403.
- Lomniczi, B. (1977) Biological properties of avian coronavirus RNA. *J. Gen. Virol.* **36**, 531–533.
- Lu, M., and Shenk, T. (1996) Human cytomegalovirus infection inhibits cell cycle progression at multiple points, including the transition from G1 to S. *J. Virol.* **70**, 8850–8857.
- Lu, W., Zheng, B. J., Xu, K., Schwarz, W., Du, L., Wong, C. K., Chen, J., Duan, S., Deubel, V., and Sun, B. (2006) Severe acute respiratory syndrome-associated coronavirus 3a protein forms an ion channel and modulates virus release. *Proc. Natl. Acad. Sci. USA.* **103**, 12540–12545.
- Lundberg, A. S., and Weinberg, R. A. (1998) Functional inactivation of the retinoblastoma protein requires sequential modification by at least two distinct cyclin-cdk complexes. *Mol. Cell. Biol.* **18**, 753–761.
- Luo, H., Chen, J., Chen, K., Shen, X., and Jiang, H. (2006) Carboxyl terminus of severe acute respiratory syndrome coronavirus nucleocapsid protein: self-association analysis and nucleic acid binding characterization. *Biochemistry* **45**, 11827–11835.
- Luo, H., Ye, F., Chen, K., Shen, X., and Jiang, H. (2005) SR-rich motif plays a pivotal role in recombinant SARS coronavirus nucleocapsid protein multimerization. *Biochemistry* **44**, 15351–15358.
- Luo, H., Zhang, J., Dastvan, F., Yanagawa, B., Reidy, M. A., Zhang, H. M., Yang, D., Wilson, J. E., and McManus, B. M. (2003) Ubiquitin-dependent proteolysis of

- cyclin D1 is associated with coxsackievirus-induced cell growth arrest. *J. Virol.* **77**, 1–9.
- Machamer, C. E., and Rose, J. K. (1987) A specific transmembrane domain of a coronavirus E1 glycoprotein is required for its retention in the Golgi region. *J. Cell. Biol.* **105**, 1205–1214.
- Machamer, C. E., Mentone, S. A., Rose, J. K., and Farquhar, M. G. (1990) The E1 glycoprotein of an avian coronavirus is targetted to the *cis*-Golgi complex. *Proc. Natl. Acad. Sci. USA* **87**, 6944–6948.
- Macleod, K. F., Sherry, N., Hannon, G., Beach, D., Tokino, T., Kinzler, K., Vogelstein, B., and Jacks, T. (1995) p53-dependent and independent expression of p21 during cell growth, differentiation, and DNA damage. *Genes Dev.* **9**, 935–944.
- Macnaughton, M. R., Davies, H. A., and Nermut, M. V. (1978) Ribonucleoprotein-like structures from coronavirus particles. *J. Gen. Virol.* **39**, 545–549.
- Maeda, J., Repass, J. F., Maeda, A., and Makino, S. (2001) Membrane topology of coronavirus E protein. *Virology* **281**, 163–169.
- Mahajan, R., Delphin, C., Guan, T., Gerace, L., and Melchior, F. (1997) A small ubiquitin-related polypeptide involved in targeting RanGAP1 to nuclear pore complex protein RanBP2. *Cell* **88**, 97–107.
- Malakhova, O. A., Yan, M., Malakhov, M. P., Yuan, Y., Ritchie, K. J., Kim, K. I., Peterson, L. F., Shuai, K., and Zhang, D. E. (2003) Protein ISGylation modulates the JAK-STAT signaling pathway. *Genes Dev.* **17**, 455–60.
- Malanchi, I., Accardi, R., Diehl, F., Smet, A., Androphy, E., Hoheisel, J., and Tommasino, M. (2004) Human papillomavirus type 16 E6 promotes retinoblastoma protein phosphorylation and cell cycle progression. *J. Virol.* **78**, 13769–13778.
- Marra, M. A., Jones, S. J., Astell, C. R., Holt, R. A., Brooks-Wilson, A., Butterfield, Y. S., Khattra, J., Asano, J. K., Barber, S. A., Chan, S. Y., Cloutier, A., Coughlin, S. M., Freeman, D., Girm, N., Griffith, O. L., Leach, S. R., Mayo, M., McDonald, H., Montgomery, S. B., Pandoh, P. K., Petrescu, A. S., Robertson, A. G., Schein, J. E., Siddiqui, A., Smailus, D. E., Stott, J. M., Yang, G. S., Plummer, F., Andonov, A., Artsob, H., Bastien, N., Bernard, K., Booth, T. F., Bowness, D., Czub, M., Drebot, M., Fernando, L., Flick, R., Garbutt, M., Gray, M., Grolla, A., Jones, S., Feldmann, H., Meyers, A., Kabani, A., Li, Y., Normand, S., Stroher, U., Tipples, G. A., Tyler, S., Vogrig, R., Ward, D., Watson, B., Brunham, R. C., Krajden, M., Petric, M., Skowronski, D. M., Upton, C., and Roper, R. L. (2003) The genome sequence of the SARS-associated coronavirus. *Science* **300**, 1399–1404.
- Masters, P. S. (1992) Localization of an RNA-binding domain in the nucleocapsid protein of the coronavirus mouse hepatitis virus. *Arch. Virol.* **125**, 141–160.

- Masters, P. S. (2006) The molecular biology of coronaviruses. *Adv. Virus Res.* **66**, 193–292.
- Matsuyama, S., and Taguchi, F. (2002) Receptor-induced conformational changes of murine coronavirus spike protein. *J. Virol.* **76**, 11819–11826.
- Matunis, M.J., Coutavas, E., and Blobel, G. (1996) A novel ubiquitin-like modification modulates the partitioning of the Ran-GTPase-activating protein RanGAP1 between the cytosol and the nuclear pore complex. *J. Cell Biol.* **135**, 1457–1470.
- Mayo, M. A. (2002) A summary of taxonomic changes recently approved by ICTV. *Arch. Virol.* **147**, 1655–1656.
- McChesney, M. B., Altman, A., and Oldstone, M. B. (1988) Suppression of T lymphocyte function by measles virus is due to cell cycle arrest in G₁. *J. Immunol.* **140**, 1269–1273.
- McIntosh, K. (1974) Coronaviruses: a comparative review. *Curr. Top. Microbiol. Immunol.* **63**, 85–129.
- Meier, C., Aricescu, A. R., Assenberg, R., Aplin, R. T., Gilbert, R. J., Grimes, J. M., and Stuart, D. I. (2006) The crystal structure of ORF-9b, a lipid binding protein from the SARS coronavirus. *Structure* **14**, 1157–1165.
- Meikrantz, W., Gisselbrecht, S., Tam, S. W., and Schlegel, R. (1994) Activation of cyclin A-dependent protein kinases during apoptosis. *Proc. Natl. Acad. Sci. USA* **91**, 3754–3758.
- Melchior, F., Schergaut, M., and Pichler, A. (2003) SUMO: ligases, isopeptidases and nuclear pores. *Trends Biochem. Sci.* **28**, 612–618.
- Mingot, J. M., Kostka, S., Kraft, R., Hartmann, E., and Gorlich, D. (2001) Importin 13: a novel mediator of nuclear import and export. *EMBO J.* **20**, 3685–3694.
- Minskaia, E., Hertzog, T., Gorbalenya, A. E., Campanacci, V., Cambillau, C., Canard, B., Ziebuhr, J. (2006) Discovery of an RNA virus 3'→5' exoribonuclease that is critically involved in coronavirus RNA synthesis. *Proc. Natl. Acad. Sci. USA.* **103**, 5108–5113.
- Mittnacht, S. (1998) Control of pRb phosphorylation. *Curr. Opin. Genet. Dev.* **8**, 21–27.
- Morgan, D. O. (1995) Principles of CDK regulation. *Nature* **374**, 131–134.
- Mortola, E., and Roy, P. (2004) Efficient assembly and release of SARS coronavirus-like particles by a heterologous expression system. *FEBS Lett.* **576**, 174–178.

- Müller, S., and Dejean, A. (1999) Viral immediate-early proteins abrogate the modification by SUMO-1 of PML and Sp100 proteins, correlating with nuclear body disruption. *J. Virol.* **73**, 5137–5143.
- Müller, S., Hoege, C., Pyrowolakis, G., and Jentsch, S. (2001) SUMO, ubiquitin's mysterious cousin. *Nat. Rev. Mol. Cell Biol.* **2**, 202–210.
- Müller, S., Led, A., and Schmidt, D. (2004) SUMO: a regulator of gene expression and genome integrity. *Oncogene* **23**, 1998–2008.
- Murray, A., and Hunt, T. (1993) *The Cell Cycle* (New York: W. H. Freeman & Co.).
- Murray, A. W. (2004) Recycling the cell cycle: cyclins revisited. *Cell* **116**, 221–234.
- Naniche, D., Reed, S. I., and Oldstone, M. B. (1999) Cell cycle arrest during measles virus infection: a G₀-like block leads to suppression of retinoblastoma protein expression. *J. Virol.* **73**, 1894–1901.
- Nakamura, H., Li, M., Zarycki, J., and Jung, J. U. (2001) Inhibition of p53 Tumor Suppressor by Viral Interferon Regulatory Factor. *J. Virol.* **75**, 7572–7582.
- Nakayama, K. (1998) Cip/Kip cyclin-dependent kinase inhibitors: brakes of the cell cycle engine during development. *Bioessays* **20**, 1020–1029.
- Narayanan, K., Chen, C. J., Maeda, J., and Makino, S. (2003) Nucleocapsid independent specific viral RNA packaging via viral envelope protein and viral RNA signal. *J. Virol.* **77**, 2922–2927.
- Narayanan, K., Maeda, A., Maeda, J., and Makina, S. (2000) Characterization of the coronavirus M protein and nucleocapsid interaction in infected cells. *J. Virol.* **74**, 8127–8134.
- Narayanan, K., and Makino, S. (2001) Cooperation of an RNA packaging signal and a viral envelope protein in coronavirus RNA packaging. *J. Virol.* **75**, 9059–9067.
- Ndolo, T., Dhillon, N. K., Nguyen, H., Guadalupe, M., Mudryj, M., and Dandekar, S. (2002) Simian Immunodeficiency Virus Nef Protein Delays the Progression of CD4⁺ T Cells through G₁/S Phase of the Cell Cycle. *J. Virol.* **76**, 3587–3595.
- Nelson, G. W., Stohlman, S. A., and Tahara, S. M. (2000) High affinity interaction between nucleocapsid protein and leader/intergenic sequence of mouse hepatitis virus RNA. *J. Gen. Virol.* **81**, 181–188.
- Neuveut, C., Low, K., G., Maldarelli, F., Schmitt, I., Majone, F., Grassmann, R., and Jeang, K. T. (1998) Human T-cell leukemia virus type 1 Tax and cell cycle progression: role of cyclin D-cdk and p110Rb. *Mol. Cell. Biol.* **18**, 3620–3632.
- Ng, M. L., Lee, J. W., Leong, M. L., Ling, A. E., Tan, H. C., and Ooi, E. E. (2004) Topographic changes in SARS coronavirus-infected cells at late stages of infection. *Emerg. Infect. Dis.* **10**, 1907–1914.

- Nguyen, V.-P., and Hogue, B. (1997) Protein interactions during coronavirus assembly. *J. Virol.* **71**, 9278–9284.
- Nicholls, J. M., Poon, L. L., Lee, K. C., Ng, W. F., Lai, S. T., Leung, C. Y., Chu, C. M., Hui, P. K., Mak, K. L., Lim, W., Yan, K. W., Chan, K. H., Tsang, N. C., Guan, Y., Yuen, K. Y., and Peiris, J. S. (2003) Lung pathology of fatal severe acute respiratory syndrome. *Lancet* **361**, 1773–1778.
- Niculescu, A. B., Chen, X., Smeets, M., Hengst, L., Prives, C., and Reed, S. I. (1998) Effects of p21(Cip1/Waf1) at both the G₁/S and the G₂/M cell cycle transitions: pRb is a critical determinant in blocking DNA replication and in preventing endoreduplication. *Mol. Cell Biol.* **18**, 629–643.
- Nishizawa, M., Kamata, M., Katsumata, R., and Aida, Y. (2000) A carboxy-terminally truncated form of the human immunodeficiency virus type 1 Vpr protein induces apoptosis via G₁ cell cycle arrest. *J. Virol.* **74**, 6058–6067.
- Nurse, P. (2004) A long twentieth century of the cell cycle and beyond. *Cell* **100**, 71–78.
- Ogryzko, V., Wong, P., and Howard, B. H. (1997) WAF1 retards S-phase progression primarily by inhibition of cyclin-dependent kinases. *Mol. Cell Biol.* **17**, 4877–4882.
- Oleksiewicz, M. B., and Alexandersen, S. (1997) S-phase-dependent cell cycle disturbances caused by aleutian mink disease parvovirus. *J. Virol.* **71**, 1386–1396.
- Op De Beeck, A., and Caillet-Fauquet, P. (1997) Viruses and the cell cycle. *Prog. Cell Cycle Res.* **3**, 1–19.
- Ortego, J., Sola, I., Almazan, F., Ceriani, J. E., Riquelme, C., Balasch, M., Plana, J., and Enjuanes, L. (2003) Transmissible gastroenteritis coronavirus gene 7 is not essential but influences in vivo virus replication and virulence. *Virology* **308**, 13–22.
- Palacios, S., Perez, L. H., Welsch, S., Schleich, S., Chmielarska, K., Melchior, F., and Locker, J. K. (2005) Quantitative SUMO-1 modification of a vaccinia virus protein is required for its specific localization and prevents its self-association. *Mol. Biol. Cell* **16**, 2822–2835.
- Parkinson, J., and Everett, R. D. (2000) Alphaherpesvirus proteins related to herpes simplex virus type 1 ICP0 affect cellular structures and proteins. *J. Virol.* **74**, 10006–10017.
- Parris, G. E. (2005) The role of viruses in cell fusion and its importance to evolution, invasion and metastasis of cancer clones. *Med. Hypotheses*. **64**, 1011–4.
- Parry, J. (2003) WHO investigates China's fall in SARS cases. *Br. Med. J.* **326**, 1285.

- Peiris, J. S., Chu, C. M., Cheng, V. C., Chan, K. S., Hung, I. F., Poon, L. L., Law, K. I., Tang, B. S., Hon, T. Y., Chan, C. S., Chan, K. H., Ng, J. S., Zheng, B. J., Ng, W. L., Lai, R. W., Guan, Y., and Yuen, K. Y. (2003a) Clinical progression and viral load in a community outbreak of coronavirus-associated SARS pneumonia: a prospective study. *Lancet* **361**, 1767–1772.
- Peiris, J. S., Guan, Y., and Yuen, K. Y. (2004) Severe acute respiratory syndrome. *Nat. Med.* **10**, S88–97.
- Peiris, J. S., Yuen, K. Y., Osterhaus, A. D., and Stohr, K. (2003b) The severe acute respiratory syndrome. *N. Engl. J. Med.* **349**, 2431–2441.
- Perlman, S. (1998) Pathogenesis of coronavirus-induced infections. Review of pathological and immunological aspects. *Adv. Exp. Med. Biol.* **440**, 503–513.
- Perlman, S., and Dandekar, A. A. (2005) Immunopathogenesis of coronavirus infections: implications for SARS. *Nat. Rev. Immunol.* **5**, 917–927.
- Peti, W., Johnson, M. A., Herrmann, T., Neuman, B. W., Buchmeier, M. J., Nelson, M., Joseph, J., Page, R., Stevens, R. C., Kuhn, P., and Wuthrich, K. (2005) Structural genomics of the severe acute respiratory syndrome coronavirus: nuclear magnetic resonance structure of the protein nsP7. *J. Virol.* **79**, 12905–12913.
- Petrik, D. T., Schmitt, K. P., and Stinski, M. F. (2006) Inhibition of Cellular DNA Synthesis by the Human Cytomegalovirus IE86 Protein Is Necessary for Efficient Virus Replication. *J. Virol.* **80**, 3872–3883.
- Pewe, L., Zhou, H., Netland, J., Tangudu, C., Olivares, H., Shi, L., Look, L., Gallagher, T., and Perlman, S. (2005) A severe acute respiratory syndrome-associated coronavirus-specific protein enhances virulence of an attenuated murine coronavirus. *J. Virol.* **79**, 11335–11342.
- Picault, J. P., Drouin, P., Guittet, M., Bennejean, G., Protais, J., L'Hospitalier, R., Gillet, J. P., Lamande, J., and Bachelier, A. L. (1986) Isolation, characterization and preliminary cross protection studies with a new pathogenic avian infectious bronchitis virus (strain PL-84084). *Avian Pathol.* **15**, 367–383.
- Pichler, A., and Melchior, F. (2002) Ubiquitin-related modifier SUMO1 and nucleocytoplasmic transport. *Traffic* **3**, 381–387.
- Poggioli, G. J., Dermody, T. S., and Tyler, K. L. (2001) Reovirus-induced sigma1-dependent G₂/M phase cell cycle arrest is associated with inhibition of p34^{cdc2}. *J. Virol.* **75**, 7429–7434.
- Poon, B., Grovit-Ferbas, K., Stewart, S. A., and Chen, I. S. (1998) Cell cycle arrest by Vpr in HIV-1 virions and insensitivity to antiretroviral agents. *Science* **281**, 266–269.

- Poon, L. L. M., Chu, D. K.W., Chan, K. H., Wong, O. K., Ellis, T. M., Leung, Y. H. C., Lau, S. K. P., Woo, P. C. Y., Suen, K. Y., Yuen, K. Y., Guan, Y., and Peiris, J. S. M. (2005) Identification of a novel coronavirus in bats. *J. Virol.* **79**, 2001–2009.
- Poon, L. L., Guan, Y., Nicholls, J. M., Yuen, K. Y., and Peiris, J. S. (2004) The aetiology, origins, and diagnosis of severe acute respiratory syndrome. *Lancet Infect. Dis.* **4**, 663–671.
- Popova, R., and X. Zhang. (2002) The spike but not the hemagglutinin/ esterase protein of bovine coronavirus is necessary and sufficient for viral infection. *Virology* **294**, 222–236.
- Raamsman, M. J. B., Krijnse Locker, J., de Hooge, A., de Vries, A. A. F., Griffiths, G., Vennema, H., and Rottier, P. J. M. (2000) Characterization of the coronavirus mouse hepatitis virus strain A59 small membrane protein E. *J. Virol.* **74**, 2333–2342.
- Rangasamy, D., and Wilson, V. G. (2000) Bovine papillomavirus E1 protein is sumoylated by the host cell Ubc9 protein. *J. Biol. Chem.* **275**, 30487–30495.
- Ratia, K., Saikatendu, K. S., Santarsiero, B. D., Barretto, N., Baker, S. C., Stevens, R. C., and Mesecar, A. D. (2006) Severe acute respiratory syndrome coronavirus papain-like protease: structure of a viral deubiquitinating enzyme. *Proc. Natl. Acad. Sci. USA* **103**, 5717–5722.
- Re, F., Braaten, D., Franke, E. K., and Luban, J. (1995) Human immunodeficiency virus type 1 Vpr arrests the cell cycle in G2 by inhibiting the activation of p34^{cdc2}-cyclin B. *J. Virol.* **69**, 6859–6864.
- Reed, M. L., Dove, B. K., Jackson, R. M., Collins, R., Brooks, G., and Hiscox, J. A. (2006) Delineation and modelling of a nucleolar retention signal in the coronavirus nucleocapsid protein. *Traffic* **7**, 833–848.
- Ricagno, S., Egloff, M. P., Ulferts, R., Coutard, B., Nurizzo, D., Campanacci, V., Cambillau, C., Ziebuhr, J., and Canard, B. (2006) Crystal structure and mechanistic determinants of SARS coronavirus nonstructural protein 15 define an endoribonuclease family. *Proc. Natl. Acad. Sci. USA* **103**, 11892–11897.
- Risco, C., Anton, I. M., Enjuanes, L., and Carrascosa, J. L. (1996) The transmissible gastroenteritis coronavirus contains a spherical core shell consisting of M and N proteins. *J. Virol.* **70**, 4773–4777.
- Ritchie, K. J., Hahn, C. S., Kim, K. I., Yan, M., Rosario, D., Li, L., de la Torre, J. C., and Zhang, D. E. (2004) Role of ISG15 protease UBP43 (USP18) in innate immunity to viral infection. *Nat Med.* **10**, 1374–1378.
- Rodriguez, M.S., Dargemont, C., and Hay, R.T. (2001) SUMO-1 conjugation in vivo requires both a consensus modification motif and nuclear targeting. *J. Biol. Chem.* **276**, 12654–12659.

- Rogel, M. E., Wu, L. I., and Emerman, M. (1995) The human immunodeficiency virus type 1 *vpr* gene prevents cell proliferation during chronic infection. *J. Virol.* **69**, 882–888.
- Roisin, A., Robin, J. P., Dereuddre-Bosquet, N., Vitte, A. L., Dormont, D., Clayette, P., and Jalinot, P. (2004) Inhibition of HIV-1 replication by cell-penetrating peptides binding Rev. *J. Biol. Chem.* **279**, 9208–9214.
- Rota, P. A., Oberste, M. S., Monroe, S. S., Nix, W. A., Campagnoli, R., Icenogle, J. P., Penaranda, S., Bankamp, B., Maher, K., Chen, M. H., Tong, S., Tamin, A., Lowe, L., Frace, M., DeRisi, J. L., Chen, Q., Wang, D., Erdman, D. D., Peret, T. C., Burns, C., Ksiazek, T. G., Rollin, P. E., Sanchez, A., Liffick, S., Holloway, B., Limor, J., McCaustland, K., Olsen-Rasmussen, M., Fouchier, R., Gunther, S., Osterhaus, A. D., Drosten, C., Pallansch, M. A., Anderson, L. J., and Bellini, W. J. (2003) Characterization of a novel coronavirus associated with severe acute respiratory syndrome. *Science* **300**, 1394–1399.
- Roulston, A., Marcellus, R. C., and Branton, P. E. (1999) Viruses and apoptosis. *Annu. Rev. Microbiol.* **53**, 577–628.
- Roussel, M. F. (1999) The INK4 family of cell cycle inhibitors in cancer. *Oncogene* **18**, 5311–5317.
- Rowland, R. R. R., Chauhan, V., Fang, Y., Pekosz, A., Kerrigan, M., and Burton, M. D. (2005) Intracellular localization of the severe acute respiratory syndrome coronavirus nucleocapsid protein: Absence of nucleolar accumulation during infection and after expression as a recombinant protein in Vero cells. *J. Virol.* **79**, 11507–11512.
- Ruan, Y. J., Wei, C. L., Ee, A. L., Vega, V. B., Thoreau, H., Su, S. T., Chia, J. M., Ng, P., Chiu, K. P., Lim, L., Zhang, T., Peng, C. K., Lin, E. O., Lee, N. M., Yee, S. L., Ng, L. F., Chee, R. E., Stanton, L. W., Long, P. M., Liu, E. T. (2003) Comparative full-length genome sequence analysis of 14 SARS coronavirus isolates and common mutations associated with putative origins of infection. *Lancet* **361**, 1779–1785.
- Saikatendu, K. S., Joseph, J. S., Subramanian, V., Clayton, T., Griffith, M., Moy, K., Velasquez, J., Neuman, B. W., Buchmeier, M. J., Stevens, R. C., and Kuhn, P. (2005) Structural basis of severe acute respiratory syndrome coronavirus ADP-ribose-1"-phosphate dephosphorylation by a conserved domain of nsP3. *Structure* **13**, 1665–1675.
- Saitoh, H., and Hinchey, J. (2000). Functional heterogeneity of small ubiquitin-related protein modifiers SUMO-1 versus SUMO-2/3. *J. Biol. Chem.* **275**, 6252–6258.
- Salinas, S. Briancon-Marjollet, A., Bossis, G., Lopez, M. A., Piechaczyk, M., Jariel-Encontre, I., Debant, A., Hipskind, R. A. (2004) SUMOylation regulates nucleo-cytoplasmic shuttling of Elk-1. *J. Cell Biol.* **165**, 767–773.

- Saltzman, A., Searfoss, G., Marcireau, C., Stone, M., Ressler, R., Munro, R., Franks, C., D'Alonzo, J., Tocque, B., Jaye, M., and Ivashchenko, Y. (1998) hUBC9 associates with MEKK1 and type I TNF- α receptor and stimulates NF κ B activity. *FEBS Lett.* **425**, 431–435.
- Santiago-Walker, A. E., Fikaris, A. J., Kao, G. D., Brown, E. J., Kazanietz, M. G., and Meinkoth, J. L. (2005) Protein kinase C δ stimulates apoptosis by initiating G₁ phase cell cycle progression and S phase arrest. *J. Biol. Chem.* **280**, 32107–32114.
- Saudan, P., Vlach, J., and Beard, P. (2000) Inhibition of S-phase progression by adeno-associated virus Rep78 protein is mediated by hypophosphorylated pRb. *EMBO J.* **19**, 4351–4361.
- Sawicki, S. G., and Sawicki, D. L. (2005) Coronavirus transcription: A perspective. *Curr. Top. Microbiol. Immunol.* **287**, 31–55.
- Schalk, A. F., and Hawn, M. C. (1931) An apparently new respiratory disease of baby chicks. *J. Am. Vet. Med. Assoc.* **78**, 413–422.
- Schang, L. M. (2003) The cell cycle, cyclin-dependent kinases, and viral infections: New horizons and unexpected connections. *Prog Cell Cycle Res* **5**, 103–124.
- Schelle, B., N. Karl, B. Ludewig, S. G. Siddell, and V. Thiel. (2005) Selective replication of coronavirus genomes that express nucleocapsid protein. *J. Virol.* **79**, 6620–6630.
- Schmidt, M., Afione, S., and Kotin, R. M. (2000) Adeno-associated virus type 2 Rep78 induces apoptosis through caspase activation independently of p53. *J. Virol.* **74**, 9441–9450.
- Scholle, F., Li, K., Bodola, F., Ikeda, M., Luxon, B. A., and Lemon, S. M. (2004) Virus-host cell interactions during hepatitis C virus replication: impact of polyprotein expression on the cellular transcriptome and cell cycle association with viral RNA synthesis. *J. Virol.* **75**, 1513–1524.
- Schwarz, B., Routledge, E., and Siddell, S. G. (1990) Murine coronavirus nonstructural protein ns2 is not essential for virus replication in transformed cells. *J. Virol.* **64**, 4784–4791.
- Schwarz, S. E., Matuschewski, K., Liakopoulos, D., Scheffner, M., and Jentsch, S. (1998) The ubiquitin like proteins smt3 and SUMO-1 are conjugated by the UBC9 E2 enzyme. *Proc. Natl. Acad. Sci. USA* **95**, 560–564.
- Seeler, J. S., and Dejean, A. (2003) Nuclear and unclear functions of SUMO. *Nat. Rev. Mol. Cell Biol.* **4**, 690–699.
- Shen, S., Lin, P. S., Chao, Y. C., Zhang, A., Yang, X., Lim, S. G., Hong, W., and Tan, Y. J. (2005) The severe acute respiratory syndrome coronavirus 3a is a novel structural protein. *Biochem Biophys Res Commun.* **330**, 286–292.

- Shen, S., Wen, Z. L., and Liu, D. X. (2003) Emergence of a coronavirus infectious bronchitis virus mutant with a truncated 3b gene: functional characterization of the 3b protein in pathogenesis and replication. *Virology* **311**, 16–27.
- Sherr, C. J., and McCormick, F. (2002) The RB and p53 pathways in cancer. *Cancer Cell* **2**, 103–112.
- Sherr, C. J., and Roberts, J. M. (1999) CDK inhibitors: positive and negative regulators of G1-phase progression. *Genes Dev.* **13**, 1501–1512.
- Shi, L., Nishioka, W. K., Th'ng, J., Bradbury, E. M., Litchfield, D. W., Greenberg, A. H. (1994) Premature p34cdc2 activation required for apoptosis. *Science* **263**, 1143–1145.
- Shimizu, T., O'Connor, P. M., Kohn, K. W., Pommier, Y. (1995) Unscheduled activation of cyclin B1/Cdc2 kinase in human promyelocytic leukemia cell line HL60 cells undergoing apoptosis induced by DNA damage. *Cancer Res.* **55**, 228–231.
- Shivakumar, C. V., Brown, D. R., Deb, S., and Deb, S. P. (1995) Wild-type human p53 transactivates the human proliferating cell nuclear antigen promoter. *Mol. Cell Biol.* **15**, 6785–6793.
- Skowronski, D. M., Astell, C., Brunham, R. C., Low, D. E., Petric, M., Roper, R. L., Talbot, P. J., Tam, T., and Babiuk, L. (2005) Severe acute respiratory syndrome (SARS): a year in review. *Annu. Rev. Med.* **56**, 357–381.
- Smits, S. L., Gerwig, G. J., van Vliet, A. L., Lissenberg, A., Briza, P., Kamerling, J. P., Vlasak, R., and de Groot, R. J. (2005) Nidovirus sialate-O-acetyl esterases: Evolution and substrate specificity of coronaviral and toroviral receptor-destroying enzymes. *J. Biol. Chem.* **280**, 6933–6941.
- Snijder, E. J., Bredenbeek, P. J., Dobbe, J. C., Thiel, V., Ziebuhr, J., Poon, L. L., Guan, Y., Rozanov, M., Spaan, W. J., and Gorbalenya, A. E. (2003) Unique and conserved features of genome and proteome of SARS-coronavirus, an early split-off from the coronavirus group 2 lineage. *J. Mol. Biol.* **331**, 991–1004.
- Song, H. D., Tu, C. C., Zhang, G. W., Wang, S. Y., Zheng, K., Lei, L. C., Chen, Q. X., Gao, Y. W., Zhou, H. Q., Xiang, H., Zheng, H. J., Chern, S. W., Cheng, F., Pan, C. M., Xuan, H., Chen, S. J., Luo, H. M., Zhou, D. H., Liu, Y. F., He, J. F., Qin, P. Z., Li, L. H., Ren, Y. Q., Liang, W. J., Yu, Y. D., Anderson, L., Wang, M., Xu, R. H., Wu, X. W., Zheng, H. Y., Chen, J. D., Liang, G., Gao, Y., Liao, M., Fang, L., Jiang, L. Y., Li, H., Chen, F., Di, B., He, L. J., Lin, J. Y., Tong, S., Kong, X., Du, L., Hao, P., Tang, H., Bernini, A., Yu, X. J., Spiga, O., Guo, Z. M., Pan, H. Y., He, W. Z., Manuguerra, J. C., Fontanet, A., Danchin, A., Niccolai, N., Li, Y. X., Wu, C. I., and Zhao, G. P. (2005) Cross-host evolution of severe acute respiratory syndrome coronavirus in palm civet and human. *Proc. Natl. Acad. Sci. USA* **102**, 2430–2435.

- Song, J., Durrin, L. K., Wilkinson, T. A., Krontiris, T. G., and Chen, Y. (2004) Identification of a SUMO-binding motif that recognizes SUMO-modified proteins. *Proc. Natl. Acad. Sci. USA* **101**, 14373–14378.
- Stadler, K., Masignani, V., Eickmann, M., Becker, S., Abrignani, S., Klenk, H.-D., and Rappuoli, R. (2003) SARS – Beginning to understand a new virus. *Nat. Rev. Microb.* **1**, 209–218.
- Steffan, J. S., Agrawal, N., Pallos, J., Rockabrand, E., Trotman, L. C., Slepko, N., Illes, K., Lukacsovich, T., Zhu, Y. Z., Cattaneo, E., Pandolfi, P. P., Thompson, L. M., and Marsh, J. L. (2004) SUMO modification of huntingtin and huntingtin's disease pathology. *Science* **304**, 100–104.
- Stewart, S. A., Poon, B., Jowett, J. B., and Chen, I. S. (1997) Human immunodeficiency virus type 1 Vpr induces apoptosis following cell cycle arrest. *J. Virol.* **71**, 5579–5592.
- Stohlman, S. A., Baric, R. S., Nelson, G. W., Soe, L. H., Welter, L. M., and Deans, R. J. (1988) Specific interaction between coronavirus leader RNA and nucleocapsid protein. *J. Virol.* **62**, 4288–4295.
- Stohlman, S., Bergmann, C., and Perlman, S. (1999) Mouse hepatitis virus. In *Persistent Viral Infection* (eds Ahmed, R. & Chen, I.) 537 – 558 (John Wiley, New York).
- Sturman, L. S., Holmes, K. V., and Behnke, J. (1980) Isolation of coronavirus envelope glycoproteins and interaction with the viral nucleocapsid. *J. Virol.* **33**, 449–462.
- Su, D., Lou, Z., Sun, F., Zhai, Y., Yang, H., Zhang, R., Joachimiak, A., Zhang, X. C., Bartlam, M., and Rao, Z. (2006) Dodecamer structure of severe acute respiratory syndrome coronavirus nonstructural protein nsp10. *J. Virol.* **80**, 7902–7908.
- Su, H. L., Liao, C. L., and Lin, Y. L. (2002) Japanese encephalitis virus infection initiates endoplasmic reticulum stress and an unfolded protein response. *J. Virol.* **76**, 4162–4171.
- Surjit, M., Kumar, R., Mishra, R. N., Reddy, M. K., Chow, V. T. K. and La, S. K. (2005) The severe acute respiratory syndrome coronavirus nucleocapsid protein is phosphorylated and localizes in the cytoplasm by 14-3-3-mediated translocation. *J. Virol.* **79**, 11476–11486.
- Surjit, M., Liu, B., Chow, V-T-K., and Lal, S. K. (2006) The Nucleocapsid Protein of Severe Acute Respiratory Syndrome-Coronavirus Inhibits the Activity of Cyclin-Cyclin-dependent Kinase Complex and Blocks S Phase Progression in Mammalian Cells. *J. Biol. Chem.* **281**, 10669–10681.

- Surjit, M., Liu, B., Jameel, S., Chow, V-T-K., and Lal, S. K. (2004a) The SARS coronavirus nucleocapsid protein induces actin reorganization and apoptosis in COS-1 cells in the absence of growth factors. *Biochem. J.* **383**, 13–18.
- Surjit, M., Liu, B., Kumar, R., Chow, V. T. K. and La, S. K. (2004b) The nucleocapsid protein of the SARS coronavirus is capable of self-association through a C-terminal 209 amino acid interaction domain. *Biochem. Biophys. Res. Commun.* **317**, 1030–1036.
- Sutton, G., Fry, E., Carter, L., Sainsbury, S., Walter, T., Nettleship, J., Berrow, N., Owens, R., Gilbert, R., Davidson, A., Siddell, S., Poon, L. L. et al. (2004) The nsp9 replicase protein of SARS-coronavirus, structure and functional insights. *Structure* **12**, 341–353.
- Swanton, C., and Jones, N. (2001) Strategies in subversion: Deregulation of the mammalian cell cycle by viral gene products. *Int J Exp Pathol* **82**, 3–13.
- Tahara, S. M., Dietlin, T. A., Bergmann, C. C., Nelson, G. W., Kyuwa, S., Anthony, R. P., and Stohlman, S. A. (1994) Coronavirus translational regulation: leader affects mRNA efficiency. *Virology* **202**, 621–630.
- Tan, M., Jing, T., Lan, K. H., Neal, C. L., Li, P., Lee, S., Fang, D., Nagata, Y., Liu, J., Arlinghaus, R., Hung, M. C., Yu, D. (2002) Phosphorylation on tyrosine-15 of p34(Cdc2) by ErbB2 inhibits p34(Cdc2) activation and is involved in resistance to taxol-induced apoptosis. *Mol. Cell* **9**, 993–1004.
- Tan, Y. W., Fang, S., Fan, H., Lescar, J., and Liu, D. X. (2006) Amino acid residues critical for RNA-binding in the N-terminal domain of the nucleocapsid protein are essential determinants for the infectivity of coronavirus in cultured cells. *Nucleic Acids Res.* **34**, 4816–4825
- Tan, Y-J., Fielding, B. C., Goh, P-Y., Shen, S., Tan, T. H. P., Lim, S. G., and Hong, W. (2004) Overexpression of 7a, a protein specifically encoded by the severe acute respiratory syndrome coronavirus, induces apoptosis via a caspase-dependent pathway. *J. Virol.* **78**, 14043–14047.
- Tan, Y. J., Lim, S. G., and Hong, W. (2005) Characterization of viral proteins encoded by the SARS-coronavirus genome. *Antiviral Res.* **65**, 69–78.
- Tang, B. S., Chan, K. H., Cheng, V. C., Woo, P. C., Lau, S. K., et al. (2005) Comparative host gene transcription by microarray analysis early after infection of the Huh7 cell line by severe acute respiratory syndrome coronavirus and human coronavirus 229E. *J. Virol.* **79**, 6180–6193.
- Taylor, W. R., Agarwal, M. L., Agarwal, A., Stacey, D. W., and Stark, G. R. (1999) p53 inhibits entry into mitosis when DNA synthesis is blocked. *Oncogene* **18**, 283–295.
- Taylor, W. R., and Stark, G. R. (2001) Regulation of G₂/M transition by p53. *Oncogene* **20**, 1803–1815.

- Teodoro, J. G., and Branton, P. E. (1997) Regulation of apoptosis by viral gene products. *J. Virol.* **71**, 1739–1746.
- Teodoro, J. G., Heilman, D. W., Parker, A. E., and Green, M. R. (2004) The viral protein Apoptin associates with the anaphase-promoting complex to induce G2/M arrest and apoptosis in the absence of p53. *Gene & Dev.* **18**, 1952–1957.
- ter Meulen, J., Bakker, A. B., van den Brink, E. N., Weverling, G. J., Martina, B. E., Haagmans, B. L., Kuiken, T., de Kruif, J., Preiser, W., Spaan, W., Gelderblom, H. R., Goudsmit, J., and Osterhaus, A. D. (2004) Human monoclonal antibody as prophylaxis for SARS coronavirus infection in ferrets. *Lancet* **363**, 2139–2141.
- Thiel, V., Ivanov, K. A., Putics, A., Hertzog, T., Schelle, B., Bayer, S., Weissbrich, B., Snijder, E. J., Rabenau, H., Doerr, H. W., Gorbalenya, A. E., and Ziebuhr, J. (2003) Mechanisms and enzymes involved in SARS coronavirus genome expression. *J. Gen. Virol.* **84**, 2305–2315.
- Thiel, V., and Siddell, S. G. (1994) Internal ribosome entry in the coding region of murine hepatitis virus mRNA5. *J. Gen. Virol.* **75**, 3041–3046.
- To, K. F., Chan, P. K., Chan, K. F., Lee, W. K., Lam, W. Y., Wong, K. F., Tang, N. L., Tsang, D. N., Sung, R. Y., Buckley, T. A., Tam, J. S., and Cheng, A. F. (2001) Pathology of fatal human infection associated with avian influenza A H5N1 virus. *J. Med. Virol.* **63**, 242–246.
- Tomoiu, A., Gravel, A., Tanguay, R. M., and Flamand, L. (2006) Functional interaction between human herpesvirus 6 immediate-early 2 protein and ubiquitin-conjugating enzyme 9 in the absence of sumoylation. *J. Virol.* **80**, 10218–10228.
- Torres, J., Parthasarathy, K., Lin, X., Saravanan, R., Kukol, A., and Liu, D. X. (2006) Model of a putative pore: the pentameric alpha-helical bundle of SARS coronavirus E protein in lipid bilayers. *Biophys. J.* **91**, 938–947.
- Torres, J., Wang, J., Parthasarathy, K., and Liu, D. X. (2005) The transmembrane oligomers of coronavirus protein E. *Biophys. J.* **88**, 1283–1290.
- Tsui, P. T., Kwok, M. L., Yuen, H., and Lai, S. T. (2003) Severe acute respiratory syndrome: clinical outcome and prognostic correlates. *Emerg. Infect. Dis.* **9**, 1064–1069.
- van den Heuvel, S., and Harlow, E. (1993) Distinct roles for cyclin-dependent kinases in cell cycle control. *Science* **262**, 2050–2054.
- van der Hoek, L., Pyrc, K., Jebbink, M. F., Vermeulen-Oost, W., Berkout, R. J., Wolthers, K. C., Wertheim-van Dillen, P. M., Kaandorp, J., Spaargaren, J., and Berkhout, B. (2004) Identification of a new human coronavirus. *Nature Med.* **10**, 368–373.

- Vannucchi, S., Chiantore, M. V., Fiorucci, G., Percario, Z. A., Leone, S., Affabris, E., and Romeo, G. (2005) TRAIL is a key target in S-phase slowing-dependent apoptosis induced by interferon- β in cervical carcinoma cells. *Oncogene* **24**, 2536–2546.
- Vennema, H., Godeke, G.-J., Rossen, J. W. A., Voorhout, W. F., Horzinek, M. C., Opstelten, D.-J. E., and Rottier, P. J. M. (1996) Nucleocapsid-independent assembly of coronavirus-like particles by co-expression of viral envelope protein genes. *EMBO J.* **15**, 2020–2028.
- Verger, A., Perdomo, J., and Crossley, M. (2003) Modification with SUMO. A role in transcriptional regulation. *EMBO Rep.* **4**, 137–142.
- Verma, S., Bednar, V., Blount, A., Hogue, B. G. (2006) Identification of functionally important negatively charged residues in the carboxy end of mouse hepatitis coronavirus A59 nucleocapsid protein. *J. Virol.* **80**, 4344–4355.
- Vogelstein, B., Lane, D., and Levine, A.J. (2000) Surfing the p53 network. *Nature* **408**, 307–310.
- von Grotthuss, M., Wyrwicz, L. S., and Rychlewski, L. (2003) mRNA cap-1 methyltransferase in the SARS genome. *Cell* **113**, 701–702.
- Wang, J. T., Wang, J. T., Sheng, W. H., Fang, C. T., Chen, Y. C., Wang, J. L., Yu, C. J., Chang, S. C., and Yang, P. C. (2004) Clinical manifestations, laboratory findings, and treatment outcomes of SARS patients. *Emerg. Infect. Dis.* **10**, 818–824.
- Wang, J. Y. (1997) Retinoblastoma protein in growth suppression and death protection. *Curr. Opin. Genet. & Dev.* **7**, 39–45.
- Wege, H., S. Siddell, and V. ter Meulen. (1982) The biology and pathogenesis of coronaviruses. *Curr. Top. Microbiol. Immunol.* **99**, 165–200.
- Weinberg, R.A. (1995) The retinoblastoma protein and cell cycle control. *Cell* **81**, 323–330.
- Weiss, S. R., and Navas-Martin, S. (2005) Coronavirus pathogenesis and the emerging pathogen severe acute respiratory syndrome coronavirus. *Microb. Mol. Biol. Rev.* **69**, 635–664.
- Williams, R. K., Jiang, G. S., and Holmes, K. V. (1991) Receptor for mouse hepatitis virus is a member of the carcinoembryonic antigen family of glycoproteins. *Proc. Natl. Acad. Sci. USA* **88**, 5533–5536.
- Wilson, L., McKinlay, C., Gage, P., and Ewart, G. (2004) SARS coronavirus E protein forms cation-selective ion channels. *Virology* **330**, 322–331.
- Wilson, V. G., and Rangasamy, D. (2001) Viral interaction with the host cell sumoylation system. *Virus Res.* **81**, 17–27.

- Wong, R. S., Wu, A., To, K. F., Lee, N., Lam, C. W., Wong, C. K., Chan, P. K., Ng, M. H., Yu, L. M., Hui, D. S., Tam, J. S., Cheng, G., and Sung, J. J. (2003) Haematological manifestations in patients with severe acute respiratory syndrome: retrospective analysis. *BMJ* **326**, 1358–1362.
- Woo, P. C., Lau, S. K., Chu, C. M., Chan, K. H., Tsoi, H. W., Huang, Y., Wong, B. H., Poon, R. W., Cai, J. J., Luk, W. K., Poon, L. L., Wong, S. S., Guan, Y., Peiris, J. S., and Yuen, K. Y. (2005) Characterization and complete genome sequence of a novel coronavirus, coronavirus HKU1, from patients with pneumonia. *J. Virol.* **79**, 884–895.
- Wootton, S. K., Raymond, R. R., and Yoo, D. (2002) Phosphorylation of the porcine reproductive and respiratory syndrome virus nucleocapsid protein. *J. Virol.* **76**, 10569–10576.
- World Health Organization. (2003) Severe acute respiratory syndrome (SARS): multi-country outbreak. World Health Organization, Geneva, Switzerland.
- World Health Organization. (2004) Summary of probable SARS cases with onset of illness from 1 November 2002 to 31 July 2003. Communicable Disease Surveillance & Response (CSR). World Health Organization, Geneva, Switzerland.
- Wu, X., Gong, X., Foley, H., Schnell, M., and Fu, Z. (2002) Both viral transcription and replication are reduced when the rabies virus nucleoprotein is not phosphorylated. *J. Virol.* **76**, 4153–4161.
- Wurm, T., Chen, H., Hodgson, T., Britton, P., Brooks, G., and Hiscox, J. A. (2001) Localization to the nucleolus is a common feature of coronavirus nucleoproteins, and the protein may disrupt host cell division. *J. Virol.* **75**, 9345–9356.
- Xiao, Z., Watson, N., Rodriguez, C., and Lodish, H. F. (2001) Nucleocytoplasmic shuttling of smad1 conferred by its nuclear localization and nuclear export signals. *J. Biol. Chem.* **276**, 39404–39410.
- Xiao, Z. X., Ginsberg, D., Ewen, M., and Livingston, D. M. (1996) Regulation of the retinoblastoma protein-related protein p107 by G₁ cyclin-associated kinases. *Proc. Natl. Acad. Sci. USA* **93**, 4633–4637.
- Xu, H. Y., Lim, K. P., Shen, S., and Liu, D. X. (2001) Further identification and characterization of novel intermediate and mature cleavage products released from the ORF 1b region of the avian coronavirus infectious bronchitis virus 1a/1b polyprotein. *Virology* **288**, 212–222.
- Xu, X., Liu, Y., Weiss, S., Arnold, E., Sarafianos, S. G., and Ding, J. (2003) Molecular model of SARS coronavirus polymerase: implications for biochemical functions and drug design. *Nucleic Acids Res.* **31**, 7117–7130.

- Yang, Y., Li, C-C. H., and Weisman, A. M. (2004a) Regulating the p53 system through ubiquitination. *Oncogene* **23**, 2096–2106.
- Yang, Y., Xiong, Z., Zhang, S., Yan, Y., Nguyen, J., Ng, B., Lu, H., Brendese, J., Yang, F., Wang, H., and Yang, X. F. (2005) Bcl-xL inhibits T-cell apoptosis induced by expression of SARS coronavirus E protein in the absence of growth factors. *Biochem. J.* **392**, 135–143.
- Yang, Z. Y., Kong, W. P., Huang, Y., Roberts, A., Murphy, B. R., Subbarao, K., and Nabel, G. J. (2004b) A DNA vaccine induces SARS coronavirus neutralization and protective immunity in mice. *Nature* **428**, 561–564.
- Yokomori, K., and Lai, M. M. C. (1991) Mouse hepatitis virus S RNA sequence reveals that nonstructural proteins ns4 and ns5a are not essential for murine coronavirus replication. *J. Virol.* **65**, 5605–5608.
- You, J., Dove, B. K., Enjuanes, L., DeDiego, M. L., Alvarez, E., Howell, G., Heinen, P., Zambon, M., and Hiscox, J. A. (2005) Subcellular localization of the severe acute respiratory syndrome coronavirus nucleocapsid protein. *J. Gen. Virol.* **86**, 3303–3310.
- Youn, S., Leibowitz, J. L., and Collisson, E. W. (2005) In vitro assembled, recombinant infectious bronchitis viruses demonstrate that the 5a open reading frame is not essential for replication. *Virology* **332**, 206–215.
- Yount, B., Curtis, K. M., Fritz, E. A., Hensley, L. E., Jahrling, P. B., Prentice, E., Denison, M. R., Geisbert, T. W., and Baric, R. S. (2003) Reverse genetics with a full-length infectious cDNA of severe acute respiratory syndrome coronavirus. *Proc. Natl. Acad. Sci. USA* **100**, 12995–13000.
- Yount, B., Denison, M. R., Weiss, S. R., and Baric, R. S. (2002) Systematic assembly of a full-length infectious cDNA of mouse hepatitis virus strain A59. *J. Virol.* **76**, 11065–11078.
- Yu, I-M., Gustafson, C. L. T., Diao, J., Burgner, J. W., Li, Z., Zhang, J., and Chen, J. (2005) Recombinant severe acute respiratory syndrome (SARS) coronavirus nucleocapsid protein forms a dimer through its C-terminal domain. *J. Biol. Chem.* **280**, 23280–23286.
- Yu, I-M., Oldham, M. L., Zhang, J., and Chen, J. (2006) Crystal structure of the SARS coronavirus nucleocapsid protein dimerization domain reveals evolutionary linkage between *Corona*- and *Arteri*- *Viridae*. *J. Biol. Chem.* **281**, 17134–17139.
- Yu, X., Bi, W., Weiss, S. R., and Leibowitz, J. L. (1994) Mouse hepatitis virus gene 5b protein is a new virion envelope protein. *Virology* **202**, 1018–1023.
- Yuan, Q., Liao, Y., Torres, J., Tam, J. P., and Liu, D. X. (2006a) Biochemical evidence for the presence of mixed membrane topologies of the severe acute

- respiratory syndrome coronavirus envelope protein expressed in mammalian cells. *FEBS Letters* **580**, 3192–3200.
- Yuan, X., Shan, Y., Zhao, Z., Chen, J., and Cong, Y. (2005) G₀/G₁ arrest and apoptosis induced by SARS-CoV 3b protein in transfected cells. *Viol. J.* **2**, 66.
- Yuan, X., Wu, J., Shan, Y., Yao, Z., Dong, B., Chen, B., Zhao, Z., Wang, S., Chen, J., and Cong, Y. (2006b) SARS coronavirus 7a protein blocks cell cycle progression at G₀/G₁ phase via the cyclin D3/pRb pathway. *Virology* **346**, 74–85.
- Yuan, Z. M., Shioya, H., Ishiko, T., Sun, X., Gu, J., Huang, Y. Y., Lu, H., Kharbanda, S., Weichselbaum, R., Kufe, D. (1999) p73 is regulated by tyrosine kinase c-Abl in the apoptotic response to DNA damage. *Nature* **399**, 814–817.
- Yueh, A., Leung, J., Bhattacharyya, S., Perrone, L. A., de los Santos, K., Pu, S. Y., and Goff, S. P. (2006) Interaction of moloney murine leukemia virus capsid with Ubc9 and PIASy mediates SUMO-1 addition required early in infection. *J. Virol.* **80**, 342–352.
- Zhai, Y., Sun, F., Li, X., Pang, H., Xu, X., Bartlam, M., and Rao, Z. (2005) Insights into SARS-CoV transcription and replication from the structure of the nsp7–nsp8 hexadecamer. *Nat. Struct. Mol. Biol.* **12**, 980–986.
- Zhang, H. S., Gavin, M., Dahiya, A., Postigo, A. A., Ma, D., Luo, R. X., Harbour, J. W., and Dean, D. C. (2000) Exit from G₁ and S phase of the cell cycle is regulated by repressor complexes containing HDAC-Rb-hSWI/SNF and Rb-hSWI/SNF. *Cell* **101**, 79–89.
- Zhang, X., Liao, C.-L., and Lai, M. M. C. (1994) Coronavirus leader RNA regulates and initiates subgenomic mRNA transcription both in *trans* and in *cis*. *J. Virol.* **68**, 4738–4746.
- Zhao, P., Cao, J., Zhao, L.-J., Qin, Z.-L., Ke, J.-S., Pan, W., Ren, H., Yu, J.-G., Qi, Z.-T. (2005) Immune responses against SARS-coronavirus nucleocapsid protein induced by DNA vaccine. *Virology* **331**, 128–135.
- Zhong, N. S., Zheng, B. J., Li, Y. M., Poon, L. L., Xie, Z. H., Chan, K. H., Li, P. H., Tan, S. Y., Chang, Q., Xie, J. P., Liu, X. Q., Xu, J., Li, D. X., Yuen, K. Y., Peiris, J. S., and Guan, Y. (2003) Epidemiology and cause of severe acute respiratory syndrome (SARS) in Guangdong, People's Republic of China, in February, 2003. *Lancet* **362**, 1353–1358.
- Zhou, M., and Collisson, E. W. (2000) The amino and carboxyl domains of the infectious bronchitis virus nucleocapsid protein interact with 30 genomic RNA. *Virus Res.* **67**, 31–39.
- Zhou, M., Williams, A. K., Chung, S. I., Wang, L., and Collisson, E. W. (1996) The infectious bronchitis virus nucleocapsid protein binds RNA sequences in the 3' terminus of the genome. *Virology* **217**, 191–199.

Zhou, Z., Post, P., Chubet, R., Holtz, K., McPherson, C., Petric, M., and Cox, M. (2006) A recombinant baculovirus-expressed S glycoprotein vaccine elicits high titers of SARS-associated coronavirus (SARS-CoV) neutralizing antibodies in mice. *Vaccine* **24**, 3624–3631.

Zhu, L., and Anasetti, C. (1995) Cell cycle control of apoptosis in human leukemic T cells. *J. Immunol.* **154**, 192–200.

Curriculum Vitae

Li, (Frank) Qisheng

EDUCATION

Ph.D. Candidate, 2002 - 2006, School of Biological Sciences, Nanyang Technological University, Singapore

MBBS (M.D. equivalent), 1990 - 1995, School of Medicine, Second Military Medical University, Shanghai, China

PROFESSIONAL EXPERIENCE

Senior Fellow, 2006 - Present, University of Washington Medical Center, Seattle, WA, USA

Research Associate, 2006 - 2006, School of Biological Sciences, Nanyang Technological University, Singapore

Attending Doctor & Instructor, 2000 - 2002, Changzheng Hospital, Shanghai, China

Medical Residency, Chief Resident, 1995 - 2000, Changzheng Hospital, Shanghai, China

PUBLICATIONS FROM PHD WORK AND PATENTS

Li FQ, Tam JP, Liu DX (2007) Cell cycle arrest and apoptosis induced by the coronavirus IBV in the absence of p53. Virology, doi:10.1016/j.virol.2007.04.015

Li Q, Xiao H, Tam JP, Liu DX (2006) Sumoylation of the nucleocapsid protein of severe acute respiratory syndrome coronavirus by interaction with Ubc9. Adv Exp Med Biol. 581, 121-126.

Li FQ, Xiao H, Tam JP, Liu DX (2005). Sumoylation of the nucleocapsid protein of severe acute respiratory syndrome coronavirus. FEBS Letters 579, 2387-2396.

Li Q, Xiao H, Tam JP, Liu DX. Interaction of the nucleocapsid protein of severe acute respiratory syndrome coronavirus with human ubiquitin conjugating enzyme 9. In: The Nidoviruses: The Control of SARS and Other Nidovirus Diseases (Perlman S & Holmes KV Eds. Springer Press), 2005.

Li K, Wang Y, Li T, **Li Q**. Methods to prepare adefovir dipivoxil and application of its crystals as drug candidates against hepatitis B virus. Patent No: CN1421449A

Li K, Wang Y, Li T, **Li Q**. Methods to prepare adefovir dipivoxil crystals. Patent No: CN1421450A

Li K, Wang Y, Li T, **Li Q**. Methods to prepare adefovir dipivoxil. Patent No: CN1421451A

Li K, Liu C, **Li Q**. A novel method to prepare β -thymidine. Patent No: ZL98121933.0

**INVITED TALKS
AND SEMINARS**

Characterization of coronaviral interactions with host factors. NIDDK, NIH, Bethesda, MD, USA (April 6, 2007)

Characterization of coronaviral interactions with host factors. Harborview Medical Center, University of Washington School of Medicine, Seattle, WA, USA (July 26, 2006)

Xth International Nidovirus Symposium: Towards Control of SARS and other Nidovirus Diseases, Colorado Springs, CO, USA (Plenary talk, June 26, 2005)